WADC TECHNICAL REPORT 54-8

AN INVESTIGATION OF A METHOD FOR PRESTRESSING FLAT PLATES TO INCREASE THEIR BUCKLING STRENGTH

C. T. WANG
A. L. ROSS
E. L. REISS

NEW YORK UNIVERSITY

FEBRUARY 1954

WRIGHT AIR DEVELOPMENT CENTER

NOTICES

When Government drawings, specifications, or other data are used for any purpose other than in connection with a definitely related Government procurement operation, the United States Government thereby incurs no responsibility nor any obligation whatsoever; and the fact that the Government may have formulated, furnished, or in any way supplied the said drawings, specifications, or other data, is not to be regarded by implication or otherwise as in any manner licensing the holder or any other person or corporation, or conveying any rights or permission to manufacture, use, or sell any patented invention that may in any way be related thereto.

The information furnished herewith is made available for study upon the understanding that the Government's proprietary interests in and relating thereto shall not be impaired. It is desired that the Judge Advocate (WCJ), Wright Air Development Center, Wright-Patterson Air Force Base, Ohio, be promptly notified of any apparent conflict between the Government's proprietary interests and those of others.

WADC TECHNICAL REPORT 54-8

AN INVESTIGATION OF A METHOD FOR PRESTRESSING FLAT PLATES TO INCREASE THEIR BUCKLING STRENGTH

C. T. Wang
A. L. Ross
E. L. Reiss

New York University

February 1954

Aeronautical Research Laboratory
Contract No. AF 33(616)-49
RDO No. 471-506

Wright Air Development Center
Air Research and Development Command
United States Air Force
Wright-Patterson Air Force Base, Ohio

McGregor & Werner, Inc., Dayton, O.
150 June, 1954

FOREWORD

This report was prepared at the College of Engineering, New York University on Air Force Contract No. AF 33(616)-49, under Research and Development Order No. 471-506, "Buckling of Flat Rectangular Panels Prestressed by Initial Curvature". The work was administered under the direction of the Aeronautical Research Laboratory, Directorate of Research, Wright Air Development Center, with Captain R. W. Rivello and Lt. E. H. Porter, Jr. acting as project engineers.

The work was carried out under the supervision and direction of Dr. Chi-Teh Wang. The theoretical portion and some of the experimental phase were carried out by Dr. Arthur L. Ross while the bulk of the experimental phase was carried out by Mr. Edward L. Reiss.

Special acknowledgement should go to Mrs. Madeline Lynar for typing the report, to Mrs. Roslyn Lawrence, Miss Maria Pan, and Miss Raquel Heller for their aid in the calculations and to Mr. Edward Fellman and Mr. Arthur Smith for their assistance in the testing laboratories.

ABSTRACT

It is proposed that flat plates can have their buckling strength increased by prestressing. The prestressing is accomplished by first cold rolling the plates into cylindrical form and then opening the plate by riveting onto or clamping into a flat frame. This prestressing will produce membrane stresses in the plane of the plate of such a magnitude and distribution as to raise its buckling load in the direction of the generator of the cylinder. The present investigation was restricted to the case of all four sides clamped.

The stresses produced by this process are measured and their effect calculated by the Rayleigh-Ritz method. The analysis shows that small stresses (1000 psi maximum) could raise the buckling load almost 50%, and probably more. These stresses would also change the buckling mode in some of the cases examined from antisymmetrical to symmetrical modes.

A testing frame was constructed to produce, and measure the effect of the proposed prestressing. The tests showed that the buckling load was raised in some cases over 100% while the average for all tests was 38%.

A theoretical evaluation of the membrane stresses and their effect was carried out which involved the solution of the non-linear plate equations of Von Karman. Because the necessity of using the rather approximate assumptions, the analysis could be subjected to questioning. Nevertheless, the analysis showed that the buckling load at one particular type of prestressed plate would be raised approximately 15%.

PUBLICATION REVIEW

This report has been reviewed and is approved.

FOR THE COMMANDER:

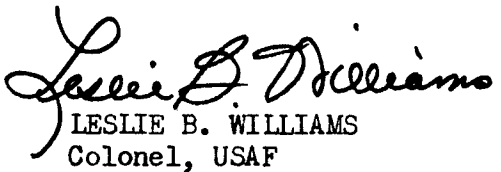

LESLIE B. WILLIAMS
Colonel, USAF
Chief, Aeronautical Research Laboratory
Directorate of Research

CONTENTS

LIST OF FIGURES

LIST OF FIGURES (Continued)

LIST OF TABLES

LIST OF TABLES (Continued)

SYMBOLS (NOTATIONS) AND UNITS

a	plate width, inches
b	plate length, inches
$b_{p,q}$	stress function coefficients, psi
D	Plate Rigidity = $\frac{Eh^3}{12(1-\nu^2)}$, in. lb.
$\delta'(x)$ or $\delta'(y)$	Pressure couple distribution using Dirac delta function
δ	Shortening of plate, inches
ε	strain, in./in.
E	Young's Modulus, psi
F	Stress Function
h	Plate thickness, inches
I	Moment of Inertia, $in.^4$
$i,j,k,l,m,n,$ p,q,r,s	Indices
K	Non-dimensional buckling coefficient = $N_{ycr}\frac{a^2}{\pi^2 D}$
l	Length, inches
M	Moment, in. lbs.
P	Load, pounds
p	Pressure, psi
$p_{r,s}$	Pressure series coefficients, psi
R	Radius, inches
σ	Stress, psi
T	Work done by Applied Load
U	Strain Energy
W	Work due to initial prestresses
w	Deflection in z-direction, inches
$w_{m,n}$	Deflection series coefficient, inches
x,y,z	Coordinates

SECTION I

Introduction

Before the advent of modern high speed aircraft, wrinkling of the covering of aircraft components due to local buckling under flight loads did not introduce any serious problems because such wrinkling does not have a material effect on the performance of the aircraft. Present day high speed aircraft, however, often operate under conditions in which the local airstream Mach number adjacent to the aerodynamic surfaces is nearly unity; consequently even slight surface irregularities, such as the appearance of wrinkles due to buckling, may cause the local velocity to become supersonic. Such changes from subsonic to supersonic flow are accompanied by the formation of shock waves in the flow which materially increase the drag of the aircraft. It is therefore desirable for these aircraft to employ a covering which will not buckle at flight loads and yet will not introduce any undue increase in the weight of the structure.

One type of such structure is sandwich construction. Sandwich construction consists of two thin external or face layers of high-strength material, such as aluminum alloy sheet, bonded to a thick internal layer or core of light-weight material, such as balsa wood or cellular cellulose acetate. The core serves to separate the strong faces a fixed distance apart, thus giving the structure a high bending and therefore buckling strength, but without a substantially increase in weight. This type of construction has been the subject of intensive investigation and considerable work has been done at the Guggenheim School of Aeronautics of New York University (1,2).

In this report an attempt is made to introduce another type of construction where buckling is delayed by a method of prestressing. The method is as follows. First, the thin sheet is curved by cold rolling in the direction perpendicular to the direction of compression, then it is opened elastically and attached to the stiffeners or the frame of the panel. By such a process, it was found that in-plane stresses are induced and the buckling loads are increased materially. Both experimental and theoretical investigations have been carried out to study this method of prestressing.

The fact that the buckling loads can be appreciably raised by first overcurving the panel and then elastically bring it to the desired curvature was first noticed by Welter (3) in his study on the effect of imperfection on the buckling loads of curved plates. Welter gave no explanation on this phenomenom. Later, Cox (4) indicated that favorable deformations occurring from the elastic bending accounted for the raising of the buckling load. This view was substantiated by Cicala (5) who showed that in certain cases the buckling load could be increased due to favorable deformations.

Although favorable deformations will doubtlessly be a factor in raising the buckling loads, an equally important cause, if not the major cause, is believed to be the presence of the induced in-plane stresses. This is born out in the present investigation where curved sheets were elastically opened to flat ones, because in general no favorable deformations can exist for a flat plate. The term "in general" is used in the above statement in deference to Cox's (4) statement that a favorable imperfection could be possible so as to develop a mode corresponding to a slightly higher buckling load.

SECTION II

OUTLINE OF THE EXPERIMENTAL PROGRAM

Before describing the experimenta carried out, Welter's (3) experiments should be reviewed at this point since it was his experiments which brought to light this particular method of prestressing thin plates to increase their buckling load. Welter presented the results of some experiments he performed with no attempt to explain the phenomenom discovered.

He performed his tests on both 17ST aluminum alloy of .036 in. thickness and 2S 3/4 H pure aluminum sheets of .032 in. thickness, both of 24 in. width and 96 in. length. The cylindrical plates were tested with a radius of curvature of 24 inches. The initial radii of curvatures of the plates varied between 6 in. and 24 in. (the latter being a non-prestressed plate) and were tested with a radius of 24 in. by opening the plate elastically to the greater radius. These tests showed increases in the buckling loads up to 50%. There were, however, a total of only nineteen tests performed and of these perhaps only half the results were conclusive.

The present experimental program can be divided into three parts: first, to determine whether objectionable deflections were produced during the prestressing process; secondly, to determine whether the prestressing process produced inplane (membrane) stresses that could be capable of raising the buckling load of the flat plate; and thirdly, to measure the buckling loads of prestressed plates and compare them with that of the corresponding non-prestressed flat plate.

SECTION III

TESTS TO DETERMINE THE INITIAL DEFLECTIONS DUE TO PRESTRESSING

Since the purpose of prestressing is to delay the occurrence of wrinkles due to buckling, it is important to determine first whether it is possible to clamp an initially curved plate without undesirable initial deflections. By "undesirable", it is inferred that the maximum deflection of the plate should be less than the thickness of the plate.

Three "flatness" tests were performed. One of the tests was performed on a half-hard brass plate while the other two were performed on 24ST aluminum plates. The brass plate was 19 1/2 by 12 inches and had a nominal thickness of 1/32 inch. The aluminum plates were 19.25 by 13.833 inches and had nominal thicknesses of .032 and .040 inches.

The clamping of the plate was executed on the compression base of the 200,000 lb. Baldwin-Southwark Universal Testing Machine. In this base there are several conveniently located, "Tee" Slots, which were used in clamping the plates to the base.

The clamping of the brass plates (see Fig. 1) was accomplished by using eight-1/2 inch thick, 1 1/4 inch wide steel bars. Two of these bars, 19 1/2 inches long were placed parallel to each other so that the edges of the bars and the "Tee" slots coincided. Two bars 9 1/2 inches long and parallel to each other were positioned on the base so that they were perpendicular to the 19 1/2 inch bars.

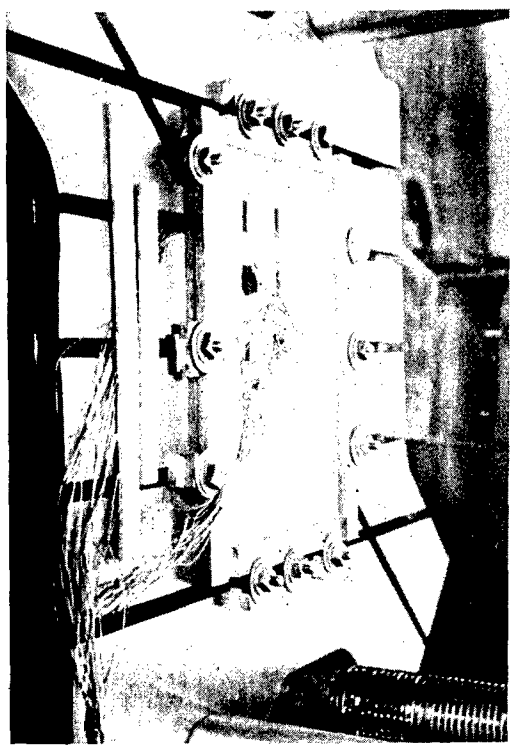

Clamping of Brass Plates for "Flatness" tests

Fig. 1

The brass test plate was set on this frame, and corresponding steel bars were oriented in similar positions on top of the brass plate, thus forming the clamping frame.

Twelve, 1/2 inch standard steel bolts whose heads were fitted with lock-washers were registered into the "Tee" slots of the compression base and were positioned as indicated in Fig. 1. The top of each bolt was fitted with a large diameter and a standard diameter steel washer. The diameter of the large steel washer was such that it extended over a considerable portion of the width of the steel clamping bars. On the side of each bolt opposite to that of the steel bar were placed three shims, two of them being 1/2 inch thick, and one being 1/32 inch thick. Thus the total thickness of the shims equaled that of the steel bars and test plate. By fitting a nut on the top of each bolt so that it bears on the washer, and tightening the nut, a clamping of the specimen between the steel bars was obtained.

After the plate was clamped by tightening down on each of the twelve bolts, the deflections of the plate at several positions were measured by a Starrett dial gage graduated with divisions of .001 inches.

The clamping of the Aluminum plates (see Fig. 2) was accomplished by using eight- 5/8 inch thick, 1 1/2 inch wide steel bars in a manner similar to the procedure used for the brass plate. In this series of tests two holes were drilled in each of the steel bars and half the bars were tapped and the other half drilled clear to accomodate bolts that would clamp the steel bars tightly to the edges of the plates. Two pairs of the steel bars were 19.25 inches long while the other two pairs were 10.75 inches long. The ends of the shorter bars which were underneath the plate were beveled to leave a passageway for the wires connected to the strain gages on the bottom surface of the plate as required in the determination of inplane strains described in the next section.

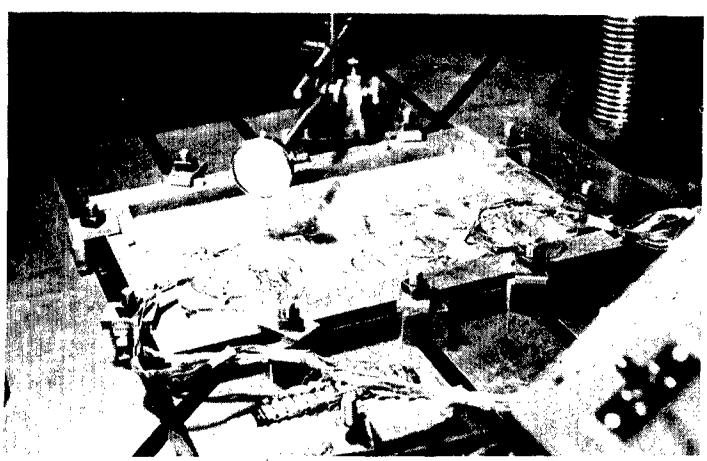

Clamping of Aluminum Plates for "Flatness" Tests

Fig. 2

The bolts for clamping the plate to the base of the testing machine were specially modified to fit the "Tee" slots thus making clamping of the plate easier. The hexagonal head of the bolt was replaced by a square head machined to fit the bottom of the "Tee" slot exactly. Instead of large washers being used to transmit the clamping force from the bolt to the steel bars, special "clamps" were made from 3/8 x 1 1/4 x 2 inch bars with holes drilled through the center to accomodate the bolt. One end of these "clamps" rested on the steel bars, forming a frame in which the plate was held, while the other end rested on bars 1.30 inches high (approximately the height of the frame).

The dial gage was fastened by means of rods to a gage "base plate". The gage was adjusted so that its measuring rod was perpendicular to the plane of the test plate. The measurements at the various positions were obtained by sliding the gage "base plate" along the surface of the compression base of the testing machine, until the rod of the gage was situated directly on the desired point. At each point, the measuring rod was lifted a small distance above the plate and then released, so as to obtain the same measuring pressure at each point.

The various measuring positions are illustrated in Figs. 3, 4, and 5 for the brass and aluminum plates. A particular point is defined by two numbers, the first indicating the position along the short side of the frame, the second along the long side.

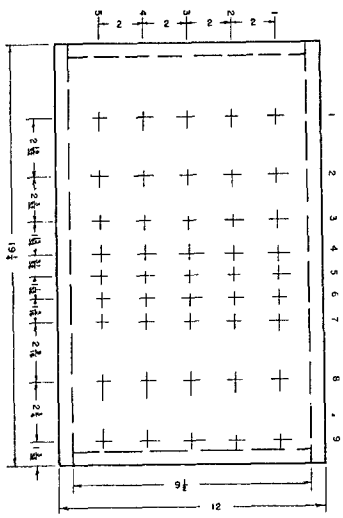

Deflection Measuring Points

Fig. 3

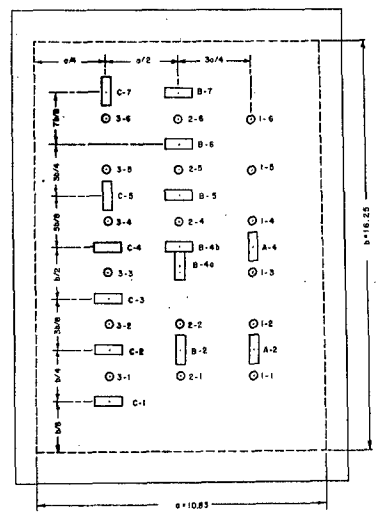

Deflection and Strain Gage Measuring Points on First Series of Aluminum Plates

Fig. 4

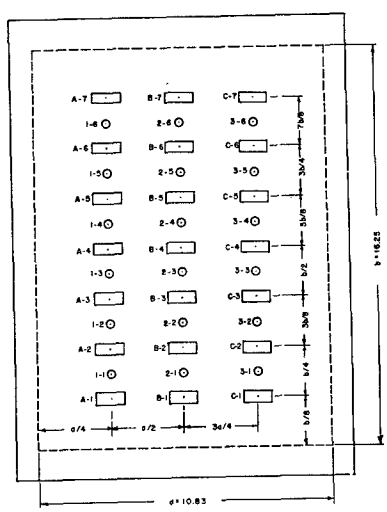

Deflection and Strain Gage Measuring Points on Second .040 inch Aluminum Plate

Fig. 5

The reference point, or the point at which the dial gage was set to zero, was arbitrarily selected at point 5-9. for the brass plate and 1-1 for the aluminum plates.

The results of the tests are in Tables 1 (a,b, and c).

The commercial designation of the brass plate was 1/32 inch with a standard commercial tolerance of ± .002 inches. From the results, it can be observed that the maximum positive deflection is + .003 (position 4-1), and the maximum negative deflection - .007 inches (position 3-3, 3-4, 3-6). Thus the percentage maximum deflections based upon the plate nominal thickness of 1/32 inch are + 9.6% and - 22.4% or a total of 32%.

The .040 inch thick aluminum plate had an initial radius of curvature of 8.7 inches, and when flattened had a maximum total deflection (the difference between the highest and lowest points on the plate) of .022 inches or 55% of the nominal thickness.

Similarly the .032 inch thick aluminum plate with an initial radius of curvature of 7 3/4 inches and a maximum total deflection of .049 inches or 153% of the nominal thickness. The unusually large deflection of this thin plate was probably caused by initial imperfections (due to the fact that this plate had been flattened several times previous to this experiment) and unavoidable errors in the measurements. However, it should be noted that deflections of this order might be expected in aircraft due to the pressure of the airforces.

SECTION IV

TESTS TO DETERMINE THE INPLANE STRESSES DUE TO PRESTRESSING

There were two series of tests performed. In the first series, three plates were tested - two brass plates and one aluminum plate. These plates were tested before any theoretical work was carried out. In the second series, tests were performed on four plates. These plates were of the same size but of different thickness. The theory indicates that the stress distribution depends on the parameters $\frac{a^2}{Rh}$ and a/b, where a is the width of the plate, b the length, h the thickness, and R is the initial radius of curvature. The radii of curvature of these plates were rolled in such a way that the parameter a^2/Rh remains a constant value, 337.5.

Each of the seven plates was clamped flat in the frames described in the preceding section. SR-4 strain gages were fastened to the plates with Duco Household cement in pans back to back at various locations. The leads of the strain gages were attached to a multichannel switching and balancing unit. The strain was measured by a standard Baldwin-Southwark Type K strain indicator.

The strain in a particular gage is obtained by subtracting the initial reading taken when the plate is standing free on its curved side and the final reading taken when the plate is clamped in the frame. The inplane strain is obtained by taking the average of the strains on both sides of the plate at a particular point.

In each case the radius of curvature was determined by tracing the outline of the plate on a piece of paper. As the surface is approximately cylindrical, the outline is approximately circular. Thus by drawing several chords of the arc and finding the intersection of the perpendicular bisectors of these chords, the radius of curvature is determined.

The tests on the two brass plates did not produce consistent results. A review of the literature of the Baldwin-Southwark Company showed that bonding of paper backed strain gages on brass is usually poor. This probably explains the inconsistent readings. However, the results of these tests did indicate that inplane strains are produced in such a process and the inplane strains in the direction of the buckling are negligible compared to the inplane strains in the perpendicular direction.

The aluminum plate tested in the first series was a 14 inch by 19 1/4 inch 24 - ST alloy plate with a thickness of .020 inch. Ten SR-4 type A-1, and two type A-5 strain gages were mounted at the position shown in Fig. 6. The test results are presented in Table 2.

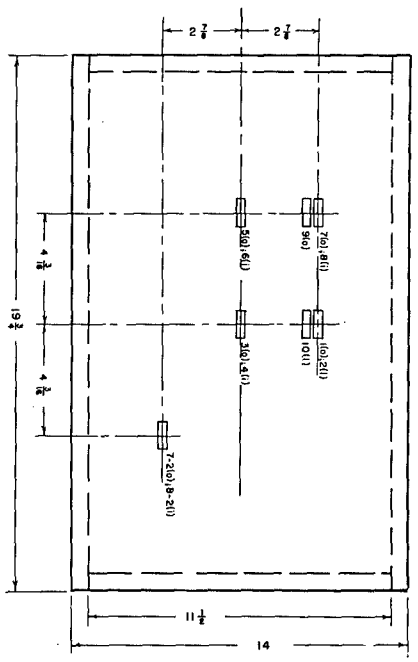

Location of Strain Gages on .020 Aluminum Plate

Fig. 6

As indicated, the first two tests were performed with gages 1 through 8 only. Since the inplane strains are not entirely as expected, it was decided to investigate the strain distribution over the top and bottom surfaces as each of them should be smooth and continuous. An investigation of the data of Table 2 reveals that on the top surfaces (gages 1,3,5,7) all gages except 7 yields a smooth distribution of strain. A similar conclusion is obtained for gage 2 on the bottom surface. It was therefore decided to mount gage 9 immediately adjacent to gage 7 and gage 10 immediately adjacent to 2. Gages 7-2 and 8-2 (see Fig. 6) were attached for checking purposes.

From the results of test 3, it is seen that by employing gages 9 and 10 instead of 7 and 2 a smooth strain distribution is obtained. By extrapolating, the values shown in Table 5 under "Test 3 (using correction)" are obtained. By comparing the axial strain at 7-2, 8-2 with 7,8, the rough extrapolations are probably somewhat in error. On a conservative basis the following inplane strains were assumed. These values will be used in calculating the buckling load.

Position	Inplane strains ($\times 10^6$)
3,4	60
5,6	80
1,2	10
7,8	15

In the second series, four aluminum plates of the size of (and including) the aluminum plates described in the preceding section were tested. The locations of the strain gages for three plates (namely one each of .032, .040, and .051 inch thickness), are shown in Fig. 4, while for the remaining test (on a .040 plate) are shown in Fig. 5.

In this series of tests the zero readings were taken with the plates standing on its curved (shorter) edge, and with and without the bars attached to the longer edges. The reason for taking zero readings with bars attached to the longer edges was to force these edges to be straight, which they would have been had adequate means been available for cold rolling the plates. The data taken for the five tests are shown in Tables 3 through 10. Note that in some cases the tests were repeated on the plates several times.

In the case of the .040 aluminum plate whose data is recorded in Table 10 many of the readings should be identical and this property of symmetry was used in analyzing the data to eliminate any unreasonable data. This analysis is shown in Figs. 7a and b where the observed data and the derived averages are indicated.

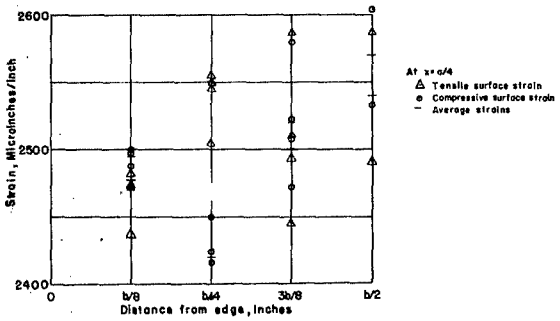

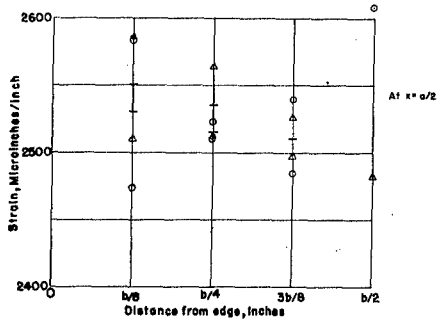

Graph Used for Averaging the Values of the .040 inch Aluminum Plate

Fig. 7a

Fig. 7b

Using Fig. 7a and b to arrive at a "reasonable "estimate for the membrane strains of the plate in the x-direction for the upper left (of Fig. 5) quadrant we obtain the values listed in Table 11. Similarly in the cases of the other plates referring to Fig. 5 we find because of symmetry; the membrane strains as listed in Table 12 through 14.

SECTION V

DETERMINATION OF THE BUCKLING LOAD BY FINITE DIFFERENCE APPROXIMATION

Assuming that the inplane stresses due to prestressing do not change while the buckling load is applied, the buckling load can be calculated by means of finite difference approximation. Two objections can be raised against such a procedure. First, since there are small initial deflections due to prestressing, the theoretical buckling load, which defines the stability limit, does not exist. Secondly, these inplane stresses due to prestressing, because of the initial deflections, certainly will change while the buckling load is applied. The excuse for using such a procedure to calculate the buckling load is as follows. Although the theoretical buckling load is not defined for a plate with initial deflections, the load for such a plate at which the deflections suddenly become large is close to the buckling load for the corresponding plate without initial deflections. Although the change in the inplane stresses due to prestressing while the buckling load is applied may introduce large errors in the calculation, in the absence of a better method, it is felt that the present method will at least give some qualitative results to compare with the experimental results described in the next section.

The differential equation governing the deflection of a thin plate with inplane forces N_x, N_y and N_{xy} is

$$\nabla^4 w = \frac{N_x}{D}\frac{\partial^2 w}{\partial x^2} + \frac{N_y}{D}\frac{\partial^2 w}{\partial y^2} + 2\frac{N_{xy}}{D}\frac{\partial^2 w}{\partial x \partial y} \qquad (1)$$

Let the plate be loaded in the y-direction only. Then $N_x = N_{x0}$, $N_y = N_{ycr} + N_{y0}$, $N_{xy} = N_{xy0}$ where the subscript 0 refers to the original inplane forces and the subscript cr refers to the buckling value.

Since $N_x = \sigma_x h$, $N_y = \sigma_y h$, $N_{xy} = \tau_{xy} h$, and from the preceding experiments it was found that $\varepsilon_{y0} = \tau_{xy0} = 0$, from Hooke's Law for plane stress we find

$$N_x = \frac{Eh}{1-\nu^2}\,\varepsilon_{x0}$$

$$N_y = N_{ycr} + \frac{\nu Eh}{1-\nu^2}\,\varepsilon_{x0}$$

$$N_{xy} = 0$$

Substituting into equation (1), we have

$$\nabla^4 w = \frac{12(1-\nu^2)}{Eh^3}\left\{\frac{Eh}{1-\nu^2}\,\varepsilon_{x0}\,\frac{\partial^2 w}{\partial x^2} + \left(N_{ycr} + \frac{\nu Eh}{1-\nu^2}\,\varepsilon_{x0}\right)\frac{\partial^2 w}{\partial y^2}\right\} \qquad (2)$$

It is convenient to put equation (2) in non-dimensional form by letting

$$w' = w/h, \quad N'_{ycr} = \frac{12(1-\nu^2)a^2}{Eh^3}\,N_{ycr} \quad x' = x/a$$

$$y' = y/a, \quad \varepsilon'_{x0} = \varepsilon_{x0}\,a^2/h^2$$

We have, therefore,

$$\nabla^4 w' - 12\,\varepsilon'_{x0}\,\frac{\partial^2 w'}{\partial x'^2} - (N'_{ycr} + 12\nu\,\varepsilon'_{y0})\,\frac{\partial^2 w'}{\partial y'^2} = 0 \qquad (3)$$

where ∇^4 is the biharmonic operator referring to the non-dimensional coordinates.

Let us now transform this equation into finite difference equations. Let the plate be divided into rectangular meshes with $\Delta y = k\Delta y$, where Δx and Δy are the sides of meshes. For the 19 1/4" x 14" .020" Aluminum alloy plate clamped by the 1 1/4" bars, the plate area is actually (19 1/4" - 2 1/2") x (14" - 2 1/2"). If we divide the plate as shown in Fig. 8, we have

$$y = b/4, \quad k = \frac{16.75}{11.5} = 1.457, \quad \nu = .3.$$

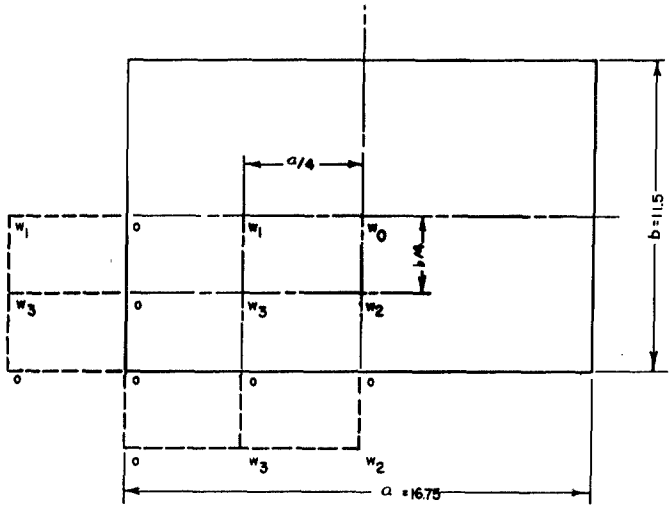

Net Points for Finite Difference Solution

Fig. 8

To approximate the boundary conditions more accurately, imaginary net points outside the plate are introduced. From the boundary conditions, they are equal to the values one mesh point inside the boundary as indicated in Fig. 8. The finite difference equations at various points are as follows:*

At w_0:

$$(177.7+18.52\ \varepsilon'_{x0}+2N'_{ycr})w_0-2(44.4+5.66\ \varepsilon'_{x0})w_1$$

$$-2(94.2+3.6\ \varepsilon'_{x0}+N'_{ycr})w_2+4(15.09)w_3 = 0 \qquad (4)$$

At w_1:

$$(177.7+18.52\ \varepsilon'_{x1}+2N'_{ycr})w_1+2(3.56)w_1$$

$$-(44.4+5.66\ \varepsilon'_{x1})w_0+2(15.09)w_2-2(94.2+3.6\ \varepsilon'_{x1}+N'_{ycr})w_3+0 \qquad (5)$$

At w_2:

$$(177.7+18.52\ \varepsilon'_{x2}+2N'_{ycr})w_2+2(16.01)w_2$$

$$-(94.2+3.6\ \varepsilon'_{x2}+N'_{ycr})w_0-2(44.4+5.66\ \varepsilon'_{x2})w_3+2(15.09)w_1 \qquad (6)$$

At w_3:

$$(177.7+18.52\ \varepsilon'_{x3}+2N'_{ycr})w_3+2(16.01)w_3+2(3.56)w_3$$

$$-(94.2+3.6\ \varepsilon'_{x3}+N'_{ycr})w_1+15.09w_0-(44.4+5.66\ \varepsilon'_{x3})w_3 = 0 \qquad (7)$$

---

* The transformation of partial differential equation to finite difference equations can be found, for example, in "Applied Elasticity" by Chi-Teh Wang, McGraw-Hill Book Co., 1953, pp. 106-143.

where the w's at various mesh points are the non-dimensional deflections.

Using the results for the inplane stresses in the .020 inch thick aluminum plate found in the previous section, we have, using the notation of this section,

$$e'_{x0} = 20 \text{ micro-inches per inch}$$

$$e'_{x1} = 25 \quad " \quad " \quad " \quad "$$

$$e'_{x2} = 3 \quad " \quad " \quad " \quad "$$

$$e'_{x3} = 5 \quad " \quad " \quad " \quad "$$

The finite difference equations can be put in matrix notation as follows.

$$\left\{[A] + [B\ N_{ycr}]\right\}[w'] = 0 \qquad (8)$$

where

$$A = \begin{bmatrix} 548 & -315 & -332 & 60 \\ -196 & 648 & 30.2 & -368 \\ -103 & 30.2 & 265 & -123 \\ 15.1 & -112.2 & -72.7 & 309 \end{bmatrix}$$

$$B = \begin{bmatrix} 2 & 0 & -2 & 0 \\ 0 & 2 & 0 & -2 \\ -1 & 0 & 2 & 0 \\ 0 & -1 & 0 & 2 \end{bmatrix}$$

$$w' = \begin{bmatrix} w' \\ 0 \\ w'_1 \\ w'_2 \\ w'_3 \end{bmatrix}$$

Equation (8) can be rewritten in the following form

$$-\left[A^{-1}\right]\left[B\right]\left[w'\right] = \frac{1}{N_{ycr}}\left[w\right] \qquad (9)$$

which is the usual form in which a solution, by iteration, for the eigen values N_y will converge to the lowest eigen value N_{ycr}.

The inverse of A can be found (18) and is

$$\left[A^{-1}\right] = \begin{bmatrix} 3.396 & 2.078 & 5.069 & 3.832 \\ 1.274 & 2.737 & 2.370 & 3.955 \\ 1.502 & 1.038 & 6.507 & 3.533 \\ .6502 & 1.137 & 2.145 & 5.318 \end{bmatrix} (10^{-3}) \tag{10}$$

Iterating Eq. (9) according to Ref. (18) the non-dimensional buckling parameter N_{ycr} for the prestressed plate is found to be

$$N_{ycr} = -99.3 \tag{11}$$

while for the ordinary plate (setting all $\epsilon_x = 0$)

$$N'_{ycr} = -47.55 \tag{12}$$

Thus using the inplane stresses found in the previous section a solution by finite difference approximations shows that the buckling load can be increased about 109%.

SECTION VI

DETERMINATION OF THE BUCKLING LOAD BY ENERGY METHOD USING HARMONIC ANALYSIS OF THE TEST DATA

The finite difference method used in the previous section loses accuracy when used with only a few net points. As an alternative, the Rayleigh-Ritz method can be used in finding the buckling loads of the prestressed and non-prestressed plates. The assumed deflection will be represented in a Fourier series and it will be convenient to represent the inplane stresses found in the previous sections also by a Fourier Series.

The Rayleigh-Ritz method will be shown in more detail in Part II of this report dealing with the theoretical analysis and only the essential points of the method will be described in this section.

Let w be the lateral deflection of the plate due to buckling. In the case of a plate with clamped edges, the bending strain energy in the plate when buckling occurs is

$$U = \frac{D}{2} \iint_A \left(\frac{\partial^2 w}{\partial x^2} + \frac{\partial^2 w}{\partial y^2}\right)^2 dx\, dy \qquad (13)$$

where D is the flexural rigidity of the plate. The work done by the inplane forces is

$$W = \frac{1}{2} \iint \bar{N}_x \left(\frac{\partial w}{\partial x}\right)^2 + \bar{N}_y \left(\frac{\partial w}{\partial y}\right)^2 dx\, dy \qquad (14)$$

where $\bar{N}_x = N_{xO}$; $N_y \approx N_{ycr}$. In the above we have assumed that the contribution to the work by the original stresses in the y-direction and by the original shear streams is negligible. At buckling we have

$$U - W = 0 \qquad (15)$$

from which we obtain

$$N_{ycr} = \frac{U - \bar{W}}{T} \qquad (16)$$

where

$$T = \frac{1}{2} \iint \left(\frac{\partial w}{\partial y}\right)^2 dx\, dy$$

and

$$\bar{W} = W - N_{ycr}\, T = \frac{1}{2} \iint \bar{N}_x \left(\frac{\partial w}{\partial x}\right)^2 dx\, dy$$

It must be emphasized that the above relations are correct only if there were no initial deflections. With the presence of the initial deflections, the values of the inplane forces due to the prestressing will probably be changed when the load N_{ycr} is applied, and therefore the above method of calculation may induce an error which is not small.

The Rayleigh-Ritz method can be carried out as follows. First, the deflection w is assumed in the form of a series every term of which satisfies the boundary conditions, but with undetermined coefficients. Substitute the series into equation (15) and carry out the integration. Then minimize the resulting expression with respect to the undetermined coefficients. This yields a system of homogeneous equations involving the buckling load N_{ycr}. A non-trivial solution is obtained if we equate the undetermined coefficients of these parameters to zero, from which N_{ycr} is determined.

The boundary conditions will be satisfied if the deflection, w, is assumed in the following form:

$$w = \sin \frac{\pi x}{a} \sin \frac{\pi y}{b} \sum_{m=1}^{\infty} \sum_{n=1}^{\infty} w_{m,n} \sin \frac{m\pi x}{a} \sin \frac{n\pi y}{b} \qquad (17)$$

As in Part II, let us introduce a stress function, F, in the form

$$F = \sum_{p=0}^{\infty} \sum_{q=0}^{\infty} b_{p,q} \cos \frac{p\pi x}{a} \cos \frac{q\pi y}{b} \qquad (18)$$

where $b_{p,q} = \bar{K}_{p,q} E h^2$, and $\sigma_{x0} = \frac{N_{x0}}{h} = \frac{\partial^2 F}{\partial y^2}$.

The first step in this analysis is to determine the coefficients of the series (18) corresponding to the data found experimentally and described in the previous sections.

Since it was experimentally impossible to determine the strains at the edges of the plate we will make use of the fact that along cross section

$$\int N_{x0} \, dy = 0 \qquad (19)$$

which results from the fact that it is assumed that no traction forces exist at the boundaries. The coefficients of the series for the stress function will be derived by the method of collocation, which is best described by actually deriving the coefficients for a specific set of test data. The problem used for illustration purposes will be the same one that was solved by the finite difference method in the previous section.

The points at which the strains were taken will be numbered as is shown in Fig. 8 just as was done in the previous section. The values of the strain in micro-inches per inch will be rewritten for clarity.

Gage Position	Strain
0	60
1	80
2	10
3	15

Two series may be written one at the section $x = a/2$ (containing points 0 and 2) the other at the section $x = a/4$. Since $e_{x0}\,dy = 0$ then the series will contain only two terms each and be of the form

$$\text{at } x = a/2 \quad \varepsilon_{x0} = \alpha_2 \cos\frac{2\pi y}{b} + \alpha_4 \cos\frac{4\pi y}{b} \tag{20}$$

$$\text{at } x = a/4 \quad \varepsilon_{x0} = \beta_2 \cos\frac{2\pi y}{b} + \beta_4 \cos\frac{4\pi y}{b} \tag{21}$$

Using the formulas listed by Scarborough (7) in his section on Harmonic Analysis and making use of the fact that by virtue of (19) α_0 and β_0 must be identically zero. The values of the coefficients are found to be

$$\begin{aligned} \alpha_2 &= -70 & \alpha_4 &= -10 \\ \beta_2 &= -95 & \beta_4 &= -15 \end{aligned} \tag{22}$$

The required two dimensional series will be of the form

$$\varepsilon_{x0} = \cos\frac{2\pi y}{b}\left[a_{0,2}+a_{2,2}\cos\frac{2\pi x}{a}\right] + \cos\frac{4\pi y}{b}\left[a_{0,4}+a_{2,4}\cos\frac{2\pi x}{a}\right] \tag{23}$$

Then substituting (21) and (22) into (23) the following conditions are arrived at for the coefficients

$$\text{at } x = a/2 \quad a_{0,2}-a_{2,2} = -70 \qquad a_{0,4}-a_{2,4} = -10$$

$$\text{at } x = a/4 \quad a_{0,2} = -95 \qquad a_{0,4} = -15$$

Solving, we obtain

$$\begin{aligned} a_{0,2} &= -95 & a_{2,2} &= -25 \\ a_{0,4} &= -15 & a_{2,4} &= -5 \end{aligned}$$

Assuming that ε_{y0} 0, Hooke's law yields

$$\sigma_{x0} = \frac{E}{1-\nu^2}\,\varepsilon_{x0} \tag{24}$$

then using Eq. (18) to relate the stress function (and coefficients) to the membrane stresses we find

$$\frac{b^2E}{\pi^2(1-\nu^2)}\ \varepsilon_{x0} = -\Sigma\Sigma\, q^2\, b_{p,q} \cos\frac{p\pi x}{a} \cos\frac{q\pi y}{b} \qquad (25)$$

or

$$\frac{b^2}{h^2\pi^2(1-\nu^2)}\ \varepsilon_{x0} = -\Sigma\Sigma\, q^2\, \bar{K}_{p,q} \cos\frac{p\pi x}{a} \cos\frac{q\pi y}{b}$$

then

$$K_{p,q} = -\frac{b^2}{h^2\pi^2(1-\nu^2)}\ \frac{a_{p,q}}{q^2}\ x\ 10^{-6} \qquad (26)$$

(the factor of 10^{-6} appears as a conversion from micro-inches to inches) then

$$\begin{aligned} K_{0,2} &= .8835 & b_{0,2} &= .8835\ E\ h^2 \\ K_{2,2} &= .2325 & b_{2,2} &= .2325\ E\ h^2 \\ K_{0,4} &= .0349 & b_{0,4} &= .0349\ E\ h^2 \\ K_{2,4} &= .0116 & b_{2,4} &= .0116\ E\ h^2 \end{aligned} \qquad \text{or} \qquad (27)$$

Assuming the deflection w to be suitably represented by the series

$$w = \sin\frac{\pi x}{a} \sin^2\frac{\pi y}{b} \left\{ w_{1,1} \sin\frac{\pi x}{a} + w_{3,1} \sin\frac{3\pi x}{a} \right\} \qquad (28)$$

The strain energy is calculated according to Eq. (13) and found to be

$$U = \frac{D\pi^4}{128a^2} \left\{ 227.92 w_{1,1}^2 + 892.59 w_{3,1}^2 - 258.08 w_{1,1} w_{3,1} \right\} \qquad (29)$$

Calculating T according to Eq. (16) results in

$$T = -\frac{\pi^2}{128}\left\{17.484\, w_{1,1}^2 + 11.656\, w_{3,1}^2 - 11.656\, w_{1,1}w_{3,1}\right\}$$

and using the non-dimensional buckling parameter defined as

$$K = N_{ycr}\frac{a^2}{\pi^2 D}$$

$$N_{ycr}T = -\frac{D\pi^4 K}{128a^2}\left\{17.484\, w_{1,1}^2 + 11.656\, w_{3,1}^2 - 11.656\, w_{1,1}w_{3,1}\right\} \tag{30}$$

Thus the governing equation for the non-prestressed plate are

$$\frac{\partial(U-N_yT)}{\partial w_{1,1}} = 0 \quad \text{and} \quad \frac{\partial(U-N_yT)}{\partial w_{3,1}} = 0 \tag{31}$$

or

$$(455.84 + 34.968K)\, w_{1,1} - (258.08 + 11.656K)\, w_{3,1} = 0$$

and

$$(258.08 + 11.656K)\, w_{1,1} - (1785.18 + 23.312K)\, w_{3,1} = 0$$

Setting the determinant of the coefficients of these two equations equal to zero, the conditions for a non-trivial solution gives

$$K^2 + 98.680K + 1099.9 = 0 \tag{32}$$

from which we find

$$K = -12.81 \text{ or } -85.87$$

$$\text{or} \quad N_{ycr} = 12.81\frac{\pi^2 D}{a^2} \tag{33}$$

which agrees with the solution given by Timoshenko on p. 323 of Ref. (19).

From Eq. (16) W_x can be calculated and making use of the values for $b_{p,q}$ (27) is

$$\bar{W}_x = -\frac{D\pi^4}{128a^2}\left\{427.30\, w_{1,1}^2 + 1953.39\, w_{3,1}^2 - 1264.28\, w_{1,1}w_{3,1}\right\} \tag{34}$$

then minimizing the expression U-W the following two equations are arrived at

$$\frac{\partial(U-\bar{W}_x-N_yT)}{\partial w_{1,1}} = (1310.44 - 34.968K)\, w_{1,1} - (1522.36 - 11.656K)\, w_{3,1} = 0 \tag{35}$$

$$\frac{\partial(U-\bar{W}_x-N_yT)}{\partial w_{3,1}} = -(1522.36 - 11.656K)\, w_{1,1} + (5691.96 - 23.312K)\, w_{3,1} = 0$$

upon setting the determinant of the coefficients equal to zero the following quadratic equation is obtained:

$$K^2 + 285.73 + 7568.6 = 0 \tag{36}$$

yielding the solution

$$K = -29.545, -256.19$$

or

$$N_{ycr} = -29.545\,\frac{\pi^2 D}{a^2} \tag{37}$$

Thus on the basis of the Rayleigh-Ritz analysis we may conclude that the stresses occurring in the .020 inch thick plate because of the pre-stressing procedure will increase the buckling load approximately 130%.

A similar set of calculations can be performed for the second .040 inch thick plate, the data for which is listed in Table 10. In this case it is found that the prestressed plate will buckle symmetrically in three half-waves even though the non-prestressed plate buckles anti-symmetrically in two half-waves.

Assuming the deflection w to be suitably represented by the series

$$w = \sin\frac{\pi x}{a}\sin\frac{\pi y}{b}\sin\frac{2\pi y}{b}\left\{w_{1,2}\sin\frac{\pi x}{a} + w_{3,2}\sin\frac{3\pi x}{a}\right\} \qquad (38)$$

the buckling load for the non-prestressed plate is found to be

$$N_{ycr} = -8.38\frac{\pi^2 D}{a^2} \qquad (39)$$

which is within 0.6% of the accepted value listed in Reference (12).

For the prestressed plate with the same assumed deflection the buckling load is

$$N_{ycr} = -11.63\frac{\pi^2 D}{a^2}$$

If however, for this same prestressed plate the deflection is assumed to be suitably represented by the series

$$w = \sin\frac{\pi x}{a}\sin\frac{\pi y}{b}\sin\frac{3\pi y}{b}\left\{w_{1,3}\sin\frac{\pi x}{a} + w_{3,3}\sin\frac{3\pi x}{a}\right\} \qquad (40)$$

the buckling load for the prestressed plate is found to be

$$N_{ycr} = -10.04\frac{\pi^2 D}{a^2} \qquad (41)$$

Thus in the case of the .040 inch plate whose data is described in Table 10 the plate will buckle symmetrically in three half-waves at a load 19.8% above that of the non-prestressed plate.

Similarly using the data for the .032 inch thick plate whose data is listed in Table 12 it is found that this plate will also buckle symmetrically into three half-waves.

For the deflection w assumed as the series (40) the buckling load is:

$$N_{ycr} = -9.47 \frac{\pi^2 D}{a^2} \qquad (42)$$

while if assumed as the anti-symmetric series (38) it is

$$N_{ycr} = -11.12 \frac{\pi^2 D}{a^2}$$

Thus in the case of the .032 inch plate a symmetric buckling mode of three half-waves occurrs at a load 13% above that of the non-prestressed plate.

SECTION VII

BUCKLING LOADS FOR PLATES WITH INITIAL IMPERFECTIONS

Before proceeding to describe the experiments for the determination of buckling loads for the non-prestressed flat plates as well as the prestressed plates, it seems desirable to review the existing methods for experimentally determining the buckling loads for plates with initial imperfections.

The three most common methods for determining the buckling load from experimental methods are the top of the knee method, the strain reversal method, and by Southwell's plot.

In the "top of the knee method", the buckling stress is taken as the stress corresponding to the top of the knee of a curve of load versus the lateral deflection. If the lateral deflection cannot be readily measured, any other quantity that increases in substantially the same manner as the lateral deflections may be plotted instead. One such quantity is, $\varepsilon_1 - \varepsilon_2$, the difference of strains, in the direction of

loading, on the two sides of the "buckle crest". The method is illustrated in Fig. 9 and the buckling loads obtained by the "top of the knee method" are indicated on the curves by small circles for three different amounts of initial imperfections. It should be noted that the larger the initial imperfections the more difficult it is to judge the "top of the knee" and consequently the buckling load.

The "strain reversal method" is best explained with the use of Fig. 10 which shows the variation of strain, ε, at opposite faces of the plate. As in Fig. 9 the method is illustrated for three different amount of initial deflections and the critical stresses found by this method are indicated by small circles. The innermost curve represents a perfect plate. The strains are elongations (or contractions) which could be found by the application of electric strain gages on opposite faces of the plate at one of the expected crests of the buckling mode. Before buckling the plate is under a uniform compression and both gages are under the same strain depending only upon the load and the Modulus of Elasticity. At the buckling load the initially perfect plate suddenly deforms thus adding to the compressive strain in the gage applied to the concave face while imposing a tensile strain (thus decreasing the compressive strain) in the gage applied to the convex face of the plate. The critical load is based on the above behavior of the perfect plate and is consequently defined as the load at which the extreme fibre strain, ε_2, on the convex side of the buckle crest stops increasing and begins to decrease. It can be seen from Fig. 10 that again the larger the initial imperfections the more difficult it is to choose the critical load.

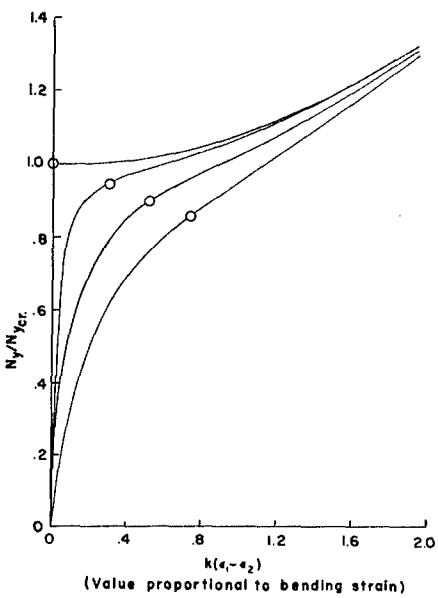

Top of Knee Method

Fig. 9

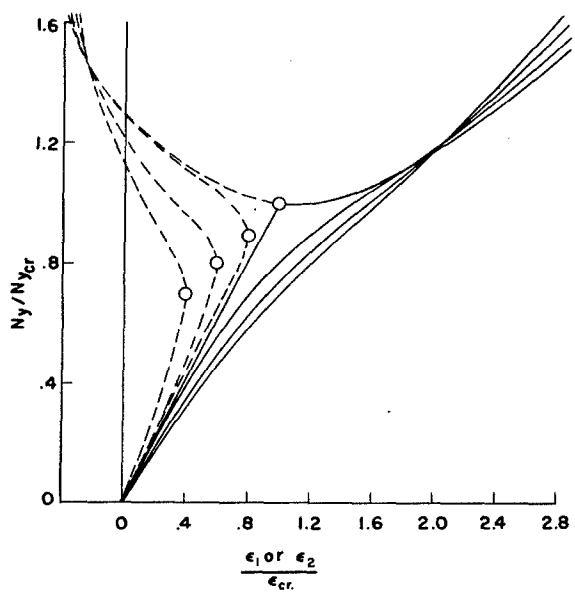

Strain Reversal Method

Fig. 10

Southwell's method has found universal acceptance in determining the buckling load of columns but has been unsatisfactory in the case of plates whose lateral motion is restrained at all four edges. In brief, Southwell's method depends on the linear relationship between the deflection of the structure and the ratio between the deflection and load, σ/P. The slope of the straight line plotted with these coordinates in the theoretical buckling load. Southwell (8) showed that there is a identifiable straight line for slender columns while Donnell (9) and Hu(10) have shown that the linear relationship will not exist as long as there are extensional strains present during the buckling process. Donnell (9) has further shown that these extensional strains do exist in the case of a simply supported plate whenever the sum of the initial imperfection and the deflections due to the load P are of the order of the plate thickness, as is usually the case.

Because of the relatively large initial deformations present in the prestressed plates the three commonly used methods for experimentally determining the buckling load mentioned above are found to be very difficult to use. For this reason a method developed by Yoshiki (11) is tried in the determination of the buckling load of the plates in this investigation.

Yoshiki's method is based upon the fact that after buckling the deflection of a theoretically perfect plate is proportional to the square of the load and therefore the load versus deflections curve is a parabola. This parabola is shown in Fig. 9 for a plate with no initial imperfections and it can be seen from the figure, that for plates with initial imperfections, these curves are assymptotic at large deflections.

When the load is plotted against the square of the deflection, or any other quantity varying in substantially the same manner, the post buckling curve will be as straight line intersecting the vertical axis of the buckling load. In Fig. 11 we have plotted the same lines as were plotted in Fig. 9 but now $(\varepsilon_1 - \varepsilon_2)2$ was used as the abscissa instead of $(\varepsilon_1 - \varepsilon_2)$. A theoretical analysis demonstrating the parabolic post buckling behavior of clamped plates is carried out in Appendix A.

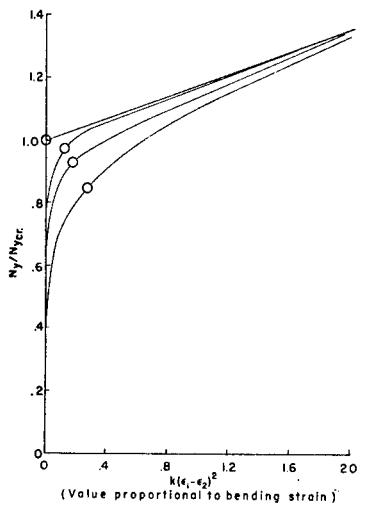

Yoshiki's Method

Fig. 11

SECTION VIII

TESTS TO DETERMINE THE BUCKLING LOADS

Having shown the probability of raising the buckling load by prestressing, and also that the prestressing caused no objectionable initial deflections, a testing program was initiated for the purpose of actually measuring the buckling load of prestressed and non-prestressed flat plates. It was recognized that the desired buckling frame should have the following properties:

1. The deflections at the edge of the plate should be zero.
2. The slope of the plate at the edges should be zero.
3. The stringers (side supports) should be flexible in order that they transmit no load.
4. The load should be applied uniformly to the ends of the plate.

The stringers designed for the testing program are shown in Figs. 12 and 13. The plate is clamped between the cantilevered "fingers" (shown in Fig. 13) which are formed at the end of the [illegible] wide roots. Since the width to depth ratio of these thin roots is about 20:1 the rigidity ratio of the cantilever beams is about 400:1. As a consequence of this high "rigidity ratio" the stringers are very flexible in the direction of the applied load and yet possesses a great deal of lateral and rotational rigidity.

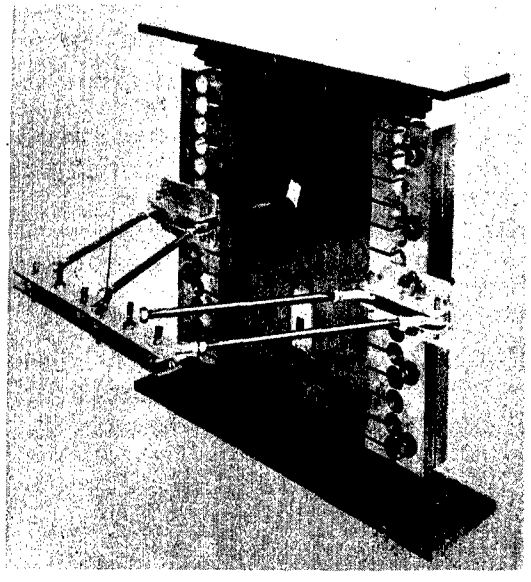

General View of Buckling Jig

Fig. 12

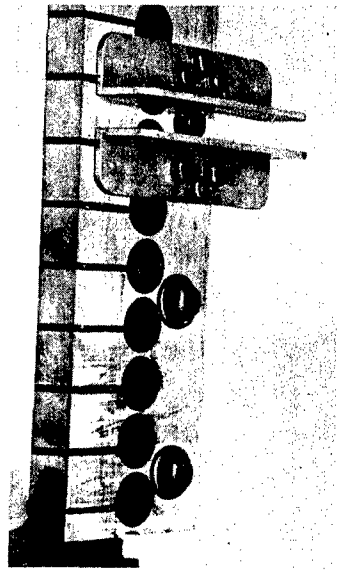

Detailed View of Stringers

Fig. 13

The flexibility of the cantilevered "fingers" reduces to a minimum the applied load being transmitted by the stringers while their lateral rigidity will produce almost zero displacement. To produce the condition that the edges of the plate will have nearly zero slopes, a four bar linkage was designed which is shown in Figs. 12 and 14. The two stringers are attached to the rod end bearings at the ends of each pair of rods shown in Fig. 14 in a manner as shown in Fig. 12. Thus they complete two similar parallelograms each of which has a cooresponding side along a common line. By thus restraining one side to a common line the opposite sides, which are the stringers, are restrained so as to always be parallel to each other although there is no other restriction on their relation rotational motion.

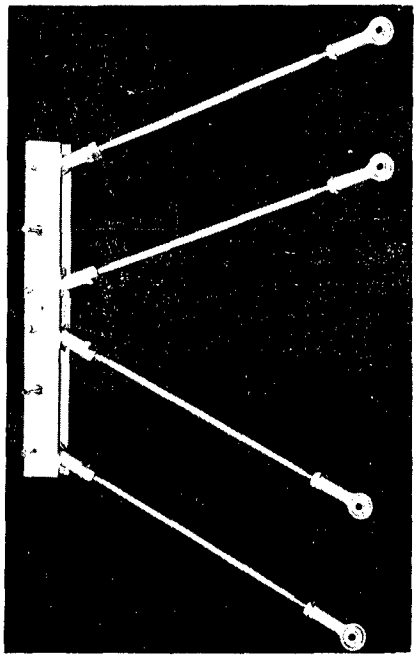

Detailed View of Four Bar Linkage

Fig. 14

In order to ensure that the four bar linkage did not restrain the movement of the plate in the direction perpendicular to the applied load (the x-direction as defined by Fig. 1) electric strain gages were placed on the plate to measure these inplane strains. The test showed that the linkage offered no restraint to the expansion (or contraction) of the plate.

The actual testing of prestressed plates was carried out in the following manner:

The side edges were clamped between the stringers and the plate flattened by moments applied to the stringers by means of monkey wrenches. The four bar linkage was then attached to the stringers thus forcing the stringers and plate to lie in a plane after removing the wrenches. The ends of the plate were then inserted between the steel angles, attached to the end plates, and firmly bolted into position. The turnbuckle connecting the end plates, was then tightened until the end plates were parallel.

The lower end plate rested on the base of the testing machine while the upper end plate was loaded through a round swivel block attached to the measuring head of the machine. The swivel head was adjusted so as to be parallel to the upper base plate of the testing jig.

It was found that if the steel angles (see Fig. 12) were clamped very tightly to the ends of the plate the friction between the angles and the plate would transmit the load uniformly from the end plates to the plate under test. This information enabled us to forego any more elaborate method of transmitting the load to the plate.

The plate was loaded to about one half the expected buckling load and then unloaded to twenty pounds to insure the proper seating of the plate in the testing jig. The strain gage indicator was then zeroed and the test begun. The two sets of strain gages were read alternately at fifty pound loading increments.

The loads measured during the tests were the total loads applied to the testing jig, that is, the sum of the loads applied to the free plate, the part of the plate supported between the stringers, and the stringers themselves. This latter part of the load should be negligible as the stringers were designed to be flexible in the direction of application of the load. The load going down the supported edge strips were, however, not negligible and were found both experimentally and analytically.

The experimental investigation of the load carried by the supported edge strip was carried out by testing .040 in. non-prestressed flat plates of the same dimensions as the prestressed plates but with four different widths of supported strips. The normal testing procedure had a one inch edge strip supported by the stringers while, in addition, for calibration purposes, tests were run with 1/2 in., 3/4 in., and 1 1/4 in. strips supported by the stringers.

In one series of tests the plates were cut to size so as to have a 1 1/4 inch strip supported by each stringer and then repeatedly trimmed down in width so as to have different widths of supported edge strips. The results of these tests are shown in Table 15.

In some cases, it was observed that the buckling load for plates with stringer grip of 1 1/4 in. buckled at a lower load than plates with 1 in. grip. The cause of these seemingly peculiar results is probably due to the variation of boundary conditions, with the width of the stringer grip, and with each test.

In another series of tests the plates were not retested but instead the plates were originally cut to sizes for testing the four different widths, 1/2, 3/4, 1, and 1 1/4 inches. The results of these tests are shown in Tables 16, 17, 18, and 19.

The results of Tables 16, 17, 18, and 19 are shown graphically in Fig. 15. Each buckling load (found by Yoshiki's method) is shown in addition to their averages shown for each initial radius of curvature. Two curves marked experimental are shown. They are straight lines drawn through the experimental values by the method of least squares. For one line, indicated by "Experimental (1/2 - 1 1/4)", a least square "average" is drawn through all the points; while for the other, indicated by "Experimental (3/4 - 1 1/4)", the points for 1/2 inch width of plate supported between each of the stringers are omitted. The results of the 1/2 inch supported width tests are omitted in this one case since it is felt that the clamping is too weak to approximate the clamped edge condition. It can be seen in Fig. 15 that the straight line found using the 1/2 inch supported width gives a "zero width" buckling load about 115 lbs. lower than that found omitting the 1/2 inch width and about 70 lbs. less than that for the ideal theoretical plate.

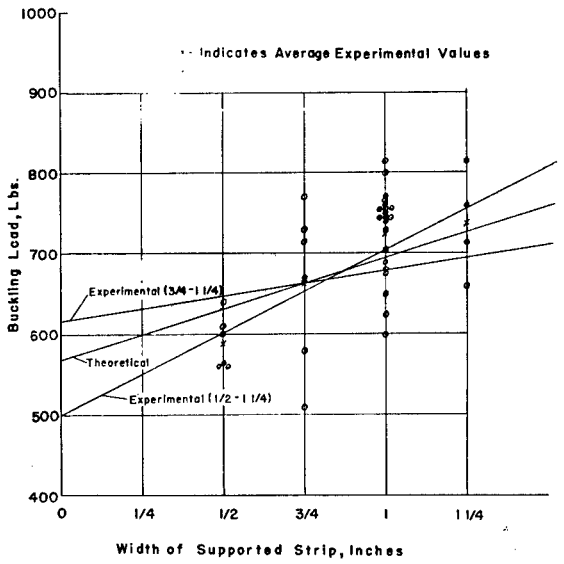

Stringer Calibration Tests
(.040 Aluminum Plates)

Fig. 15

Since it can be seen that the line representing the buckling loads of the theoretical plate falls well within all the experimental points (except perhaps the ones tested with 1/2 inch supported edges) this "theoretical" line will be used for calibration purposes.

The line labeled theoretical is obtained by assuming that supported edge strips undergo the same total compression as an ideal plate would at the inception of buckling. Then the load per unit length carried by the edge strip will be equal to the buckling load per unit length of the plate. S. Levy (12) has found this for aspect ratio 3:2 to be:

$$N_y = 8.33 \frac{\pi^2 D}{a^2}$$

where $h = .040$, $a = 9$, $\nu^2 = .1$, and $E = 10.5 \times 10^6$ psi

$$N_y = 63.2 \text{ lb./in.}$$

Thus the buckling load for our plate with a = 9 in. is 569 lbs. and for strips of the widths tested are shown in Table 20. Table 20 is calculated by multiplying the buckling load per unit length by the width of the supported strip.

Now, if each of these values are added to the buckling load of the theoretical plate (569 lbs.) the values of the buckling loads for theoretical plates with the various supported widths (stringer grips) are obtained. These are the values that determine the plot labeled "theoretical".

Very close agreement between the "theoretical" and the experimental curve can not be expected since the calculations of the "theoretical" curve in no way takes into account the variation of degree of clamping with the different widths of stringer grips; and in an actual plate the end shortening will be greater than in the theoretical case. Therefore a larger load will be carried by the supported strips than originally computed. Moreover, no account has been taken of load carried by the stringers. From these considerations, the experimentally determined buckling loads will be larger than those calculated from theory.

Nevertheless, in spite of those objections, the plot of Fig. 15 still gives a reasonable indication of the degree of clamping that is attained by the buckling jig.

Having shown that, after accounting for the load transmitted by the strip of plate clamped between the stringers, the buckling loads are close to the values computed from the accepted theory, the program of testing prestressed plates was begun and is described in the following paragraphs.

Because of the unsymmetrical buckling of prestressed plate two sets of strain gages were used in order to increase the likliehood of the gages being at the crest of the buckling modes.

The results of testing of non-prestressed flat plates were very consistent and the results of a representative test is shown in Fig. 16. Both $(\epsilon_1-\epsilon_2)$ and $(\epsilon_1-\epsilon_2)^2$ are plotted and since these are proportional to deflection and the square of deflection respectively the methods previously described may be used in determining the buckling load. The plate shown is numbered F40-1, 5-11 where F indicates that it was an non-prestressed flat plate (prestressed plates are indicated by the letter C), the first set of numbers indicates the plate thickness to be .040 inches, the second set of numbers indicates that the aspect ratio was

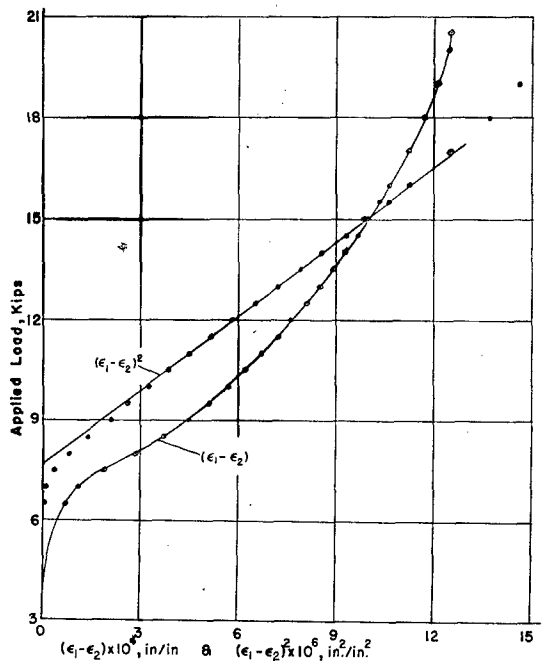

Typical Load-Deflection Diagram for Ordinary Flat Plate

Fig. 16

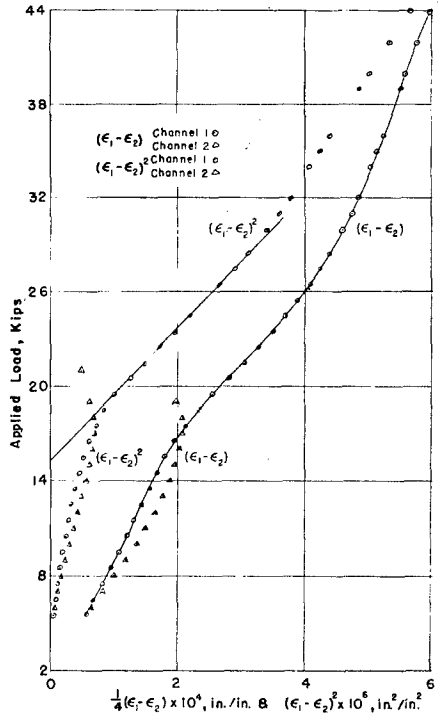

"Normal" Type Buckling of Prestressed Plate

Fig. 17

1.5, while the third series of numbers indicates that this was the eleventh plate of this type tested.

The plots of the test data of prestressed flat plates were of three general types shown in Figs. 17, 18, and 19. The curves of Fig. 17 are what will be called the "normal" type, that is, they are of the type expected theoretically. The curves of Fig. 18 will be called the "double parabola" type in that the post buckling behavior is characterized by two parabolas, instead of one. Thus if plates of the "double parabola" type are analyzed by means of the $(\epsilon_1-\epsilon_2)^2$ plot there will result two different buckling loads corresponding to the two parabolic post buckling behaviors of the plate. The significance of these two parabolas is not obvious, and is a puzzling characteristic of prestressed plates. The curves of Fig. 19 will be called the "mode jump" type, that is, they occur when the plate buckling form changes suddenly during the test. The change is from two half-waves to three half-waves and is sometimes so sudden as to be accompanied by a loud popping sound.

Flat plates with an aspect (length to width) ratio of 1.5 should, according to theory, buckle in two half waves. It is felt that initial imperfections are a major cause for the formation of three wave form. If the plates had longitudinal initial deflections of the form shown in Fig. 20a which is shown to be the case for prestressed plates (see Fig. 20), the plate could be forced to buckle into three instead of two half waves.

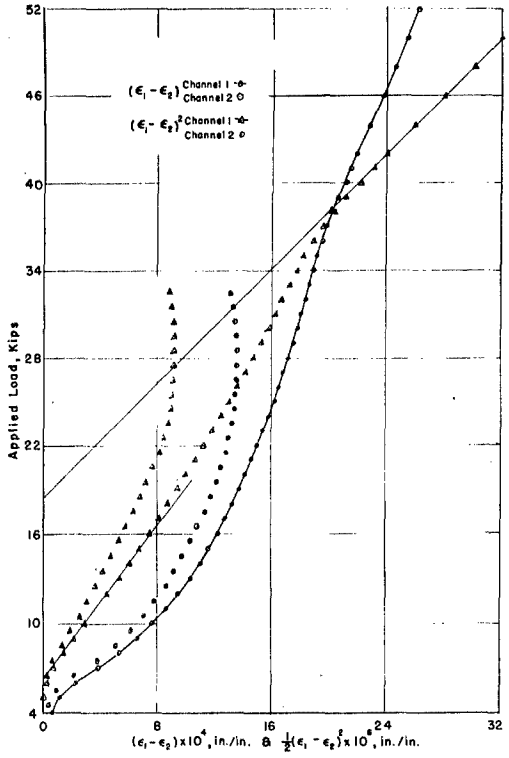

"Double Parabola" Type of Buckling of Prestressed Plate

Fig. 18

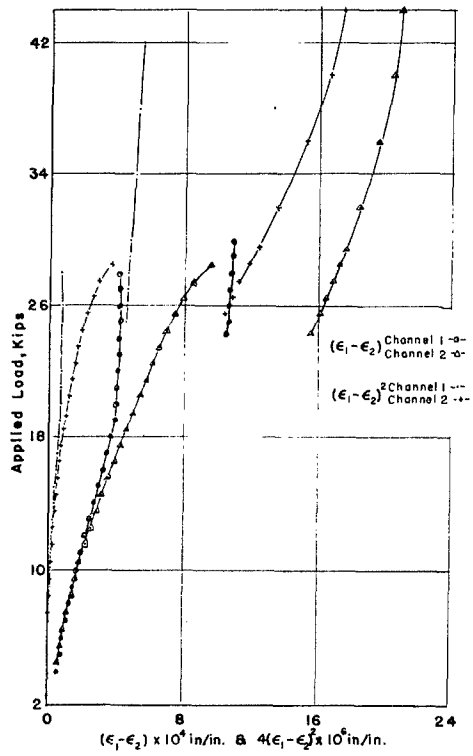

"Mode Jump" Type of Buckling of Prestressed Plate

Fig. 19

The hypothesis can be visualized with the help of Fig. 20. If the initial deflections of one half wave shown in Fig. 20a are added to the usual buckling form of two waves shown in Fig. 20b, an unsymmetrical two wave form, shown in Fig. 20c, results. This wave form is actually a characteristic of the prestressed plates. It is possible that the longer half wave of Fig. 20c becomes unstable and this buckles into two more waves giving a total of three half waves shown in Fig. 20d.

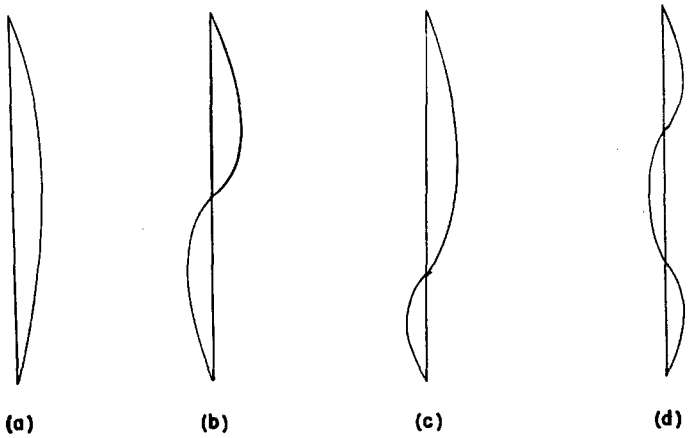

Effect of Initial Deflections on Buckling Mode

Fig. 20

The above hypothesis, although conjectural, is somewhat substantiated by experience with non-prestressed flat plates. During the testing of non-prestressed flat plates it was observed that the plates "popping" into three waves were those with the largest initial deformations in the form of one wave. After noticing this the testing of non-prestressed plates were restricted to those that appeared, to the naked eye, to be flat. Thereafter, no trouble was encountered with this "popping" phenomenon. Unfortunately, initial deflections are inherent in the prestressing process, thus necessitating a larger number of tests to compensate for the tests discarded because of "popping".

Another possibility for explaining this "popping" is the formation of inplane stresses that would be of such a nature as to cause the plate to buckle into three half-waves. The probability of this hypothesis being a major factor is strengthened considerably by the results of the Rayleigh-Ritz analises shown in the previous section.

It was shown that for some stress distributions occurring during the prestressing process (particularly that found by the experiments performed on the second .040 inch thick Aluminum plate) the plate will buckle into three half-waves. In some plates (particularly the .020 inch thick aluminum plate) the energy level at which the plate will buckle is very nearly the same for the symmetric or antisymmetric modes of failure. It was also shown that there is a wide scattering in the stress distribution found experimentally. Since there will also be some variation in the degree of clamping at the boundaries and some non-homogeneity of the plate and also since the prestress distribution will vary somewhat upon deflecting under the applied buckling load it is quite likely that in some cases a plate will buckle in two half-waves while in other cases an apparently similar plate will buckle in three half-waves.

The results of buckling tests performed on non-prestressed flat plates of .040, .032, and .051 inch thickness are shown in Tables 18, 21, and 22, respectivley. The results of buckling tests performed on prestressed plates of thicknesses of .040, .032, .051 inches are shown in Tables 23, 24, and 25, respectively.

The results of the buckling tests performed on non-prestressed flat plates of .032 and .051 inch thicknesses which were listed in Tables 21 and 22 are shown graphically in Figures 21 and 22 respectively. These figures are similar to Fig. 15 which showed the tests of .040 non-prestressed flat plate tests for calibration purposes.

Since the calibration tests showed that very good results were obtained by assuming that the supported edge strips undergo the same total compression as an ideal plate would, the calibration tests were dispensed with in the case of plates of .032 and .051 inch thicknesses.

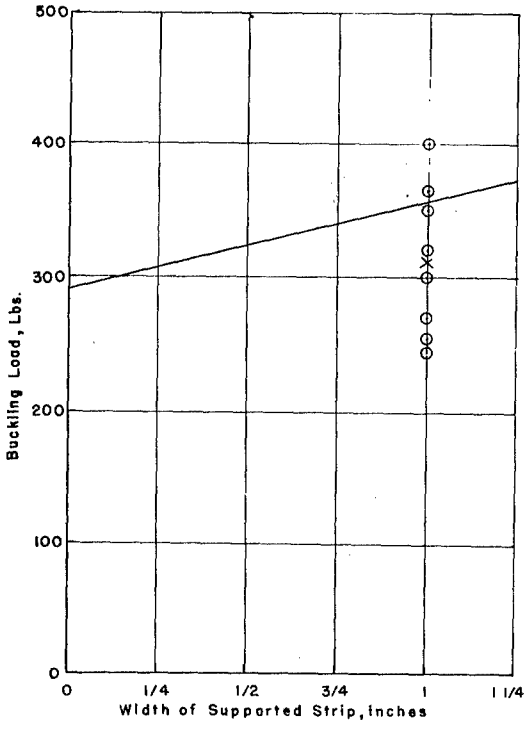

.032 Ordinary Flat Plate Tests

Fig. 21

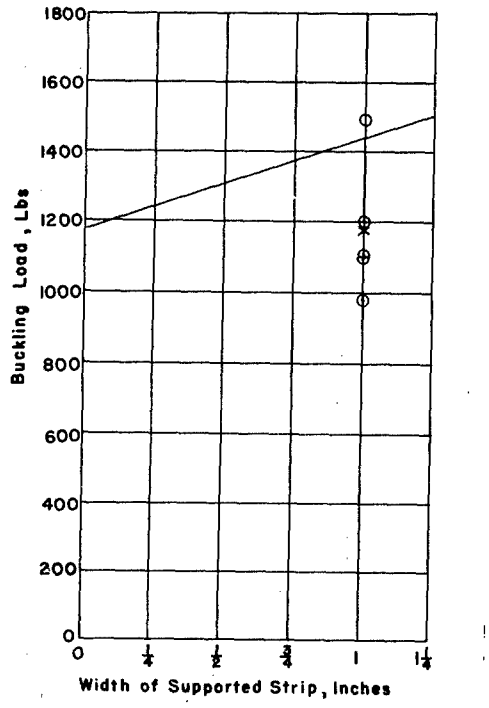

.051 Ordinary Flat Plate Tests

Fig. 22

The theoretical buckling loads of .032 and .051 inch thick non-prestressed flat plates with different widths of supported edge strips are shown in Figs. 21 and 22 along with the experimentally determined values (by Yoshiki's method). The theory indicates that for .032, .040, and .051 inch plates the load supported by the 1 inch supported strips at both edges will be 63, 126, and 262 pounds respectively.

Making use of these values and subtracting them from the loads listed in Tables 23, 24, and 25 (and shown graphically in Figs. 23, 24, and 25) the net buckling loads were determined. The average experimental "total" buckling loads are listed in Tables 26, 27, and 28 for the .040, .032, and .051 inch thick prestressed plates respectively while the net loads are listed in Table 29.

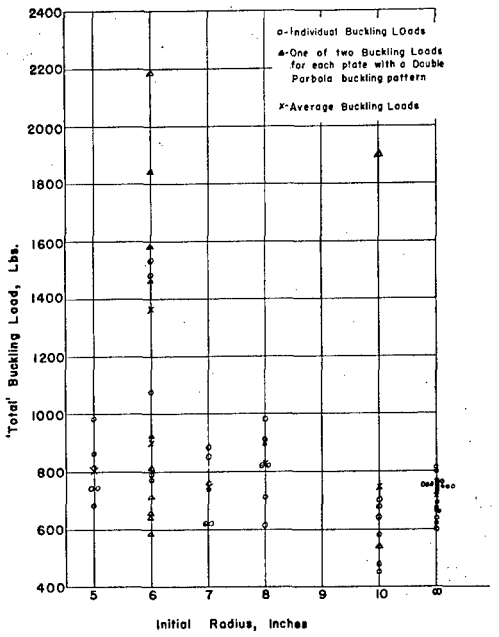

Buckling Loads of .040 Prestressed Flat Plates

Fig. 23

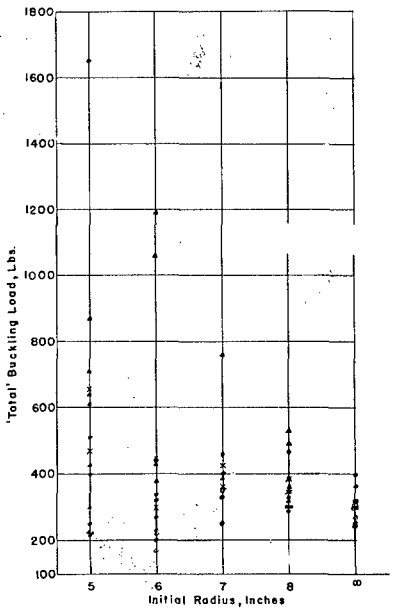

Buckling Loads of .032 Prestressed Flat Plates

Fig. 24

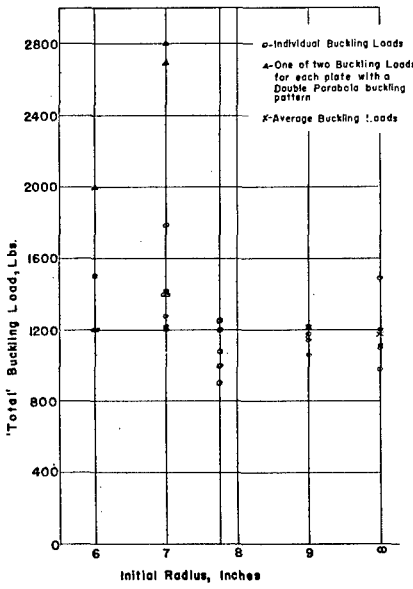

Buckling Loads of .051 Prestressed Flat Plates

Fig. 25

From the data listed in the above tables, it is felt that Yoshiki's method, though convenient to use for non-prestressed plates, may not be applicable to the prestressed plates as indicated by the occurrence of double parabola in the plate. As a result, the top of the knee method was used. The buckling loads thus determined indicate the loads at which the deflections suddenly become large. The net loads supported by the "free" plate are listed in Table 29 together with their percentage increases over the buckling loads of the corresponding non-prestressed plates, both measured by the top of knee method. For purpose of comparison, the values determined by Yoshiki's method are given in the parentheses after the net buckling loads in Table 29.

SECTION IX

Remarks on the "Buckling" Criteria

The current methods of testing make use of the form of the Load-strain diagram rather than the actual values of the deflections in the diagram. These methods all have as a basis the load-strain relations existing in a theoretically flat plate which does not deflect until the buckling load is reached at which point the deflections suddenly occurs. The actual plate with initial deflections, does not exhibit this sudden increase in deflection and in fact in some cases the evidences of the behavior of the ideal plate is indiscernable. As was mentioned in the Introduction, a factor of major significance is the ratio of plate deflection to applied load. It can be seen from Fig. 26 that a lower value of this ratio does not necessarily occur with a higher buckling load of the equivalent ideal plate. In this figure two Load - deflection diagrams are shown along with their extensions (shown by dashed lines) which would represent the diagram of the equivalent ideal plate. The intersection of this dashed line with the ordinate is the buckling load which all of the measuring methods attempt to find. It can be seen, however, that in the case shown the plate with the highest theoretical buckling load also has the largest deflection to load ratio, a distinctly undesirable characteristic.

Because of the relatively large deflections inherent in prestressed plates the importance of low values of Deflection to Load ratios is especially important. It is felt that the "buckling load" in such a case should be defined as the load at which the maximum deflection in the plate reaches a certain prescribed value. Further research on prestressed plates with this new "buckling" criteria would seem to be of great value.

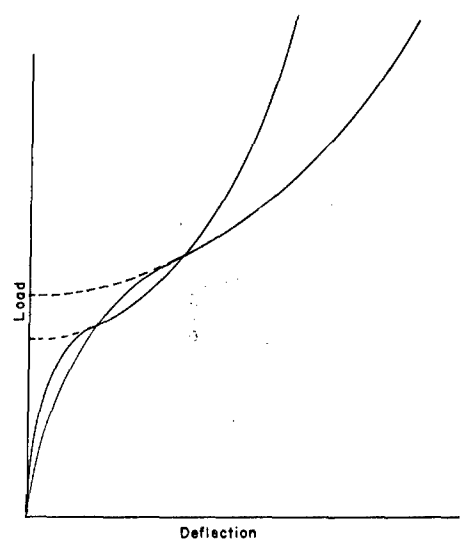

Illustration of Buckling Criterias

Fig. 26

SECTION X

FORMULATION OF THE PROBLEM

The theoretical treatment of the problem consists of two parts. First, it is necessary to find the inplane stresses induced in the plate due to the clamping of a curved plate into a flat frame. Next, with these inplane stresses determined, the buckling load will be calculated for a flat plate with such initial stresses.

The first problem can be formulated by considering the process of clamping the curved plate into a flat frame to occur in three steps. First, the cylindrically curved plate is bent into an identically flat form by pure moments applied at the edge. Secondly, the edges of the plate in this identically flat form, will be clamped. Note that the clamping will induce no additional deflections or stresses.

Thirdly, the pure moments applied in step one will be removed by the application of equal and opposite moments thus leaving the clamping action at the edges as the only restraining force on the plate.

It may be pointed out that initial bending stresses do not affect the buckling load of plates but inplane (or membrane) stresses do. Since the first step produces only pure bending stresses and the second step induces no stresses in the plate, our analysis will be concerned exclusively in analyzing the deflections and stresses induced by the loadings of the third step. This analysis will yield the deflections and inplane stresses ocurring when a cylindrically curved plate is clamped into a flat frame.

The problem of determining the buckling load for a prestressed flat plate problem can be solved by the use of the Rayleigh-Ritz energy method. In using the energy method, it will be assumed that when buckling occurs these inplane stresses will remain unchanged.

SECTION XI

BENDING OF A CYLINDRICALLY CURVED PLATE INTO FLAT FORM

If the curved plate originally is in the form of a cylindrical surface, it is possible to bend it into an identically flat form by inextensional bending. This is because both the cylindrical and flat surfaces are developable surfaces. The problem of bending one developable surface into another one can be found in many texts on Elasticity, for example, ref. 13. The edge moments necessary to bend such a plate (Fig. 27) are

$$M_x = D\left(\frac{1}{R_x} + \nu \frac{1}{R_y}\right) \tag{43}$$

$$M_y = D\left(\frac{1}{R_y} + \nu \frac{1}{R_x}\right) \tag{44}$$

where $\frac{1}{R_x}$ and $\frac{1}{R_y}$ are the changes in curvature. In our case $\frac{1}{R_x} = 0$ and $\frac{1}{R_y} = \frac{1}{R}$. Thus

$$M_x = \nu D/R \tag{45}$$

$$M_y = D/R \tag{46}$$

In order to apply equal and opposite moments to the plate when the plate has been clamped at the edges, it is necessary to represent these moments in the form of equal and opposite pressures applied near the edges of the plate (see Fig. 28). This can be done by expressing the pressure distributions in terms of Dirac delta functions (14). According to usual notation for these delta functions, $\delta(x-c)$ indicates the delta function which intersects the abscissa at $x = c$. δ' indicates the first derivation of δ.

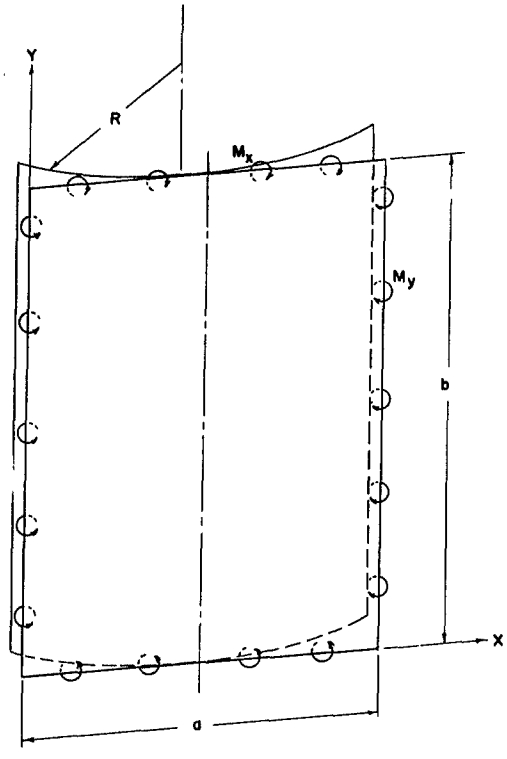

Coordinate System
Fig. 27

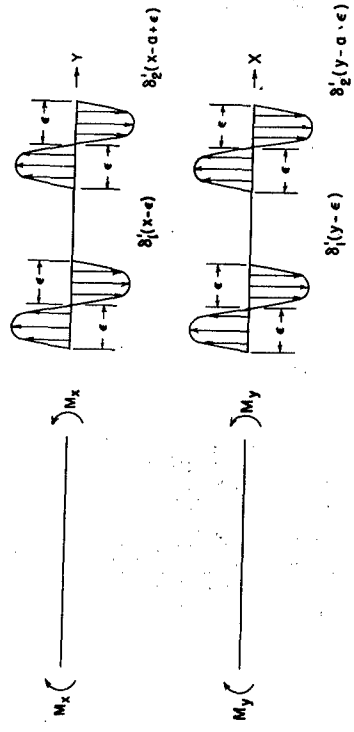

Representation of Edge Moments
by Pressure Couples
Fig. 28

The pressure distributions $\delta'(x)$ and $\delta'(y)$ must have the following properties:

$$\int_0^b \delta'_1(y-\varepsilon)\,dy = \int_0^b \delta'_2(y-b+\varepsilon)\,dy = 0 \qquad (47)$$

$$\int_0^a \delta'_1(x-\varepsilon)\,dx = \int_0^a \delta'_2(x-a+\varepsilon)\,dx = 0$$

$$\int_0^b (y-\varepsilon)\,\delta'_1(y-\varepsilon)\,dy = -\int_0^b (y-b+\varepsilon)\,\delta'_2(y-b+\varepsilon)\,dy = M_x$$

$$\int_0^b (x-\varepsilon)\,\delta'_1(x-\varepsilon)\,dx = -\int_0^b (x-a+\varepsilon)\,\delta'_2(x-a+\varepsilon)\,dx = M_y \qquad (48)$$

In addition, the derivative of the Dirac delta function has the following useful integration properties:

$$\int_0^b f(y)\,\delta'_1(y-\varepsilon)\,dy = M_x \frac{f'(\varepsilon+0) + f'(\varepsilon-0)}{2} \approx M_x\, f'(\varepsilon)$$

$$\int_0^b f(y)\,\delta'_2(y-b+\varepsilon)\,dy = -M_x \frac{f'(b-\varepsilon+0) + f'(b-\varepsilon-0)}{2} \approx -M_x\, f'(b-\varepsilon) \qquad (49)$$

$$\int_0^a f(x)\,\delta'_1(x-\varepsilon)\,dx = M_y \frac{f'(\varepsilon+0) + f'(\varepsilon-0)}{2} \approx M_y\, f'(\varepsilon)$$

$$\int_0^a f(x)\,\delta'_2(x-a+\varepsilon)\,dx = -M_y \frac{f'(a-\varepsilon+0) + f'(a-\varepsilon-0)}{2} \approx -M_y\, f'(a-\varepsilon)$$

This delta function pressure distribution can be written in terms of a Fourier series and the Fourier coefficients easily found by using the above integration properties of Dirac delta functions. Let

$$\delta'(x) = \delta'_1(x-\epsilon) + \delta'_2(x-a+\epsilon)$$

$$\delta'(y) = \delta'_1(y-\epsilon) + \delta'_2(y-b+\epsilon)$$

δ' may be written as Fourier series by noting that

$$\delta'(x) = \frac{a_0}{2} + \sum a_m \cos \frac{m\pi x}{a} + \sum b_m \sin \frac{m\pi x}{a}$$

$$\delta'(y) = \frac{a_0}{2} + \sum c_n \cos \frac{n\pi y}{b} + \sum d_n \sin \frac{n\pi y}{b} \qquad (50)$$

where

$$a_m = \frac{2}{a} \int_0^a \delta'(x) \cos \frac{m\pi x}{a} \, dx$$

$$b_m = \frac{2}{a} \int_0^a \delta'(x) \sin \frac{m\pi x}{a} \, dx \qquad (51)$$

$$c_n = \frac{2}{b} \int_0^b \delta'(y) \cos \frac{n\pi y}{b} \, dy$$

$$d_n = \frac{2}{b} \int_0^b \delta'(y) \sin \frac{n\pi y}{b} \, dy$$

Making use of the integration properties of δ' the Fourier coefficients (51), may be evaluated.

$$a_m = \frac{2}{a} \int_0^a \delta'(x-\varepsilon) \cos \frac{m\pi x}{a} \, dx + \frac{2}{a} \int_0^a \delta'_2(x-a+\varepsilon) \cos \frac{m\pi x}{a} \, dx$$

$$= \frac{2}{a} \left[- M_y \frac{m\pi}{a} \sin \frac{m\pi 0}{a} - M_y \frac{m\pi y}{a} \sin \frac{m\pi a}{a} \right]$$

$$a_m = 0 \qquad (52)$$

Similarly,

$$c_n = 0$$

$$b_m = \frac{2}{a} \int_0^a \delta'_1(x-\varepsilon) \sin \frac{m\pi x}{a} \, dx + \frac{2}{a} \int_0^a \delta'_2(x-a+\varepsilon) \sin \frac{m\pi x}{a} \, dx$$

$$= \frac{2}{a} \left[M_x \frac{m\pi}{a} \cos \frac{m\pi 0}{a} - M_x \frac{m\pi}{a} \cos \frac{m\pi a}{a} \right]$$

$$= \frac{2m\pi}{a^2} M_x \left[1 - \cos m\pi \right]$$

$$b_m = 0 \quad \text{for even } m$$

and $b_m = \frac{4m\pi}{a^2} M_y$ for odd m

similarly

$$d_n = 0 \quad \text{for even } n$$

$$d_n = \frac{4n\pi}{b^2} M_y \text{ for odd } n \qquad (53)$$

Substituting (50) and (53) in eqs. (50) we find

$$\delta'(x) = \frac{4\pi}{a^2} M_y \sum_{m=1,3,5}^{\infty} m \sin \frac{m\pi x}{a}$$

$$\delta'(y) = \frac{4\pi}{b^2} M_x \sum_{n=1,3,5}^{\infty} n \sin \frac{n\pi y}{b} \tag{54}$$

We will now proceed to use the above results in determining the Fourier series representing the applied pressure, p_e, which in turn approximates the effect of a moment equal and opposite to the moments M_x and M_y required to open the plate to an identically flat form.

By definition,

$$p_e = \delta'(x) + \delta'(y) \tag{55}$$

Substituting eqs. (45), (46), and (54) in (55), we find

$$p_e = 4\pi M_y \left\{ \sum_{m=1,3,5}^{\infty} \frac{m}{a^2} \sin \frac{m\pi x}{a} + \sum_{n=1,3,5}^{\infty} \frac{\nu n}{b^2} \sin \frac{n\pi y}{b} \right\} \tag{56}$$

Since it is more convenient in the later analysis to use a double Fourier series, we shall expand $4\pi M_y/a^2$ and $4\pi M_y \nu/b^2$ into sine series as follows:

$$\frac{4\pi M_y}{a^2} = \sum_{s=1}^{\infty} e_s \sin \frac{s\pi y}{b}$$

$$\frac{4\pi M_y \nu}{b^2} = \sum_{r=1}^{\infty} f_r \sin \frac{r\pi x}{a} \tag{57}$$

It is easy to verify that

$$e_s = \frac{16M_y}{a^2}\,\frac{1}{s} \quad \text{for odd } s$$

$$e_s = 0 \text{ for even } s$$

$$f_r = \frac{16M_y\nu}{b^2}\,\frac{1}{r} \quad \text{for odd } r$$

$$f_r = 0 \text{ for even } r \tag{58}$$

Hence,

$$p_e = 16M_y \sum_{r=1,3,5}^{\infty} \sum_{s=1,3,5}^{\infty} \left(\frac{r}{s}\frac{1}{a^2} + \frac{s}{r}\frac{\nu}{b^2}\right) \sin\frac{r\pi x}{a} \sin\frac{s\pi y}{b} \tag{59}$$

In addition to the above pressure equivalent to the applied forces (hereafter referred to simply as the equivalent pressure), there will also be a clamping pressure, p_c, which will be the equivalent of the moments occuring at the edges of the clamped plate. This pressure will be expanded in a trigonometric series containing arbitrary coefficients which will be determined by the use of the boundary conditions due to the clamping of the edge.

The clamping effect will be replaced by equivalent edge moments m_x and m_y (at $x = 0$, a and $y = 0$, b respectively). Using Eq. (56)

$$p_c = \sum_{r=1,3,5}^{\infty} \frac{4\pi m_y}{a^2}\, r \sin\frac{r\pi x}{a} + \sum_{s=1,3,5}^{\infty} \frac{4\pi m_x}{b^2}\, s \sin\frac{s\pi y}{b} \tag{60}$$

m_x and m_y may be expressed by a trigonometric series in terms of arbitrary coefficients K_r and T_s

$$m_x = \nu M_y \frac{4}{\pi} \sum_{r=1,3,5}^{\infty} K_r \sin\frac{r\pi x}{a}$$

$$m_y = M_y \frac{4}{\pi} \sum_{s=1,3,5}^{\infty} T_s \sin\frac{s\pi y}{b} \tag{61}$$

combining Eqs. (60) and (61) gives the equivalent clamping pressure

$$p_c = 16M_y \sum_{r=1,3,5}^{\infty} \sum_{s=1,3,5}^{\infty} \left(\frac{T_s}{a^2} r + \nu \frac{K_r}{b^2} s\right) \sin \frac{r\pi x}{a} \sin \frac{s\pi y}{b} \tag{62}$$

The addition of the equivalent applied pressure, p_e, and the equivalent clamping pressure, p_c, will be called the total applied pressure, p_T. Thus,

$$p_T = p_e + p_c = 16M_y \sum_{r=1,3,5}^{\infty} \sum_{s=1,3,5}^{\infty} \frac{r}{a^2} \left(T_s + \frac{1}{s}\right) + \nu \frac{s}{b^2} \left(K_r + \frac{1}{r}\right) \sin \frac{r\pi x}{a} \sin \frac{s\pi y}{b} \tag{63}$$

To simplify the writing, let

$$p_T = \sum_{r=1,3,5}^{\infty} \sum_{s=1,3,5}^{\infty} p_{r,s} \sin \frac{r\pi x}{a} \sin \frac{s\pi y}{b} \tag{64}$$

where

$$p_{r,s} = 16M_y \left[\frac{r}{a^2} \left(T_s + \frac{1}{s}\right) + \nu \frac{s}{b^2} \left(K_r + \frac{1}{r}\right)\right] = \frac{16D}{R} \left[\frac{r}{a^2} \left(T_s + \frac{1}{s}\right) + \frac{\nu s}{b^2} \left(K_r + \frac{1}{r}\right)\right] \tag{65}$$

since $M_y = \frac{D}{R}$.

It should be pointed out that (54) are divergent series and consequently Eqs. (59), (60), (62), and (65) consist of divergent series. The paradox of obtaining a convergent solution to an equilibrium problem under the action of a load represented by a divergent series has already been noted by S. Levy (15).

The explanation of this paradox would require further mathematical research. It can be shown that, for instance, if the divergent representation (Eq. 65) for the applied pressure is summed according to the Borel summation (one of many types of summations useful in summing divergent series) it is indeed found to be zero at, for instance, the center of the plate, as it should be. The physical meaning behind such a means for

summing divergent series seems rather nebulous and no concrete conclusions can be drawn from such a summation yielding the desired results.

The view that his paradox is not an accidental one is strengthened considerably by noting its occurrence in a rather simple linear problem.

The pure bending of a simply supported beam of length "a" by equal moments, M_y, applied at its ends can be solved by replacing these moments by equivalent pressures exactly in the same manner as has been done in the previous section for the clamped plate. Solving this problem by the method under question will lead to the exact solution.

Using equation (54) the moment equivalent pressure may be written as

$$p_{eq} = -\frac{4\pi}{a^2} M_y \sum_{m=1,3,5\ldots}^{\infty} m \sin \frac{m\pi x}{a}$$

The equilibrium equation for a beam under a pressure load is:

$$E I \frac{d^4 w}{dx^4} = -p$$

For our problem the boundary conditions at $x = 0$ and $x = a$ are

$$w = 0 \text{ and } \frac{d^2 w}{dx^2} = 0$$

These boundary conditions are satisfied termwise by assuming the deflection in the fomr of the following infinite series:

$$w = \sum_{m=1}^{\infty} w_m \sin \frac{m\pi x}{a}$$

Substituting the above two infinite series into the equilibrium equation, we obtain

$$E I \sum_{m=1}^{\infty} w_m \left(\frac{m\pi}{a}\right)^4 \sin \frac{m\pi x}{a} = -\frac{4\pi}{a^2} M_y \sum_{m=1,3,5,\ldots}^{\infty} m \sin \frac{m\pi x}{a}$$

Equating coefficients we find

$$w_m = -\frac{4a^2}{m^3\pi^3}\frac{M_y}{EI}$$

or

$$w = \frac{4a^2}{\pi^3}\frac{M_y}{EI}\sum_{m=1,3,5,\ldots}^{\infty}\frac{1}{m^3}\sin\frac{m\pi x}{a}$$

For purposes of comparison we find

$$\frac{d^2w}{dx^2} = -\frac{4}{\pi}\frac{M_y}{EI}\sum_{m=1,3,5,\ldots}^{\infty}\frac{1}{m}\sin\frac{m\pi x}{a}$$

Making use of the following formula No. 808 listed by B.O. Pierce (17):

$$\pi/4 = \sum_{m=1,3,5,\ldots}^{\infty}\frac{1}{m}\sin\frac{m\pi x}{a}$$

we find

$$\frac{d^2w}{dx^2} = -\frac{M_y}{EI}$$

which is well known to be the exact solution for the second derivative of a beam bent by pure moments.

The success of using a divergent representation for the pressure, which arises from the use of the Dirac delta function, seems to be hinged upon the order of the differential equation. Note that if the above equation were a first order differential equation, e.g.

$$EI\frac{dw}{dx} = -p$$

the solution for w would then be expressed by a divergent series and the solution could not be correct.

SECTION XII

THE DETERMINATION OF THE INPLANE STRESSES

Next, we shall calculate the inplane stresses in a flat plate clamped at four edges and under some distribution of lateral pressure which is equivalent to the edge moments applied. In this case, the von Karman's large deflection equations for thin plates (19) will be used. They are

$$D \nabla^4 w = p_T + h\left\{\frac{\partial^2 F}{\partial y^2}\frac{\partial^2 w}{\partial x^2}\frac{\partial^2 w}{\partial y^2} - 2\frac{\partial^2 F}{\partial x \partial y}\frac{\partial^2 w}{\partial x \partial y}\right\} \tag{66}$$

$$\nabla^4 F = E\left\{\left(\frac{\partial^2 w}{\partial x \partial y}\right)^2 - \frac{\partial^2 w}{\partial x^2}\frac{\partial^2 w}{\partial y^2}\right\} \tag{67}$$

where the pressure p_T is the equivalent pressure derived in the previous section and the stress function, F, is defined in terms of the inplane stresses by the following relations:

$$\sigma_{x0} = \frac{\partial^2 F}{\partial y^2}, \sigma_{y0} = \frac{\partial^2 F}{\partial x^2}, \tau_{xy0} = -\frac{\partial^2 F}{\partial x \partial y}$$

The boundary conditions on the deflection, w, are as follows:

$$\begin{aligned} &\text{at } x = 0,a \qquad w = 0, \quad \frac{\partial w}{\partial x} = 0 \\ &\text{at } y = 0,b \qquad w = 0, \quad \frac{\partial w}{\partial y} = 0 \end{aligned} \tag{68}$$

The boundary conditions on the stress function F are such that

1. The resultant load (at any cross section of the plate) must be zero in the x-direction and in the y-direction.
2. The boundaries of the plate must remain straight.

(69)

The deflection, w, and the stress function, F, will be assumed in the form of the following trigonometric series with arbitrary coefficients:

$$w = \sum_{m=1}^{\infty} \sum_{n=1}^{\infty} w_{m,n} \sin \frac{m\pi x}{a} \sin \frac{n\pi y}{b} \tag{70}$$

$$F = \sum_{p=0}^{\infty} \sum_{q=0}^{\infty} b_{p,q} \cos \frac{p\pi x}{a} \cos \frac{q\pi y}{b} \tag{71}$$

Note that the pressure p_T has already been expanded in the form of a Fourier series, namely,

$$p_T = \sum_{r=1,3,5}^{\infty} \sum_{s=1,3,5}^{\infty} p_{r,s} \sin \frac{r\pi x}{a} \sin \frac{s\pi y}{b} \tag{72}$$

To satisfy the differential equations, the coefficients $b_{p,q}$ and $w_{m,n}$ are to be determined as follows. We first substitute (70) and (71) into equation (67). By equating the coefficients of like terms, $b_{p,q}$ can be expressed in terms of $w_{m,n}$ in the following form.

$$b_{p,q} = \frac{E}{4(p^2 \frac{b}{a} + q^2 \frac{a}{b})^2} \sum_{i=1}^{9} B_i \tag{73}$$

where B_i are functions of $w_{m,n}$ and are listed in Appendix B. Next, substitute (70), (71), (72) into equation (66) and equate the coefficients of like terms. Since $b_{p,q}$ are now functions of $w_{m,n}$, we obtain

$$Dw_{r,s}(r^2 \frac{\pi^2}{a^2} + s^2 \frac{\pi^2}{b^2})^2 + \frac{h\pi^4}{4a^2b^2} \sum_{i=1}^{9} A_i = p_{r,s} \tag{74}$$

where A_i are function of $w_{m,n}$ and are listed in Appendix C. The derivation is the same as that carried out by Levy (20). Note that in this problem due to symmetry the coefficients $p_{r,s}$ and $w_{m,n}$ are restricted to odd subscripts only. Because of this, it is found that $b_{p,q}$ are restricted to even subscripts only.

Before we attempt to carry out the solution of $w_{m,n}$ let us examine the boundary conditions.

It is obvious that the assumed series, (70), is termwise identically zero at $x = 0$, $x = a$, $y = 0$, and $y = b$; hence the first set of the boundary conditions on w is satisfied. Also

$$\frac{\partial w}{\partial x} = \frac{\pi}{a} \sum_{m=1}^{\infty} \sum_{n=1}^{\infty} m\, w_{m,n} \cos \frac{m\pi x}{a} \sin \frac{n\pi y}{b}$$

and

$$\frac{\partial w}{\partial y} = \frac{\pi}{b} \sum_{m=1}^{\infty} \sum_{n=1}^{\infty} n\, w_{m,n} \sin \frac{m\pi x}{a} \cos \frac{n\pi y}{b}$$

To satisfy the conditions $\frac{\partial w}{\partial x} = 0$ at $x = 0$ and at $x = s$, we must have

$$\frac{\pi}{a} \sum_{m=1}^{\infty} \sum_{n=1}^{\infty} m\, w_{m,n} \sin \frac{n\pi y}{b} = 0$$

$$\frac{\pi}{a} \sum_{m=1}^{\infty} \sum_{n=1}^{\infty} m(-1)\, m w_{m,n} \sin \frac{n\pi y}{b} = 0$$

or

$$\sum_{m=1}^{\infty} m\, w_{m,n} = 0$$

$$\sum_{m=1}^{\infty} m(-1)m\, w_{m,n} = 0 \qquad (75)$$

The conditions of zero slope at the edges y = 0, b lead to similar equations

$$\sum_{n=1}^{\infty} n\, w_{m,n} = 0$$

$$\sum_{n=1}^{\infty} n(-1)\, n\, w_{m,n} = 0 \qquad (76)$$

The two relations in (75) and also those in (76) become the same if m and n are either odd or even.

In our problem, m and n must be odd, the boundary conditions of zero slope therefore lead to the following requirements on the deflection coefficients

$$\sum_{m=1,3,5}^{\infty} m\, w_{m,n} = 0 \qquad (77)$$

$$\sum_{n=1,3,5}^{\infty} n\, w_{m,n} = 0 \qquad (78)$$

Now let us examine the boundary conditions, (69).

The first condition may be shown to be satisfied in the following manner. Defining the load in the plane of the plate as p_x in the x-direction and p_y in the y-direction. Then

$$p_x = \int_0^b h\, \sigma_{x0}\, dy$$

where h is the thickness of the plate and is a constant. But

$$\sigma_{x0} = \frac{\partial^2 F}{\partial y^2}$$

Then

$$p_x = h \int_0^b \frac{\partial^2 F}{\partial y^2}\, dy = h \left[\left(\frac{\partial F}{\partial y}\right)_{y=b} - \left(\frac{\partial F}{\partial y}\right)_{y=0} \right]$$

Now,

$$F = \sum_{p=0}^{\infty} \sum_{q=0}^{\infty} b_{p,q} \cos \frac{p\pi x}{a} \cos \frac{q\pi y}{b}$$

therefore $p_x = 0$ (79)

Proceeding in a similar fashion, we find

$$p_y = h \int_0^a \frac{\partial^2 F}{\partial x^2} dx = h \frac{\partial F}{\partial x} \Bigg|_0^b = 0 \quad (80)$$

The second boundary condition can be shown to be satisfied as follows. Displacement of edges in x-direction.

$$\delta_x = \int_0^a \left[\varepsilon_x - \frac{1}{2} \left(\frac{\partial w}{\partial x} \right)^2 \right] dx \quad (81)$$

Displacement of edges in the y-direction

$$\delta_y = \int_0^b \left[\varepsilon_y - \frac{1}{2} \left(\frac{\partial w}{\partial y} \right)^2 \right] dy \quad (82)$$

where ε_x and ε_y are the inplane strain components which may be written in terms of the stress function as follows

$$\varepsilon_x = \frac{1}{E} \left(\frac{\partial^2 F}{\partial y^2} - \nu \frac{\partial^2 F}{\partial x^2} \right)$$

$$\varepsilon_y = \frac{1}{E} \left(\frac{\partial^2 F}{\partial x^2} - \nu \frac{\partial^2 F}{\partial y^2} \right) \quad (83)$$

Substituting the expressions for w and F into the above relations and then combining terms, we find finally

$$\delta_x = -\frac{\pi^2}{8a} \sum_{m=1} \sum_{n=1} m^2 w_{m,n}^2$$

$$\delta_y = -\frac{\pi^2}{8b} \sum_{m=1} \sum_{n=1} n^2 w_{m,n}^2 \qquad (84)$$

It is evident that these relations are independent of x and y and consequently the conditions of straight edges are satisfied. Since the detail of calculation is not obvious and is not included in Levy's reports, it is included in Appendix D.

Having examined the boundary conditions, let us now proceed to solve for the coefficients $w_{m,n}$. Since the problem was set up in a manner analogous to that of Levy and Greenman (21), much of the numerical work done by them may be used in this investigation. First, let us express the coefficients $b_{p,q}$ in terms of $w_{m,n}$. This is listed in Table 30. Next, let us substitute $b_{p,q}$ in terms of $w_{m,n}$ and $p_{r,s}$ as given by (65) into (74). We obtain

$$w_{1,1}/h = (.089783 + .011057K_1, + .078726T_1)\ a^2/Rh - D_1/h^3$$

$$w_{1,3}/h = (.0049583 + .0027683K_1 + .0065702T_3)\ a^2/Rh - D_2/h^3$$

$$w_{3,1}/h = (.0056107 + .00025863K_3 + .0055245T_1)\ a^2/Rh - D_3/h^3$$

$$w_{3,3}/h = (.0011085 + .00040949K_3 + .0029158T_3)\ a^2/Rh - D_4/h^3$$

$$w_{1,5}/h = (.0010103 + .00078637K_1 + .0011198T_5)\ a^2/Rh - D_5/h^3$$

$$w_{5,1}/h = (.0012757 + .000035632K_5 + .0012685T_1)\ a^2/Rh - D_6/h^3$$

$$w_{7,1}/h = (.00047166 + .0000094360K_7 + .00047031T_1)\ a^2/Rh - D_7/h^3$$

$$w_{9,1}/h = (.00022325^{+} + .0000034778K_9 + .00022287T_1)\ a^2/Rh - D_8/h^3$$

$$w_{11,1}/h = (.00012265^{-} + .0000015640K_{11} + .00012250T_1)\ a^2/Rh - D_9/h^3$$

$$w_{13,1}/h = (.000074433 + .00000080346K_{13} + .000074372T_1)\ a^2/Rh - D_{10}/h^3$$

$$w_{15,1}/h = (.000048506 + .00000045389K_{15} + .000048475T_1)\ a^2/Rh - D_{11}/h^3$$

$$w_{5,3}/h = (.00034197 + .000082290K_5 + .00097655^{-}T_3)\ a^2/Rh - D_{12}/h^3$$

$$w_{7,3}/h = (.00013996 + .000024629K_7 + .000409323T_3)\ a^2/Rh - D_{13}/h^3$$

$$w_{9,3}/h = (.000069267 + .0000095788K_9 + .00020462T_3)\ a^2/Rh - D_{14}/h^3$$

$$w_{11,3}/h = (.000038948 + .0000044292K_{11} + .00011564T_3)\ a^2/Rh - D_{15}/h^3$$

$$w_{13,3}/h = (.000023969 + .0000023123K_{13} + .000071346T_3)\ a^2/Rh - D_{16}/h^3$$

$$w_{3,5}/h = (.00033873 + .00028518K_3 + .0012183T_5)\ a^2/Rh - D_{17}/h^3$$

$$w_{5,5}/h = (.00014365 + .000088453K_5 + .00062981T_5)\ a^2/Rh - D_{18}/h^3$$

$$w_{7,5}/h = (.000068202 + .000031922K_7 + .00031821T_5)\ a^2/Rh - D_{19}/h^3$$

$$w_{9,5}/h = (.000036358 + .000013595^{-}K_9 + .00017424T_5)\ a^2/Rh - D_{20}/h^3$$

$$w_{11,5}/h = (.000021305 + .0000066087K_{11} + .00010352T_5)\ a^2/Rh - D_{21}/h^3$$

$$w_{13,5}/h = (.000013438 + .0000035555K_{13} + .000065824T_5)\ a^2/Rh - D_{22}/h^3$$

$$w_{1,7}/h = (.00035647 + .00031124K_1 + .00031659T_7)\ a^2/Rh - D_{23}/h^3$$

$$w_{3,7}/h = (.00013114 + .00017047K_3 + .00052020T_7)\ a^2/Rh - D_{24}/h^3$$

$$w_{5,7}/h = (.000068377 + .000073798K_5 + .00037533T_7)\ a^2/Rh - D_{25}/h^3$$

$$w_{7,7}/h = (.000037394 + .000032236K_7 + .00022953T_7)\ a^2/Rh - D_{26}/h^3$$

$$w_{9,7}/h = (.000021690 + .000015287K_9 + .00013994T_7)\ a^2/Rh - D_{27}/h^3$$

$$w_{11,7}/h = (.000013382 + .0000079213K_{11} + .000088632T_7)\ a^2/Rh - D_{28}/h^3$$

$$w_{1,9}/h = (.000164988 + .00015166\ K_1 + .00011998T_9)\ a^2/Rh - D_{29}/h^3$$

$$w_{3,9}/h = (.000061214 + .00010253K_3 + .00024334T_9)\ a^2/Rh - D_{30}/h^3$$

$$w_{5,9}/h = (.000035683 + .000055796K_5 + .00022071T_9)\ a^2/Rh - D_{31}/h^3$$

$$w_{7,9}/h = (.000021786 + .000028737K_7 + .00015914T_9)\ a^2/Rh - D_{32}/h^3$$

$$w_{9,9}/h = (.000013684 + .000015167K_9 + .00010799T_9)\ a^2/Rh - D_{33}/h^3$$

$$w_{13,7}/h = (.0000087224 + .0000044368K_{13} + .000058668T_7)\ a^2/Rh$$

$$w_{11,9}/h = (.0000089101 + .0000084230K_{11} + .000073302T_9)\ a^2/Rh$$

$$w_{13,9}/h = (.0000060254 + .000004940K_{13} + .000050810T_9)\ a^2/Rh$$

$$w_{1,11}/h = (.000089546 + .000084569K_1 + .000054742T_{11})\ a^2/Rh$$

$$w_{3,11}/h = (.000032830 + .000064388K_3 + .00012504T_{11})\ a^2/Rh$$

$$w_{5,11}/h = (.000020208 + .000040889K_5 + .00013233T_{11})\ a^2/Rh$$

$$w_{7,11}/h = (.000013327 + .000024022K_7 + .00010885T_{11})\ a^2/Rh$$

$$w_{9,11}/h = (.0000089504 + .000013970K_9 + .000081382T_{11})\ a^2/Rh$$

$$w_{11,11}/h = (.0000061323 + .000008307OK_{11} + .000059148T_{11})\ a^2/Rh$$

$$w_{13,11}/h = (.0000043047 + .000005113OK_{13} + .000043024T_{11})\ a^2/Rh$$

$$w_{1,13}/h = (.000053951 + .000051770K_1 + .000028355T_{13})\ a^2/Rh$$

$$w_{3,13}/h = (.000019488 + .000042391K_3 + .00006954T_{13})\ a^2/Rh$$

$$w_{5,13}/h = (.000012288 + .000029922K_5 + .000081944T_{13})\ a^2/Rh$$

$$w_{7,13}/h = (.0000085232 + .000019469K_7 + .000074644T_{13})\ a^2/Rh$$

$$w_{9,13}/h = (.0000060332 + .000012306K_9 + .000060659T_{13})\ a^2/Rh$$

$$w_{11,13}/h = (.0000043226 + .0000077975K_{11} + .000046979T_{13})\ a^2/Rh$$

$$w_{13,13}/h = (.0000031436 + .0000050327K_{13} + .000035834T_{13})\, a^2/Rh$$

(85)

where the expressions $D_1, D_2, \ldots, D_{33}$ are given in Table 31, with the assumption that the non-linear terms not involving $w_{1,1}$, $w_{1,3}$, $w_{3,1}$, $w_{3,3}$, $w_{1,5}$ and $w_{5,1}$ are negligible as compared to terms involving only these six terms. Table 31 should be read in such a manner that $D_1 = 1.451\, w_{1,1}^3 - .972\, w_{1,1}^2 w_{1,3} - .1920\, w_{1,1}^2 w_{3,1} + \ldots$.

In order to satisfy the boundary conditions (68) on the slope of the edges, equations (85) are substituted in equations (77) and (78). The resulting equations may be written in matrix notation as follows:

$$\frac{a^2}{Rh}\,[A_{ij}][K_j] = \frac{a^2}{Rh}\,[F_i] + \frac{1}{h^3}\,[C_i]$$

where the matrix $[A_{ij}]$ is given in Table 32 partitioned so that

$$A = \left[\begin{array}{c|c} P & Q \\ \hline R & S \end{array}\right]$$

and

$$K_j = \begin{bmatrix} K_1 \\ K_3 \\ K_5 \\ K_7 \\ K_9 \\ K_{11} \\ K_{13} \end{bmatrix} \qquad F_i = \begin{bmatrix} -.115376 \\ -.012713 \\ -.00420168 \\ -.00194778 \\ -.0010647 \\ -.00064353 \\ -.00041703 \\ -.120621 \\ -.0123367 \\ -.00395848 \\ -.0018093 \\ -.000979049 \\ -.000586332 \\ -.000376233 \end{bmatrix}$$

$$K_j = \begin{bmatrix} T_1 \\ T_3 \\ T_5 \\ T_7 \\ T_9 \\ T_{11} \\ T_{13} \end{bmatrix} \tag{86}$$

and C_i ($i = 1$ to 14) are non-linear functions of $w_{m,n}$ as listed in Table 33. Table 33 should be read in such a manner that $C_i = 1.370\ w_{1,1}^3 + .298\ w_{1,1}^2 w_{1,3} - .069\ w_{1,1}^2 w_{3,1} + \cdots$

With the non-linear terms not involving $w_{1,1}$, $w_{1,3}$, $w_{3,1}$, $w_{3,3}$, $w_{1,5}$, $w_{5,1}$ neglected the problem can be solved as follows. First, we note that equations (86) are linear equations in terms of the unknowns K_j. It is therefore possible to solve these equations for K_j in terms of the non-linear functions of $w_{m,n}$. In matrix form, we have

$$\frac{a^2}{Rh}\left[K_j\right] = \frac{a^2}{Rh}\left[A_{ij}^{-1}\right]\left[F_i\right] + \frac{1}{h}\left[A_{ij}^{-1}\right]\left[C_i\right] \tag{87}$$

where A_{ij}^{-1} denotes the inverse of the matrix A_{ij} and is given in Table 34 shown partitioned according to $A^{-1} = \begin{matrix} P & Q \\ R & S \end{matrix}$. The inversion of of the matrix A_{ij} was carried out by the use of high speed electronic calculating machines. Since we have neglected all non-linear terms of $w_{m,n}$ except those involving $w_{1,1}$, $w_{1,3}$, $w_{3,1}$, $w_{3,3}$, $w_{1,5}$, $w_{5,1}$ with K_j found as functions of these deflection coefficients, we can substitute these K_j into the first six equations of (85) and obtain a system of six non-linear equations in terms of these deflection coefficients. In

matrix notations, the first six equations of (85) may be written as follows:

$$\frac{1}{h}\,{}^{i}\left[w_i\right] = \frac{a^2}{Rh}\,{}^{i}\left[\,{}^{j}B_{ij}\right]\left[K_j\right] + \frac{a^2}{Rh}\,{}^{i}\left[E_i\right] - \frac{1}{h^3}\,{}^{i}\left[D_i\right] \tag{88}$$

where

$$w_i = \begin{bmatrix} w_{1,1} \\ w_{1,3} \\ w_{3,1} \\ w_{3,3} \\ w_{1,5} \\ w_{5,1} \end{bmatrix} \qquad E_i = \begin{bmatrix} .089783 \\ .0049583 \\ .0056107 \\ .0011085 \\ .0010103 \\ .0012757 \end{bmatrix}$$

and

$$B_{ij} = \begin{array}{c} i \\ j \end{array}$$

.011057	0	0	0	0	0	.078726	0	0	0	0	0	0
.0027683	0	0	0	0	0	0	.0065702	0	0	0	0	0
0	.00025863	0	0	0	0	.0055245	0	0	0	0	0	0
0	.00040949	0	0	0	0	0	.0029158	0	0	0	0	0
.00078637	0	0	0	0	0	0	0	.0011198	0	0	0	0
0	0	.000035632	0	0	0	.0012685	0	0	0	0	0	0

By substituting (87) into (88), we obtain

$$\frac{1}{h}\left[w_i\right] = \frac{a^2}{Rh}\left[B_{ij}\right]\left[A_{ij}^{-1}\right]\left[F_i\right] + \frac{1}{h^3}\left[B_{ij}\right]\left[A_{ij}^{-1}\right]\left[C_i\right] + \frac{a^2}{Rh}\left[E_i\right] - \frac{1z}{h^3}\left[D_i\right]$$

To simplify the notation, let

$$\frac{a^2}{Rh}\left[B_{ij}\right]\left[A_{ij}^{-1}\right]\left[F_i\right] + \frac{a^2}{Rh}\left[E_i\right] = \frac{a^2}{Rh}\left[G_i\right]$$

and

$$\frac{1}{h^3}\left[B_{ij}\right]\left[A_{ij}^{-1}\right]\left[C_i\right] - \frac{1}{h^3}\left[D_i\right] = \left[H_i\right]$$

then

$$\frac{1}{h}\left[w_i\right] = \frac{a^2}{Rh}\left[G_i\right] + \left[H_i\right] \qquad (89)$$

The above matrix operations have been carried out and we obtain the following results:

$$G_i = \begin{bmatrix} .0242193 \\ -.00335124 \\ .00274422 \\ .00016766 \\ -.00120163 \\ .00120163 \end{bmatrix} \quad \text{and} \quad H_i = \begin{bmatrix} H_1 \\ H_2 \\ H_3 \\ H_4 \\ H_5 \\ H_6 \end{bmatrix} \qquad (90)$$

where the H_i are listed in Table 35.

The six non-linear equations (88) can be solved by an iteration method as follows. Consider at first the first equation. Assume that all deflection coefficients except $w_{1,1}$ are zero. Then we have a cubic equation in $w_{1,1}$. This equation can be solved by trial and error which gives a first approximation to $w_{1,1}$. Next, consider the first two

equations and assume that all deflection coefficients except $w_{1,1}$ and $w_{1,3}$ are zero. Substituting the value of $w_{1,1}$ obtained previously into the second equation, a first approximation to the value of $w_{1,3}$ can be obtained. Next substitute this value of $w_{1,3}$ into the first equation and calculate the second approximation to the value of $w_{1,1}$. This process is repeated until the desired accuracy is obtained. It may be pointed out that after the second cycle, it is not necessary to compute the $w_{1,1}$ by using the value of $w_{1,3}$ computed in the previous cycle and a value which appears to give a more rapid convergence can be used. In this way the rapidity of convergence can be accelerated. By taking more equations and solving for more unknowns, all six unknown deflection coefficients can finally be solved.

It was found that the convergence of the solution is fairly rapid if the iteration of the first equation is carried out according to the scheme

$$\frac{w_{1,1}}{h}^{(n+1)} = \left\{ \frac{1}{.620} \left(.0242193 \frac{a^2}{Rh} - \frac{w_{1,1}}{h}^{(n)} + \bar{H}_1^{(n)} \right) \right\}^{1/3} \qquad (91)$$

where $\bar{H}_1^{(n)} = H_1(w_{1,1}^{(n)}, w_{1,3}^{(n)}, w_{3,1}^{(n)}, w_{3,3}^{(n)}, w_{1,5}^{(n)}, w_{5,1}^{(n)})$ with the $(\frac{w_{1,1}}{h}^{(n)})^3$ term deleted; and the remaining five equations are iterated according to the scheme:

$$\frac{w_i}{h}^{(n+1)} = \frac{a^2}{Rh} \left[G_i \right] + H_i^{(n)} \qquad (92)$$

where $H_i^{(n)} = H_i^{(n)}(w_{1,1}^{(n)}, w_{1,3}^{(n)}, w_{3,1}^{(n)}, w_{1,5}^{(n)}, w_{5,1}^{(n)})$.

In the above equations, the superscript (n+1) indicates the (n+1)-th approximation and n indicates the value assumed before the (n+1)-th cycle is computed. Since these equations are cubic equations, it is possible that these equations may have more than one set of solutions. To show the uniqueness of the solution is a very difficult task although it is intuitively clear that there should be only one equilibrium configuration in this problem. This is partially born out by solving

the first equation when only $w_{1,1}$ is assumed to be different from zero. It was found that, in this case, we have one real root and two complex ones.

The iteration of the six equations according to the scheme of Eqs. (91) and Eq. (92) are shown graphically in Fig. 29. In this figure the solid lines lead from the assumed values, $w_i(n)$ to the iterated values, $w_i^{(n+1)}$ while the broken lines show the next guess made from the results of the previous iterated value which is used in the next iteration. The iteration converges to the values for w_i with

$$\frac{a^2}{Rh} = 337.5 \quad (a = 9", \quad R = 6", \text{ and } h = .040")$$

as follows:

$$\frac{w_{1,1}}{h} = 1.824, \quad \frac{w_{1,3}}{h} = 0.116, \quad \frac{w_{3,1}}{h} = .527, \quad \frac{w_{3,3}}{h} = .0194, \quad \frac{w_{1,5}}{h} = -.071, \quad \frac{w_{5,1}}{h} = .2025$$

These values for w_i are used in computing C_i from Table 33 and D_i from Table 31. We obtain therefore,

$C_1 = 15.08h^3$
$C_2 = .4988h^3$
$C_3 = .039917h^3$
$C_4 = -.0002530h^3$
$C_5 = .00001019h^3$
$C_6 = .00001045h^3$
$C_7 = -.0000002114h^3$
$C_8 = 20.33h^3$
$C_9 = -1.075h^3$
$C_{10} = -.07069h^3$
$C_{11} = .009659h^3$
$C_{12} = .0001135h^3$
$C_{13} = -.00003037h^3$
$C_{14} = -.00000006266h^3$

and

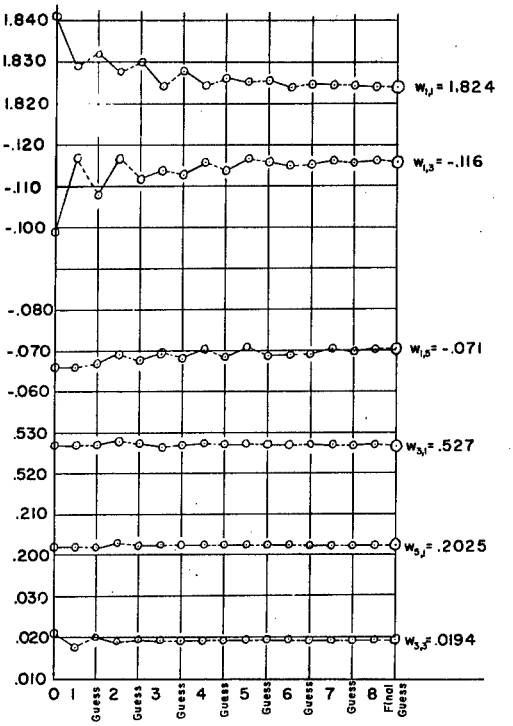

Iteration of the Six Non-Linear Equations

Fig. 29

$$D_1 = 16.9219h^3 \qquad D_{15} = .0000011h^3$$
$$D_2 = .9018h^3 \qquad D_{16} = -.04668h^3$$
$$D_3 = .1300h^3 \qquad D_{17} = -.006135h^3$$
$$D_4 = .001054h^3 \qquad D_{18} = -.00057689h^3$$
$$D_5 = -.00000934h^3 \qquad D_{19} = -.00008891h^3$$
$$D_6 = -.00000687h^3 \qquad D_{20} = .00001768h^3$$
$$D_7 = -.00000024h^3 \qquad D_{21} = .00000798h^3$$
$$D_8 = -.00000002h^3 \qquad D_{22} = .00000001h^3$$
$$D_9 = -.5360h^3 \qquad D_{23} = .00008837h^3$$
$$D_{10} = -.1290h^3 \qquad D_{24} = .001891h^3$$
$$D_{11} = -.01286h^3 \qquad D_{25} = .0006802h^3$$
$$D_{12} = -.0004967h^3 \qquad D_{26} = .00007449h^3$$
$$D_{13} = -.00002564h^3 \qquad D_{27} = .00000208h^3$$
$$D_{14} = -.00000339h^3 \qquad D_{28} = -.00000251h^3$$

Using these values for C_i and D_i, the K_i's can be computed according to Eq. (87) by which we obtain

$$\frac{a^2}{Rh} K_1 = -3032 \qquad \frac{a^2}{Rh} K_{11} = -27664 \qquad \frac{a^2}{Rh} T_7 = 2411$$
$$\frac{a^2}{Rh} K_3 = -7765 \qquad \frac{a^2}{Rh} K_{13} = -32664 \qquad \frac{a^2}{Rh} T_9 = 3183$$
$$\frac{a^2}{Rh} K_5 = -12703 \qquad \frac{a^2}{Rh} T_1 = 278.3 \qquad \frac{a^2}{Rh} T_{11} = 3817$$
$$\frac{a^2}{Rh} K_7 = -16553 \qquad \frac{a^2}{Rh} T_3 = 924.4 \qquad \frac{a^2}{Rh} T_{13} = 4520$$
$$\frac{a^2}{Rh} K_9 = -22669 \qquad \frac{a^2}{Rh} T_5 = 1694$$

Substituting these results into equations (85), the values of $w_{m,n}$ are as follows:

$w_{1,1}/h = 1.77$

$w_{1,3}/h = -.110$

$w_{3,1}/h = .521$

$w_{3,3}/h = .018$

$w_{1,5}/h = -.099$

$w_{5,1}/h = .201$

$w_{7,1}/h = .133$

$w_{1,7}/h = -.060$

$w_{3,7}/h = -.027$

$w_{5,7}/h = -.010$

$w_{7,7}/h = .032$

$w_{9,7}/h = -.0018$

$w_{11,7}/h = -.00094$

$w_{13,7}/h = -.00054$

$w_{1,9}/h = -.022$

$w_{3,9}/h = -.00085$

$w_{5,9}/h = .0059$

$w_{9,1}/h = .059$

$w_{11,1}/h = .032$

$w_{13,1}/h = .020$

$w_{5,3}/h = -.014$

$w_{7,3}/h = .018$

$w_{9,3}/h = -.0046$

$w_{11,3}/h = -.0025$

$w_{7,9}/h = .038$

$w_{9,9}/h = .0046$

$w_{11,9}/h = .0033$

$w_{13,7}/h = .0024$

$w_{1,11}/h = -.017$

$w_{3,11}/h = -.012$

$w_{5,11}/h = -.0075$

$w_{7,11}/h = .022$

$w_{9,11}/h = -.0030$

$w_{13,3}/h = -.0015$

$w_{3,5}/h = -.030$

$w_{5,5}/h = -.0076$

$w_{7,5}/h = .034$

$w_{9,5}/h = -.00076$

$w_{11,5}/h = -.00028$

$w_{13,5}/h = -.000097$

$w_{11,11}/h = -.0020$

$w_{13,11}/h = -.0014$

$w_{1,13}/h = -.011$

$w_{3,13}/h = -.0078$

$w_{5,13}/h = -.0056$

$w_{7,13}/h = .018$

$w_{9,13}/h = -.0028$

$w_{11,13}/h = -.0019$

$w_{13,13}/h = -.0014$

Comparing the values of these deflection coefficients, it is observed that it is reasonably accurate to neglect all the non-linear terms in these equations except the first six. The derivation of the values of the first six deflection coefficients so computed from the results obtained earlier is probably due to the accumulated errors in the substitution, especially since the matrix inversion A^{-1} was found to no more than four significant figures.

The stress function coefficients $b_{p,q}$ can be computed by substituting the values of these deflection coefficients into Table 30 from which we obtain

$b_{0,2} = .569Eh^2$
$b_{0,4} = .0072Eh^2$
$b_{0,6} = -.0013Eh^2$
$b_{0,8} = -.00068Eh^2$
$b_{0,10} = .00027Eh^2$
$b_{0,12} = -.00006Eh^2$
$b_{2,0} = .020Eh^2$
$b_{2,2} = .079Eh^2$
$b_{2,4} = .0004Eh^2$
$b_{2,6} = -.0019Eh^2$
$b_{2,8} = -.0012Eh^2$
$b_{2,10} = .00005Eh^2$
$b_{2,12} = -.00009Eh^2$
$b_{4,0} = .0048Eh^2$
$b_{4,2} = .0041Eh^2$
$b_{4,4} = -.0017Eh^2$
$b_{4,6} = -.0025Eh^2$
$b_{4,8} = .00034Eh^2$
$b_{6,0} = .0016Eh^2$
$b_{6,2} = -.00084Eh^2$
$b_{6,4} = -.00098Eh^2$
$b_{6,6} = .00022Eh^2$
$b_{8,0} = .00018Eh^2$
$b_{8,2} = -.00002Eh^2$
$b_{8,4} = -.000009Eh^2$
$b_{10,0} = .00002Eh^2$

With the values of $w_{m,n}$ and $b_{p,q}$ determined, we thus obtain the solution to our problem of clamping a curved plate in a flat frame. The actual distribution of the deflection and stresses can be found from the relations previously listed and shown below:

$$w = \sum \sum w_{m,n} \sin \frac{m\pi x}{a} \sin \frac{n\pi y}{b} \qquad (70)\ \text{bis}$$

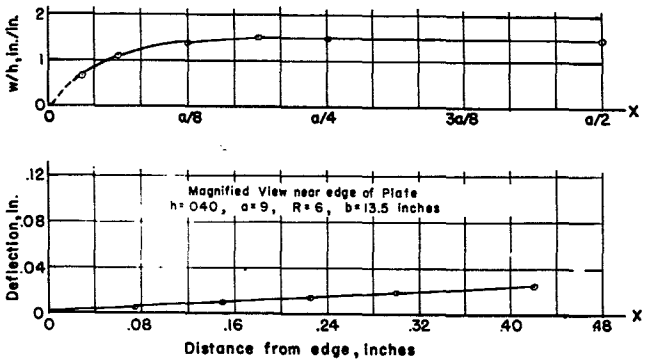

Plate Deflection at y = b/2

Fig. 30

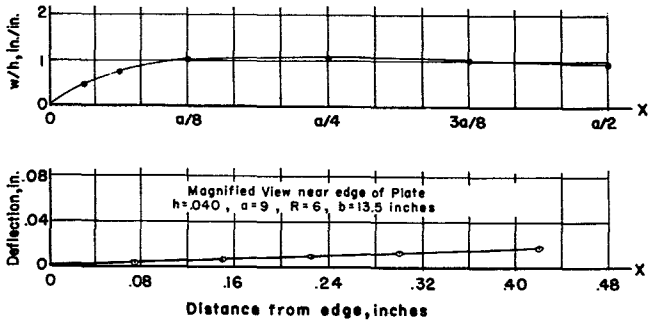

Plate Deflection at y = b/4

Fig. 31

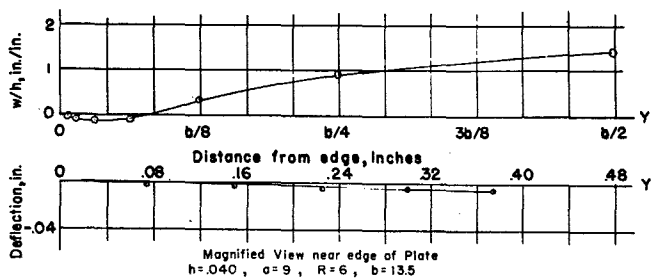

Plate Deflection at x = a/2

Fig. 32

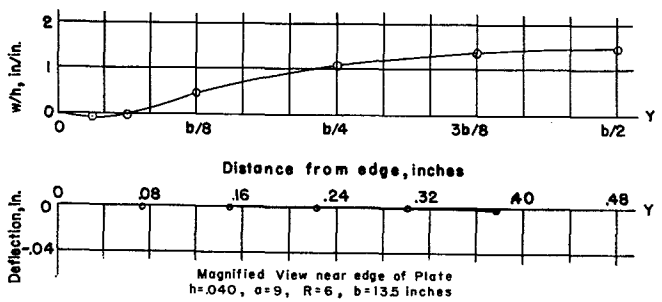

Plate Deflection at x = a/4

Fig. 33

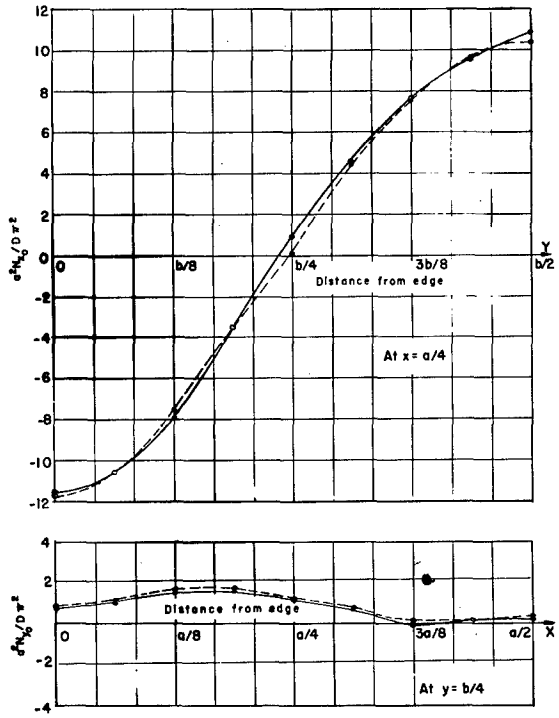

Unit Membrane Normal Forces
(at x = a/4 and y = b/4)
Fig. 34

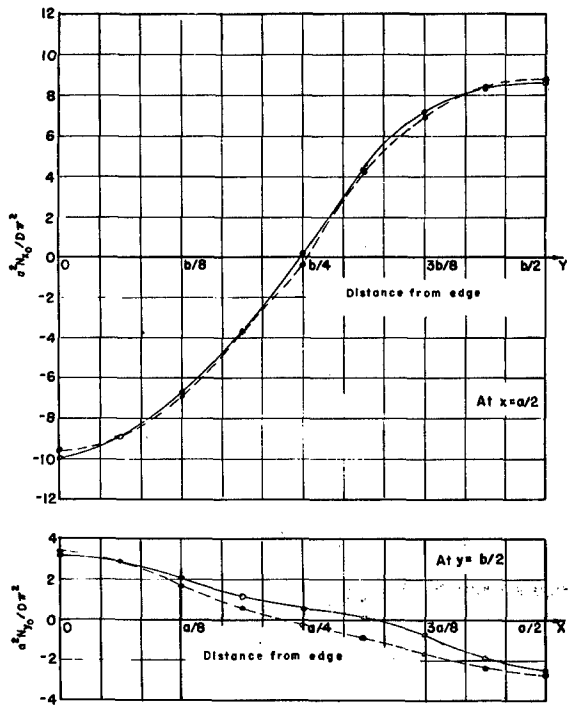

Unit Membrane Normal Forces
(at x = a/2 and y = b/2)
Fig. 35

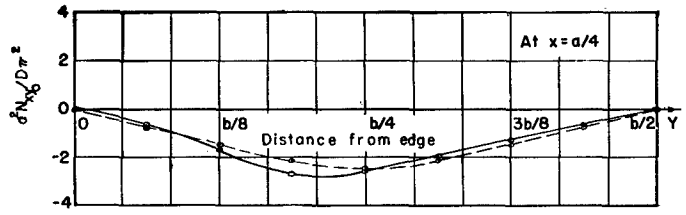

Unit Membrane Shear Forces
(at x = a/4)

Fig. 36

and

$$\sigma_{x0} = \frac{\partial^2 F}{\partial y^2}$$

$$\sigma_{y0} = \frac{\partial^2 F}{\partial x^2}$$

$$\sigma_{xy0} = \frac{\partial^2 F}{\partial x \partial y}$$

where

$$F = \sum \sum b_{p,q} \cos \frac{p\pi x}{a} \cos \frac{q\pi y}{b} \qquad (71) \text{ bis}$$

The variation of the non-dimensional unit membrane forces and deflections are computed using the finite number of terms obtained above. They are plotted along four sections of the plate, that is along $x = a/4$ and $a/2$ and along $y = b/2$ and $b/4$. The values are plotted for only one-quarter of the plate ($0 \leq x \leq a/2$, $0 \leq y \leq b/2$) in Figs. 30-36 because of the symmetry of σ_x, σ_y and w. The computed non-dimensionalized forces are represented by the solid lines of Figs. 34-36. In Figs. 30-33 the deflection curves are shown magnified for the portions of the plate near the boundaries. It can be seen from these magnified views that the boundary conditions on the deflections which theoretically require zero slope and deflection, seem to be well approximated by taking the finite number of terms.

SECTION XIII

DETERMINATION OF THE BUCKLING LOAD FOR A PRESTRESSED PLATE

Having determined the inplane forces in the prestressed plate, the next problem is to find the buckling load. Here the use of the term buckling load can be subjected to objection, because the prestressed plate will have initial deflections and there will not be a definite load at which the "flat" form of plate becomes unstable. However, if we assume that these initial deflections do not exist, then we may determine the "buckling load" by the Rayleigh-Ritz method.

Let w be the lateral deflection of the plate due to buckling. Then the bending strain energy in the plate with all edges clamped when buckling occurs is

$$U = \frac{D}{2} \iint_A \left(\frac{\partial^2 w}{\partial x^2} + \frac{\partial^2 w}{\partial y^2}\right)^2 dx\, dy \qquad (93)$$

where D is the flexural rigidity of the plate. The work done by the inplane forces is

$$W = \frac{1}{2} \iint_A \left[\bar{N}_x \left(\frac{\partial w}{\partial x}\right)^2 + \bar{N}_y \left(\frac{\partial w}{\partial y}\right)^2 + 2\bar{N}_{xy} \frac{\partial w}{\partial x} \frac{\partial w}{\partial y}\right] dx\, dy \qquad (94)$$

where $\bar{N}_x = N_{x0}$, $\bar{N}_y = N_{ycr} + N_{y0}$, $\bar{N}_{xy} = N_{xy0}$, the subscript 0 refers to the original inplane forces and the subscript cr refers to the buckling value. At buckling, we have

$$U - W = 0 \qquad (95)$$

from which we obtain

$$N_{ycr} = \frac{U - \bar{W}}{T} \qquad (96)$$

where

$$T = \frac{1}{2} \iint_A \left(\frac{\partial w}{\partial y}\right)^2 dx\, dy$$

and

$$\bar{W} = W - N_{ycr}\, T$$

It must be emphasized that the above relations are correct only if there were no initial deflections. With the presence of the initial deflections, the values of the inplane forces originally due to the prestressing will be changed when the load N_{ycr} is applied and therefore the above method of calculation may induce an error which is not small. However, in the absence of a better method, it was decided to try to use the Rayleigh-Ritz method.

The Rayleigh-Ritz method can be carried out as follows. First, the deflection w is assumed in the form of a series, every term of which satisfies the boundary conditions but with undetermined parameters. Substitute the series into equation (95) and carry out the integration. Then minimize the resulting expression with respect to the undetermined parameters. This gives us a system of homogeneous equations involving the buckling load N_{ycr}. A non-trivial solution is obtained if we equate

the determinant of the coefficients of these parameters to zero, from which N_{ycr} is calculated.

The boundary conditions for a clamped plate are that the deflection and the slope normal to the edge are zero at the edge, i.e.

$$\text{at } x = 0,a \qquad w = \frac{\partial w}{\partial x} = 0$$

$$\text{at } y = 0,b \qquad w = \frac{\partial w}{\partial y} = 0$$

To satisfy these conditions, we may assume w in the following form.

$$w = \sin\frac{\pi x}{a} \sin\frac{\pi y}{b} \sum_{m=1} \sum_{n=1} w_{m,n} \sin\frac{m\pi x}{a} \sin\frac{n\pi y}{b} \tag{97}$$

where $w_{m,n}$ are undetermined coefficients.

Substituting (97) in (93), we find

$$U = \frac{D\pi^4}{2} \int_0^b \int_0^a \left\{ \sum \sum \frac{w_{m,n}}{b^2} \sin\frac{\pi x}{a} \sin\frac{m\pi x}{a} \left[(n+1)^2 \cos\frac{(1+n)\pi y}{b} \right.\right.$$

$$\left. - (n-1)^2 \cos\frac{(1-n)\pi y}{b} \right] + \frac{w_{m,n}}{a^2} \sin\frac{\pi y}{b} \sin\frac{n\pi y}{b}$$

$$\left.\left[(n+1)^2 \cos\frac{(1+n)\pi y}{b} - (n-1)^2 \cos\frac{(1-n)\pi y}{b} \right] \right\}^2 dx\, dy \tag{98}$$

Performing the indicated integration, we obtain

$$U = \frac{D\pi^4}{128a^2} \left\{ \sum_{m=1}^{\infty} 2w_{m,1}^2 \left(\frac{b}{a}\right) (m^4+6m^2+1) \right.$$

$$+ \sum_{n=1}^{\infty} 2w_{1,n}^2 \left(\frac{a}{b}\right)^3 (n^4+6n^2+1)$$

$$- \sum_{n=1}^{\infty} w_{1,n-2}w_{1,n} \left(\frac{a}{b}\right)^3 2 \left[(n+1)^2+8n\right]$$

$$- \sum_{m=1}^{\infty} w_{m-2,1}w_{m,1} \left(\frac{b}{a}\right) 2 \left[(m+1)^2+8m\right]$$

$$+ \sum_{m=1}^{\infty} \sum_{n=1}^{\infty} 4w_{m,n}^2 \left[\left(\frac{b}{a}\right)(m^4+6m^2+1)+\left(\frac{a}{b}\right)^3 (n^4+6n^2+1)\right.$$

$$\left. + 2 \left(\frac{a}{b}\right)(m^2+1)(n^2+1)\right]$$

$$- \sum_{m=1}^{\infty} \sum_{n=3}^{\infty} 2w_{m,n-2}w_{m,n} \left[\left(\frac{a}{b}\right)^3 (n^4-6n^2+8n-3)\right.$$

$$\left. + \left(\frac{b}{a}\right)(m^4+6m^2+1)+2\left(\frac{a}{b}\right)(m^2+1)(n-1)^2\right]$$

$$- \sum_{m=3}^{\infty} \sum_{n=1}^{\infty} 2w_{m-2,n}w_{m,n} \left[\left(\frac{b}{a}\right)(m^4-6m^2+8m-3)\right.$$

$$\left. + \left(\frac{a}{b}\right)^3 (n^4+6n^2+1)+2\left(\frac{a}{b}\right)(m-1)^2(n^2+1)\right]$$

$$+ \sum_{m=3}^{\infty} \sum_{n=3}^{\infty} w_{m-2,n-2}\, w_{m,n} \left[\left(\frac{a}{b}\right)^3 (n^4-6n^2+8n-3) \right.$$

$$\left. + \left(\frac{b}{a}\right)(m^4-6m^2+8m-3) + 2\left(\frac{a}{b}\right)(m-1)^2(n-1)^2 \right]$$

$$- \sum_{m=1}^{\infty} \sum_{n=1}^{\infty} 2w_{m,n+2}\, w_{m,n} \left[\left(\frac{a}{b}\right)^3 (n^4-6n^2-8n-3) \right.$$

$$\left. + \left(\frac{b}{a}\right)(m^4+6m^2+1) + 2\left(\frac{a}{b}\right)(m^2+1)(n+1)^2 \right]$$

$$- \sum_{m=1}^{\infty} \sum_{n=1}^{\infty} 2w_{m+2,n}\, w_{m,n} \left[\left(\frac{b}{a}\right)(m^4-6m^2-8m-3) \right.$$

$$\left. + \left(\frac{a}{b}\right)^3 (n^4+6n^2+1) + 2\left(\frac{a}{b}\right)(m+1)^2(n^2+1) \right]$$

$$+ \sum_{m=3}^{\infty} \sum_{n=1}^{\infty} w_{m-2,n+2}\, w_{m,n} \left[\left(\frac{b}{a}\right)(m^4-6m^2+8m-3) \right.$$

$$\left. + \left(\frac{a}{b}\right)^3 (n^4-6n^2-8n-3) + 2\left(\frac{a}{b}\right)(m-1)^2(n+1)^2 \right]$$

$$+ \sum_{m=1}^{\infty} \sum_{n=3}^{\infty} w_{m+2,n-2}\, w_{m,n} \left[\left(\frac{a}{b}\right)^3 (n^4-6n^2+8n-3) \right.$$

$$\left. + \left(\frac{b}{a}\right)(m^4-6m^2-8m-3) + 2\left(\frac{a}{b}\right)(m+1)^2(n-1)^2 \right]$$

$$+ \sum_{m=3}^{\infty} \sum_{n=3}^{\infty} w_{m+2,n+2}\, w_{m,n} \left[\left(\frac{a}{b}\right)^3 (n^4-6n^2-8n-3) \right.$$

$$\left. + \left(\frac{b}{a}\right)(m^4-6m^2-8m-3)+2\left(\frac{a}{b}\right)(m+1)^2(n+1)^2 \right] \qquad (99)$$

It may be mentioned that we obtain the above general form for U if all terms in the assumed series for w are taken. If only a finite number of particular terms are taken, the coefficients of those terms omitted naturally should be deleted from the above expressions.

Substituting the assumed form for **w**, into the expression for T and integrating, we obtain

$$T = -\frac{\pi^2 a}{128b} \left[\sum \sum w_{m,n} \quad 2(1+n^2)(2w_{m,n} - w_{m-2,n} \right.$$

$$+ w_{2-m,n} - w_{2+m,n}) + (n^2-1)(-2w_{m,n-2} - 2w_{m,n+2}$$

$$+ 2w_{m,2-n} + w_{m-2,n-2} + w_{m-2,n+2} - w_{m-2,2-n}$$

$$\left. - w_{2-m,n-2} - w_{2-m,n+2} + w_{2-m,2-n} + w_{2+m,n-2} + w_{2+m,2+n} - w_{2+m,2-n}) \right]$$

(100)

The work expression due to the prestresses existing in the plate will now be computed assuming that these stresses remain the same as before the buckling load is applied and remain constant during buckling. Thus

$$N_{x0} = h\frac{\partial^2 F}{\partial y^2}, \quad N_{y0} = h\frac{\partial^2 F}{\partial x^2}, \quad N_{xy0} = -h\frac{\partial^2 F}{\partial x \partial y} \qquad (101)$$

and

$$F = \sum_{p=0}^{\infty} \sum_{q=0}^{\infty} b_{p,q} \cos \frac{p\pi x}{a} \cos \frac{q\pi y}{b}$$

To simplify the writing, let

$$\bar{W}_x = + \frac{1}{2} \iint_A N_{x0} \left(\frac{\partial w}{\partial x}\right)^2 dx\, dy$$

$$\bar{W}_y = + \frac{1}{2} \iint_A N_{y0} \left(\frac{\partial w}{\partial y}\right)^2 dx\, dy$$

$$\bar{W}_{xy} = + \iint_A N_{xy0} \frac{\partial w}{\partial x} \frac{\partial w}{\partial y} dx\, dy \qquad (102)$$

Then, after substitution and integration, we find

$$\bar{W}_x = \frac{h\pi^4}{512a^2} \sum_{m=1}^{\infty} \sum_{n=1}^{\infty} \sum_{k=1}^{\infty} \sum_{t=1}^{n} w_{m,n} w_{k,t} \frac{a}{b} \Big[2(n-t)^2 b_{s,n-t} - 2(n+t)^2 b_{s,n+t}$$

$$- (t-n+2)^2 b_{s,t-n+2} - (n-t-2)^2 b_{s,n-t-2} - (n-t+2)^2 b_{s,n-t+2}$$

$$+ (n+t-2)^2 b_{s,t+n-2} + (n+t+2)^2 b_{s,n+t+2} \Big] \Big[2 - \delta_k^m \delta_t^n \Big]$$

$$\Big[(2mk+2)\, \delta_s^{m-k} + (2mk+2)\, \delta_s^{k-m} + (2mk-2)\, \delta_s^{m+k}$$

$$+(-mk+1-2m)\ \delta_s^{k-m+2} +(-mk+1-2m)\ \delta_s^{m-k-2}$$

$$+(-mk+1+2m)\ \delta_s^{m-k+2} +(-mk+1+2m)\ \delta_s^{k-m-2}$$

$$+(-mk-1+2m)\ \delta_s^{2-m-k} +(-mk-1+2m)\ \delta_s^{m+k-2}+(-mk-1-2m)\ \delta_s^{m+k+2}$$

(103)

where $\delta_j^i = 1$ when $i = j$ and $\delta_j^i = 0$ when $i \neq j$

$$\bar{W}_y = \frac{h\pi^4}{512a^2} \sum_{m=1}^{\infty} \sum_{n=1}^{\infty} \sum_{k=1}^{k=M} \sum_{t=1}^{\infty} W_{m,n} W_{k,t} \left(\frac{a}{b}\right) \Big[2(m-k)^2 b_{m-k,s}$$

$$-(m-k-2)^2 b_{m-k-2,s} -(2-m+k)^2 b_{2-m+k,s} -(m-k+2)^2 b_{m-k+2,s}$$

$$+(m+k-2)^2 b_{m+k-2,s} -2(m+k)^2 b_{m+k,s} +(m+k+2)^2 b_{m+k+2,s}\Big]$$

$$\Big[2-\delta_k^m\ \delta_t^n\Big]\Big[(2nt+2)\ \delta_s^{n-t}+(2nt+2)\ \delta_s^{t-n}+(2nt-2)\ \delta_s^{n+t}$$

$$+(-nt+1-2n)\ \delta_s^{2-n-t}+(-nt+1-2n)\ \delta_s^{-2+n-t}+(-nt+1+2n)\ \delta_s^{2+n-t}$$

$$+(-nt+1+2n)\ \delta_s^{t-2-n}+(-nt-1+2n)\ \delta_s^{2-n-t}$$

$$+(-nt-1+2n)\ \delta_s^{-2+n+t}+(-nt-1-2n)\ \delta_s^{2+n+t}\Big]$$

(104)

$$\bar{W}_{xy} = \frac{hm^4}{256a^2} \sum_{m=1}^{\infty}\sum_{n=1}^{\infty}\sum_{k=1}^{\infty}\sum_{t=1}^{\infty} w_{m,n}w_{k,t}\left(\frac{a}{b}\right)$$

$$\Big\{\Big[(2+m-k)b_{2+m-k,s}+(2-m+k)b_{2-m+k,s}-(2+m+k)b_{2+m+k,s}$$

$$-(m-k-2)b_{m-k-2,s}+(m+k-2)b_{m+k-2,s}\Big]\Big[2n(t-n)\,\delta_s^{t-n}$$

$$-2n(n-t)\,\delta_s^{n-t}+2n(n+t)\,\delta_s^{n+t}+(n+1)(2+n-t)\,\delta_s^{2+n-t}$$

$$+(1-n)(2-n+t)\,\delta_s^{2-n+t}-(1+n)(n+t+2)\,\delta_s^{n+t+2}+(n-1)(n-t-2)\delta_s^{n-t-2}$$

$$-(1+n)(t-n-2)\,\delta_s^{t-n-2}+(1-n)(n+t-2)\,\delta_s^{n+t-2}\Big]$$

$$+\Big[-2(m-k)b_{m-k,s}+2(m+k)b_{m+k,s}+(2+m-k)b_{2+m-k,s}$$

$$-(2-m+k)b_{2-m+k,s}-(2+m+k)b_{2+m+k,s}+(m-k-2)b_{m-k-2,s}$$

$$-(m+k-2)b_{m+k-2,s}\Big]\Big[m(1-t)(2+n-t)\,\delta_s^{2+n-t}+m(1+t)(2+t-n)\delta_s^{2+t-n}$$

$$-m(1+t)(n+t+2)\delta_s^{n+t+2}-m(1+t)(n-t-2)\delta_s^{n-t-2}+m(t-1)(t-n-2)\delta_s^{t-n-2}$$

$$+m(1-t)(n+t-2)\delta_s^{n+t-2}\Big]\Big\}\,(2-\delta_k^m\,\delta_t^n) \qquad (105)$$

To obtain numerical answers, let us consider a plate with the following dimension ratios:

$$b/a = 1.5, \quad \frac{a^2}{Rh} = 337.5 \tag{106}$$

These ratios are those corresponding to the plate tested having a thickness of .040 in. and an initial radius of curvature of 6 in.

Using eqs. (99), (100), (103), (104), and (105), and taking only one term in assumed form of deflection, namely,

$$w = w_{1,2} \sin^2 \frac{\pi x}{a} \sin \frac{\pi y}{b} \sin \frac{2\pi y}{b} \tag{107}$$

we find

$$\begin{aligned}
U &= 1.361 \frac{\pi^4 D}{a^2} w_{1,2}^2 \\
T &= -.156 \pi^2 w_{1,2}^2 \\
\bar{W}_x &= -.285 \frac{\pi^4 D}{a^2} w_{1,2}^2 \\
\bar{W}_y &= +.049 \frac{\pi^4 D}{a^2} w_{1,2}^2 \\
\bar{W}_{xy} &= +.034 \frac{\pi^4 D}{a^2} w_{1,2}^2
\end{aligned} \tag{108}$$

Substituting the expressions (107) into the buckling criteria yields the following equations:

$$2\left(1.563 \frac{\pi^4 D}{a^2} + .156 \pi^2 N_y\right) w_{1,2} = 0$$

$$\text{or } N_y = 10.02 \frac{\pi^2 D}{a^2} \tag{109}$$

The buckling load for a non-prestressed plate of the same dimensions can be found in an analogous manner by equating to zero the work done by in-plane forces due to prestressing, i.e., omitting $\bar{W}_x$, $\bar{W}_y$ and $\bar{W}_{xy}$.

The buckling criteria for the corresponding non-prestressed flat plate yields

$$2(1.361\,\frac{\pi^4 D}{a^2} + .156\,\pi^2 N_y)\,w_{1,2} = 0$$

$$\text{or } N_y = -8.72\,\frac{\pi^2 D}{a^2} \qquad (110)$$

From the above calculations, we find that, by assuming the deflection in the form of (107) and assuming that the in-plane forces remain constant when the buckling load is applied, the Rayleigh-Ritz analysis shows that the buckling load is increased 14.9% by prestressing. It may be mentioned that a more accurate value for the buckling load of a non-prestressed clamped rectangular plate with b/a = 3/2 is (12)

$$N_{ycr} = -8.33\,\frac{\pi^2 D}{a^2} \qquad (111)$$

which is 4.7% lower than the value just computed.

To study the effect of taking more terms in the assumed deflection series (97), we consider next the following deflection form

$$w = (w_{1,2}\sin\frac{\pi x}{a} + w_{3,2}\sin\frac{3\pi x}{a})\sin\frac{\pi x}{a}\sin\frac{\pi y}{b}\sin\frac{2\pi y}{b} \qquad (112)$$

Substituting this deflection form into (99), (100), (103), (104) and (105), we obtain

$$U = \frac{D\pi^4}{64a^2}\left\{87.11\,w_{1,2}^2 - 137.63 w_{1,2}w_{3,2} + 565.63 w_{3,2}^2\right\}$$

$$T = -\frac{\pi^2}{64}\left\{10 w_{1,2}^2 - 6.67 w_{1,2}w_{3,2} + 6.67 w_{3,2}^2\right\}$$

$$\bar{W}_x = -\frac{D\pi^4}{64a^2}\left\{18.20w_{1,2}^2-31.35w_{1,2}w_{3,2}+85.40w_{3,2}^2\right\}$$

$$\bar{W}_y = -\frac{D\pi^4}{64a^2}\left\{-3.13w_{1,2}^2+7.88w_{1,2}w_{3,2}-2.70w_{3,2}^2\right\}$$

$$\bar{W}_{xy} = -\frac{D\pi^4}{64a^2}\left\{-2.27w_{1,2}^2+2.97w_{1,2}w_{3,2}-.11w_{3,2}^2\right\} \qquad (113)$$

First, let us calculate the buckling load for a non-prestressed plate. Let

$$K = N_{ycr}\, a^2/\pi^2 D \qquad (114)$$

then, we have

$$U-N_{ycr}T = \frac{D\pi^4}{64a^2}\left\{(87.11+10K)w_{1,2}^2-(137.63+6.67K)w_{1,2}w_{3,2}+(565.63+6.67K)w_{3,2}^2\right\} \qquad (115)$$

Minimizing the above expression with respect to the undetermined coefficients $w_{3,2}$ and $w_{1,2}$ we obtain the following two equations at buckling,

$$\frac{\partial(V-T)}{\partial w_{1,2}} = \frac{D\pi^4}{64a^2}\left\{(174.22+20K)w_{1,2}-(137.63+6.67K)w_{3,2}\right\} = 0$$

$$\frac{\partial(V-T)}{\partial w_{3,2}} = \frac{D\pi^4}{64a^2}\left\{-(137.63+6.67K)w_{1,2}-(1131.26+13.33K)w_{3,2}\right\} = 0 \qquad (116)$$

Setting the determinant of the coefficients of these two equations equal to zero, the conditions for a non-trivial solution give

$$K^2 + 104.06K + 802.10 = 0 \qquad (117)$$

from which we find

$$K = -8.38, \text{ or } -95.7 \qquad (118)$$

or

$$N_{ycr} = 8.38 \frac{\pi^2 D}{a^2}$$

Although this answer was arrived at using only two terms of the series, it is only.06% higher than the more accurate value found by Levy (12) and listed as Eq. (111). For the prestressed plate, we have

$$V-T-T_{0_x}-T_{0_y}-T_{0_{xy}} = \frac{D\pi^4}{64a^2}\left\{(99.9+10K)w_{1,2}^2-(158.1+6.67K)w_{1,2}w_{3,2}+(648.21+6.67K)w_{3,2}^2\right\} \qquad (119)$$

Minimizing this expression with respect to $w_{1,2}$ and $w_{3,2}$, we obtain the following two equations

$$(199.8+20K)w_{1,2} - (158.12+6.67K)w_{3,2} = 0$$

$$-(158.12+6.67K)w_{1,2} + (1296.4+13.34K)w_{3,2} = 0 \qquad (120)$$

The condition for a non-trivial solution is

$$K^2 + 119.1K + 1052.7 = 0 \qquad (121)$$

from which we find

$$K = -9.61, \text{ or } -109.52$$

or

$$N_{ycr} = 9.61 \frac{\pi^2 D}{a^2} \qquad (122)$$

Although the actual values of $w_{1,2}$ or $w_{3,2}$ cannot be found there ratio can be calculated using either of Eqs. (119).

The first of Eqs. (119) may be rewritten as

$$(199.8+20K) \frac{w_{1,2}}{w_{3,2}} - 158.12 + 6.67K = 0$$

Substituting K = - 9.61 the equation becomes

$$7.6 \frac{w_{1,2}}{w_{3,2}} - 222.22 = 0 \qquad (123)$$

or

$$\frac{w_{1,2}}{w_{3,2}} = 29.2 \qquad (124)$$

for the prestresssed plate.

The buckling loads and ratio of deflection coefficients were computed for both the non-prestressed and prestressed plates using other coefficients and combinations of coefficients in the assumed deflection series (109). The results are tabulated in Tables 36 and 37 and shown graphically in Fig. 37 for various percentages of the calculated amounts of prestressing.

Note that due to orthogonality relations between the assumed deflection form and the stress function series taking a limited number of terms of the deflection form ($w_{m,n}$) will automatically limit the number of terms describing the stress function ($b_{p,q}$). The stresses computed with these limited number of terms (due to considering only one term, $w_{1,2}$ in the deflection series) are compared with those computed with a larger number of terms in Fig. 34, 35, and 36. In these figures the stresses corresponding to the limited number of terms are shown with broken lines while the more exact representations are shown with solid lines.

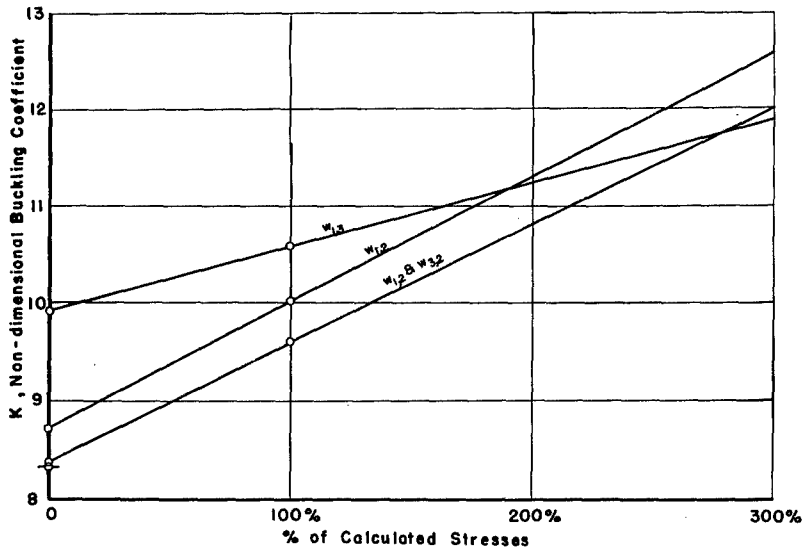

Results of Rayleigh Ritz Analysis

Fig. 37

SECTION XIV

TABLES

TABLE 1

"Flatness Test Results" (see Fig. 3)

Pos.*	Defl. (10^3 in.)	Pos.	Defl. (10^3 in.)	Pos.	Defl. (10^3 in.)	Pos.	Defl. (10^3 in.)	Pos.	Defl. (10^3 in.)
1-1	+1	2-1	+2.5	3-1	+2.5	4-1	+3	5-1	-1
1-2	-.5	2-2	-1	3-2	-3.5	4-2	-1	5-2	-3
1-3	-.5	2-3	-4	3-3	-7	4-3	-4	5-3	-3.5
1-4	-1	2-4	-5	4-4	-7	4-4	-3.5	5-4	-3
1-5	-1.5	2-5	-6	4-5	-6	4-5	-3	5-5	-2
1-6	-2.5	2-6	-6	4-6	-7	4-6	-5.5	5-6	-3
1-7	-1	2-7	-4	4-7	-6	4-7	-6	5-7	-3
1-8	-2.5	2-8	-3	4-8	-5	4-8	-1	5-8	0
1-9	-2	2-9	+1	4-9	-1	4-9	0	5-9	0

* minus indicated downward deflection

These results were duplicated within $\pm$ .001 inches for similar tests.

TABLE 1 - 1b

(Flatness tests on .032 inch Aluminum Plate)

Position	Deflection x 10^{-3} inches	Position	Deflection x 10^{-3} inches	Position	Deflection x 10^{-3} inches
1-1	0	2-1	-18	3-1	-12
1-2	-15	2-2	-38	3-2	-27
1-3	-23	2-3	-	3-3	-37
1-4	-27	2-4	-49	3-4	-30
1-5	-25	2-5	-46	3-5	-28
1-6	-18	2-6	-35	3-6	-20

(minus indicates downward deflection)

TABLE 1 - 1c

(Flatness tests on .040 inch Aluminum Plate)

Position	Deflection x 10^{-3} inches	Position	Deflection x 10^{-3} inches	Position	Deflection x 10^{-3} inches
1-1	0	2-1	0	3-1	+3
1-2	-6	2-2	-9	3-2	-1
1-3	-14	2-3	-19	3-3	-10
1-4	-12	2-4	-17	3-4	-13
1-5	-8	2-5	-11	3-5	-13
1-6	-5	2-6	-5	3-6	-6

TABLE 2

Test Data For Determining Initial Stresses in .020 Aluminum Alloy Plate

e = Final Reading - Initial Reading

Gage No.	1	2	3	4	5	6	7	8	9	10	7-2	8-2
Test 1												
Initial Rd.	6900	6640	6765	5851	7020	6171	5533	6072				
Final Rd.	5282	8171	5149	7590	5453	7888	3479	7845				
$e(10^{-6})$ in./in.	-1618	1531	-1616	1739	-1567	1717	-2054	1773				
Test 2												
Initial Rd.	6930	6642	6790	5855	7041	6171	5558	6073				
Final Rd.	5320	8200	5140	7648	5440	7935	3578	7857				
$e(10^{-6})$ in./in.	-1610	1558	-1650	1793	-1601	1764	-1980	1784				
Test 3												
Initial Rd.	6499	6648	6866	5849	6938	6130	5496	6044	4991	7866	3932	4728
Final Rd.	4908	8191	5246	7611	3398	7839	3508	7819	3369	9542	2372	6315
$e(10^{-6})$ in./in.	-1591	1543	-1620	1762	-1540	1709	-1998	1775	-1622	1676	-1560	1587

Note: Gage Numbers refer to those indicated in Fig. 6

TABLE 3

Results of Tests on 24 S-T Al. Alloy Plate
Radius of Curvature - 9 1/4 inches

e_a (10^{-6}) in./in.

Gage	Test 1	Test 2	Test 3	Test 3	(using corrections)
1,2	-43.5	-26	-24	(1.10)	+42
3,4	+61.5	+71.5	+71.0		+71
5,6	+75.0	+81.5	+84.5		+84.5
7,8	-140.5	-98	-111.5	(8,9)	+76.5
7-2,8-2	X	X	X		+13.5

Note: + = tensile
- = compressive

TABLE 4

Test Data for Determining Initial Stresses

in .040 Aluminum Plate

Initial Radius = 8.70 inches

e_a = membrane strain (micro-inches per inch) see Fig. 4 for placement of gages

Test 1

Zero position taken with side bars clamped on

Gage No. (see Fig. 4)	A-2	A-4	B-2	B-4a	B-4b	B-5	B-6	B-7
	-11 1/2	+24	+2 1/2	+5	-18 1/2	+43 1/2	-21	-16
e_a	-16	+18	0	0	-19	-38 1/2	-26	-21

Gage No.	C-1	C-2	C-3	C-4	C-5	C-7
	-16	-10	14	21	-8 1/2	5
e_a	-26	-9	10	19 1/2	-11	-1

Zero position taken without side bars clamped on

Gage No.	A-2	A-4	B-2	B-4a	B-4b	B-5	B-6	B-7
	+4	+30	+10	+5	-11 1/2	48 1/2	-21	-16
e_a	-2 1/2	+24	+3 1/2	-1 1/2	-16 1/2	43 1/2	-23 1/2	-18 1/2

Gage No.	C-1	C-2	C-3	C-4	C-5	C-7
	-24 1/2	-5	14	18 1/2	4	5
	-26	-10	5	15	-2	5

Strain gage readings were not taken at each surface, but instead, they were averaged electrically and only the averages (membrane strains) recorded.

TABLE 5

Test Data for Determining Initial Stresses

in .051 Aluminum Plate

Initial Radius = 6.82

e = strain at surface (micro-inches per inch)
e_a = membrane strain (micro-inches per inch)

Zero position taken with side bars clamped on

Gage No. (see Fig. 4)	A-2	A-4	B-2	B-4a	B-4b	B-5	B-6	B-7
	-6	+82	-44	+180	+2398	+2518	+2534	+2512
e(concave side)	+4	+102	-55	+168	+2284	+2403	+2399	+2361
	+11	-203	+12	-181	-2507	-2547	-2398	-2425
e(convex side)	+31	-186	+0	-194	-2368	-2408	-2260	-2273
	-21 1/2	-60 1/2	+16	- 1/2	-54 1/2	-14 1/2	+68	+43 1/2
e_a	+17 1/2	-42	-27 1/2	-13	-42	-2 1/2	+69 1/2	+44

Gage No.	C-1	C-2	C-3	C-4	C-5	C-7
e(concave side)	+2167	+2198	+2338	+2408	+104	-42
	+2130	+2132	+2253	+2305	+100	-39
e(convex side)	-2252	-2286	-2403	-2459	-175	+1
	-2200	-2203	-2295	-2342	-170	+2
	-42 1/2	-44	-32 1/2	-25 1/2	-35 1/2	-20 1/2
e_a	-37	-35 1/2	-21	-18 1/2	-35	-18 1/2

Note: Because of thickness of plate the cold rolling of the plate was poorly done, i.e,m the initial shape of the plate is not purely cylindrical.

TABLE 5 (continued)

Zero position taken without side bars clamped on

Gage No.	A-2	A-4	B-2	B-4a	B-4b	B-5	B-6	B-7
e(concave side)	-24	+76	-15	+218	+2461	+2551	+2507	+2451
	-12	+87	-32	+207	+2351	+2444	+2390	+2317
e(convex side)	-49	-158	+54	-149	-2581	-2597	-2392	-2385
	-14	-145	+32	-159	-2450	-2466	-2267	-2252
e_a	-36 1/2	-41	+19 1/2	+34 1/2	-60	-23	+115	+66
	-13	-29	0	+24	-49 1/2	-11	+123	+65

Gage No.	C-1	C-2	C-3	C-4	C-5	C-7
e(concave side)	+2282	+2216	+2203	+2186	+80	-53
	+2214	+2138	+2128	+2113	+93	-43
e(convex side)	-2356	-2272	-2260	-2243	-158	-37
	-2290	-2190	-2176	-2165	-148	-23
e_a	-37	-28	-28 1/2	-28 1/2	-78	-45
	-38	-26	-24	-26	-55	-33

TABLE 6

Test Data for Determining Initial Stresses

in .051 Aluminum Plate

e = strain at surface (micro-inches per inch)

e_a = membrane strain (micro-inches per inch)

Test 2

Zero position taken with side bars clamped on

Gage No.	A-2	A-4	B-2	B-4a	B-4b	B-5	B-6	B-7
e(concave side)	-7 -20	+115 +105	-59 -59	+190 +189	+2307 +2300	+2415 +2420	+2401 +2401	+2352 +2372
e(convex side)	+82 +52	-170 -203	+27 +21	-198 -208	-2390 -2389	-2414 -2415	-2248 -2259	-2240 -2270
e_a	+37 1/2 +16	-27 1/2 -49	-16 -19	-4 -9 1/2	-41 1/2 -44 1/2	+ 1/2 +2 1/2	+76 1/2 +71	+56 +51

Gage No.	C-1	C-2	C-3	C-4	C-5	C-7
e(concave side)	+2079 +2090	+2061 +2072	+2212 +2217	+2288 +2283	+112 +102	-31 -41
e(convex side)	-2231 -2241	-2231 -2240	-2307 -2315	-2340 -2341	-160 -171	+49 +29
e_a	-76 -75 1/2	-85 -84	-47 1/2 -49	-26 -29	-24 -34 1/2	+9 -11 1/2

TABLE 6 (continued)

Zero position taken without side bars clamped on

Gage No.	A-2	A-4	B-2	B-4a	B-4b	B-5	B-6	B-7
	-18	+105	-29	+238	+2378	+2467	+2406	+2324
e(concave side)	-29	+95	-29	+230	+2353	+2445	+2379	+2312
	+31	-125	+82	-157	-2440	-2445	-2240	-2210
e(convex side)	+21	-160	+70	-168	-2440	-2445	-2240	-2220
	+6 1/2	-10	+26 1/2	+40 1/2	-31	+11	+84	+57
e_a	-4	-32 1/2	+20 1/2	+31	-43 1/2	0	+69 1/2	+46

Gage No.	C-1	C-2	C-3	C-4	C-5	C-7
	+2181	+2099	+2114	+2123	+115	-26
e(concave side)	+2171	+2090	+2104	+2111	+108	-33
	-2291	-2200	-2175	-2152	-130	+30
	-2303	-2215	-2190	-2162	-142	+19
	-55	-50 1/2	-30 1/2	-14 1/2	-7 1/2	+2
e_a	-66	-62 1/2	-43	-25 1/2	-17	-7

TABLE 7

Test Data For Determining Initial Stresses

in .032 Aluminum Plate

Initial Radius = 7 3/4 inches

e = strain at surface (micro-inches per inch)

e_a = membrane strain (micro-inches per inch)

Test 1

Zero position taken without side bars clamped on

Gage No. (see Fig. 4)	A-2	A-4	B-2	B-4a	B-4b	B-5	B-6	B-7
	+63	+30	+151	+72	+2565	+2663	+2695	+2317
e(concave side)	+65	+40	+160	+81	+2570	+2660	+2697	+2324
	-148	-114	+20	-27	-2531	-2771	-2629	-2711
e(convex side)	-146	-106	+29	-27	-2521	-2754	-2629	-2691
	-42 1/2	-42	+85 1/2	+22 1/2	+17	-54	+33	-197
e_a	-40 1/2	-33	+94 1/2	+27	+24 1/2	-47	+34	-185 1/2

Gage No.	C-1	C-2	C-3	C-4	C-5	C-7
	+2212	+2395	+2505	+2420	+40	+151
e(concave side)	+2197	+2385	+2497	+2417	+41	+160
	-2482	-2385	-2442	-2422	-89	+20
e(convex side)	-2467	-2363	-2431	-2409	-79	+29
	-135	+5	+31 1/2	-1	-24 1/2	+85 1/2
e_a	-135	+11	+33	+4	-19	+94 1/2

Note: There are two readings for each gage because readings were taken during both the flattening and the unflattening process.

TABLE 7 (continued)

Zero position taken with side bars clamped on

Gage No.	A-2	A-4	B-2	B-4a	B-4b	B-5	B-6	B-7
e(concave side)	+74 +63	+30 +30	+140 +55	+62 +80	+2470 +2490	+2582 +2582	+2635 +2635	+2284 +2270
e(convex side)	-142 -159	-95 -114	+29 +31	-23 -25	-2421 -2441	-2672 -2674	-2558 -2564	-2662 -2632
e_a	-34 -48	-32 1/2 -42	+84 1/2 +43	+19 1/2 +27 1/2	+ 24 1/2 +24 1/2	-45 -46	+38 1/2 +35 1/2	-189 -176 1/2

Gage No.	C-1	C-2	C-3	C-4	C-5	C-7
e(concave side)	+2132 +2162	+2349 +2385	+2485 +2516	+2410 +2430	+30 +40	+61 +81
e(convex side)	-2392 -2424	-2328 -2348	-2410 -2430	-2390 -2409	-89 -89	-130 -130
e_a	-130 -131	+10 1/2 +18 1/2	+37 1/2 +43	+10 +10 1/2	-29 1/2 -24 1/2	-34 1/2 -24 1/2

TABLE 8

Test Data For Determining Initial Stresses

in .032 Aluminum Plate

Initial Radius = 7 3/4 inches

e = strain at surface (micro-inches per inch)

e_a = membrane strain (micro-inches per inch)

Test2

Zero position taken without side bars clamped on

Gage No.	A-2	A-4	B-2	B-4a	B-4b	B-5	B-6	B-7
e(concave side)	+5 -2	+59 +67	+131 +138	+120 +124	+2551 +2548	+2639 +2637	+2650 +2648	+2300 +2312
e(convex side)	-128 -140	-35 -53	-127 -127	-128 -128	-2352 -2535	-2734 -2735	-2568 -2563	-2591 -2601
e_a	-61 1/2 -71	+12 +7	+2 +5 1/2	-4 -2	+99 1/2 +6 1/2	-47 1/2 -49	+41 +42 1/2	-145 1/2 -144 1/2

Gage No.	C-1	C-2	C-3	C-4	C-5	C-7
e(concave side)	+2376 +2366	+2503 +2502	+2530 +2529	+2401 +2401	+41 +50	+85 +95
e(convex side)	-2486 -2495	-2463 -2465	-2511 -2516	-2459 -2460	-59 -59	-138 -130
e_a	-55 -64 1/2	+20 +18 1/2	+9 1/2 +6 1/2	-29 -29 1/2	-9 -4 1/2	-26 1/2 -17 1/2

TABLE 8 (continued)

Zero position taken with side bars clamped on

Gage No.	A-2	A-4	B-2	B-4a	B-4b	B-5	B-6	B-7
e(concave side)	+15 +14	+68 +68	+138 +140	+123 +125	+2592 +2520	+2678 +2609	+2697 +2628	+2359 +2310
e(convex side)	-145 -145	-30 -26	-132 -117	-129 -118	-2561 -2492	-2763 -2695	-2595 -2530	-2639 -2581
e_a	-65 -65 1/2	+38 +42	+3 +11 1/2	-3 -3 1/2	+15 1/2 +14	-42 1/2 -43	+51 +49 1/2	-140 -135 1/2

Gage No.	C-1	C-2	C-3	C-4	C-5	C-7
e(concave side)	+2390 +2356	+2555 +2515	+2620 +2569	+2500 +2447	+50 +49	+87 +87
e(convex side)	-2495 -2465	-2504 -2465	-2590 -2526	-2545 -2475	-69 -71	-152 -142
e_a	-52 1/2 -54 1/2	+25 1/2 +25	+15 +21 1/2	-22 1/2 -14	-9 1/2 -11	-32 1/2 -27 1/2

TABLE 9

Test Data For Determining Initial Stresses

in .032 Aluminum Plate

Initial Radius = 7 3/4 inches

e = strain at surface (micro-inches per inch)

e_a = membrane strain (micro-inches per inch)

Test 3

Zero position taken without side bars clamped on

Gage No.	A-2	A-4	B-2	B-4a	B-4b	B-5	B-6	B-7
e(concave side)	+27 +40	+77 +93	+109 +120	+114 +129	+2485 +2485	+2570 +2578	+2581 +2584	+2454 +2474
e(convex side)	-25 -63	-110 -150	-89 -121	-124 -159	-2422 -2442	-2618 -2648	-2473 -2495	-2521 -2558
e_a	+1 -11 1/2	-16 1/2 -28 1/2	+10 - 1/2	-5 -15	+31 1/2 +21 1/2	-24 -35	+54 +44 1/2	-33 1/2 -42

Gage No.	C-1	C-2	C-3	C-4	C-5	C-7
e(concave side)	+2341 +2343	+2459 +2466	+2508 +2508	+2403 +2403	+50 +59	+0 +7
e(convex side)	-2399 -2499	-2368 -2407	-2442 -2472	-2410 -2439	-57 -87	-80 -110
e_a	-29 -78	+45 1/2 +29 1/2	+33 +18	-3 1/2 -18	-3 1/2 -14	-40 -51 1/2

TABLE 9 (continued)

Test 3

Zero position taken with side bars clamped on

Gage No. (see Fig. 4)	A-2	A-4	B-2	B-4a	B-4b	B-5	B-6	B-7
e(concave side)	+37 +41	+75 +87	+90 +118	+104 +127	+2457 +2436	+2541 +2530	+2562 +2543	+2460 +2443
e(convex side)	-18 -34	-130 -149	-103 -108	-136 -139	-2402 -2380	-2598 -2588	-2455 -2435	-2532 -2508
e_a	+9 1/2 +3 1/2	-27 1/2 -31	-6 1/2 +5	-16 -6	+27 1/2 +28	-28 1/2 -29	+53 1/2 +54	-36 +32 1/2

Gage No.	C-1	C-2	C-3	C-4	C-5	C-7
e(concave side)	+2312 +2317	+2459 +2470	+2536 +2529	+2443 +2423	+40 +60	-10 +0
e(convex side)	-2392 -2370	-2388 -2378	-2475 -2462	-2449 -2430	-77 -87	-100 -110
e_a	-40 -26 1/2	+35 1/2 +46	+30 1/2 +33 1/2	-3 -3 1/2	-18 1/2 -13 1/2	-60 -55

TABLE 10

Test Data For Determining Initial Stresses

in .040 Aluminum Plate

Initial Radius = 8.70 inches

e = strain at surface (micro-inches per inch)

e_a = membrane strain (micro-inches per inch)

Zero position taken with side bars clamped on

Gage No. (see Fig. 5)	A-1	A-2	A-3	A-4	A-5	A-6	A-7
	+2472	+2550	+2510	+2587	+2493	+2504	+2437
e(concave side)	+2442	+2512	+2442	+2503	+2411	+2432	+2355
	-2499	-2424	-2580	-2604	-2472	-2390	-2487
e(convex side)	-2489	-2390	-2531	-2536	-2415	-2329	-2428
e_a							
	B-1	B-2	B-3	B-4	B-5	B-6	B-7
	+2586	+2563	+2526	+2491	+2497	+2512	+2510
e(concave side)	+2454	+2424	+2420	+2427	+2428	+2443	+2447
	-2473	-2522	-2539	-2608	-2483	-2509	-2583
e(convex side)	-2368	-2415	-2456	-2546	-2420	-2451	-2533
e_a							
	C-1	C-2	C-3	C-4	C-5	C-6	C-7
	+2492	+2455	+2445	+2490	+2586	+2545	+2473
e(concave side)	+2432	+2365	+2327	+2388	+2496	+2478	+2413
	-2348	-2451	-2522	-2533	-2508	-2416	-2498
e(convex side)	-2293	-2368	-2427	-2446	-2428	-2362	-2450
e_a							

TABLE 10 (continued)

Zero position taken without side bars clamped on

Gage No.	A-1	A-2	A-3	A-4	A-5	A-6	A-7
e(concave side)	+2498 +2439	+2551 +2492	+2447 +2374	+2499 +2422	+2426 +2355	+2503 +2439	+2485 +2410
e(convex side)	-2480 -2469	-2378 -2336	-2492 -2444	-2490 -2433	-2386 -2333	-2364 -2310	-2513 -2455
e_a							

Gage No.	B-1	B-2	B-3	B-4	B-5	B-6	B-7
e(concave side)	+2553 +2421	+2565 +2424	+2579 +2450	+2570 +2478	+2572 +2473	+2544 +2460	+2491 +2430
e(convex side)	-2414 -2317	-2497 -2397	-2562 -2472	-2658 -2580	-2525 -2452	-2510 -2443	-2555 -2507
e_a							

Gage No.	C-1	C-2	C-3	C-4	C-5	C-6	C-7
e(concave side)	+2526 +2457	+2432 +2350	+2392 +2295	+2382 +2310	+2465 +2392	+2507 +2443	+2508 +2430
e(convex side)	-2342 -2302	-2405 -2342	-2458 -2382	-2421 -2370	-2398 -2348	-2360 -2310	-2506 -2456
e_a							

TABLE 11

Membrane strains for second .040 Aluminum Plate

Gage Position see Fig. 5	Membrane strain micro-inches per inch
A-1	-10
A-2	+65
A-3	-10
A-4	-15
B-1	+10
B-2	+10
B-3	0
B-4	-60

TABLE 12

Membrane strains for first .040 Aluminum Plate

Gage Positions (see Fig. 5)	Gage Positions (see Fig. 4)	Membrane strain micro-inches per inch	Assumed Value
C-1	A-1	-16 -26	-21
C-2	A-2	-10 -9	-10
C-3	A-3	+14 +10	+12
C-4	A-4	+21 +19 1/2	+20
B-7	B-1	-16 -21	-18
B-6	B-2	-21 -26	-23
B-5	B-3	+43 1/2 +38 1/2	+41
B-4b	B-4	-18 1/2 -19	-19

TABLE 13

Membrane strains for .032 Aluminum Plate

Gage Positions (see Fig. 5)	Gage Positions (see Fig. 4)	Membrane strain micro-inches per inch Test 1	Test 2	Test 3	Assumed Value
C-1	A-1	-130	-52 1/2	-40	-70
		-131	-54 1/2	-26 1/2	
C-2	A-2	+10 1/2	+25 1/2	+35 1/2	+30
		+18 1/2	+25	+46	
C-3	A-3	+37 1/2	+15	+30 1/2	+30
		+43	+21 1/2	+33 1/2	
C-4	A-4	+10	-22 1/2	-3	-5
		+10 1/2	-14	-3 1/2	
B-7	B-1	-189	-140	-36	-120
		-176 1/2	-135 1/2	-32 1/2	
B-6	B-2	+38 1/2	+51	+53 1/2	+45
		+35 1/2	+49 1/2	+54	
B-5	B-3	-45	-42 1/2	-28 1/2	-40
		-46	-43	-29	
B-4b	B-4	+24 1/2	+15 1/2	+27 1/2	+20
		+24 1/2	+14	+28	

TABLE 14

Membrane strains for .051 Aluminum Plate

Gage Positions (see Fig. 5)	Gage Positions (see Fig. 4)	Membrane strain micro-inches per inch Test 1	Test 2	Assumed Value
C-1	A-1	-42 1/2 -37	-76 -75 1/2	-60
C-2	A-2	-44 -35 1/2	-85 -84	-60
C-3	A-3	-32 1/2 -21	-47 1/2 -49	-35
C-4	A-4	-25 1/2 -18 1/2	-26 -29	-25
B-7	B-1	+43 1/2 +44	+56 +51	+50
B-6	B-2	+68 +69 1/2	+76 1/2 +71	+70
B-5	B-3	-14 1/2 -2 1/2	+ 1/2 +2 1/2	-5
B-4b	B-4	-54 1/2 -42	-41 1/2 -44 1/2	-45

TABLE 15

Calibration Tests
Performed on Flat Plates

Plate No.*	Width of supported edge	Buckling load, lbs.
F,40,1.5,30		
	1 1/4	715
	1	755
F,40,1.5,31		
	1 1/4 (a)	670
	1 1/4 (b)	650
	1	675
	3/4	730
	1/2	600
F,40,1.5,32		
	1 1/4	760
	1	740
	3/4	715
F,40,1.5,33		
	1 1/4	815
	1	625
	3/4	770
	1/2	640

* The designation of the plate number is as follows: F indicates non-prestressed flat plates, the first set of numbers indicates the plate thickness is .040 in., the second set of numbers indicates that the aspect ratio is 1.5, while the last series of numbers indicates that this was the 30th of the type tested.

TABLE 16

Buckling Tests of Flat Plates
With 1/2 Inch Supported Edges

Plate No.	Buckling load, lbs.
F,40,1.5,22	565
23	3 waves
24	560
25	610
29D	560
31D	600
33D	640

Average value = 589 lbs.

TABLE 17

Buckling Tests of Flat Plates
With 3/4 Inch Supported Edges

Plate No.	Buckling load, lbs.
F,40,1.5,26	510
27	580
28	670
29A	crimped Plate
31C	730
32C	715
33C	770

Average value = 663 lbs.

TABLE 18

Buckling Tests of Flat Plates

With 1 Inch Supported Edges

Plate No.	Buckling Load lbs. (Yoshiki's Method)
F,40,1.5,1	750*
2	770*
3	760*
4	-
5	745
6	800*
7	-
8	765
9	745
10	705
11	755
12	755
13	815
14	745
15	600
16	3 waves
17	650
18	730
19	680
20	3 waves
21	690
30B	755
31B	675
32B	740
33B	625

Average value = 726 lbs.

* Gage poorly located - determined buckling load by load vs. bending graph, not shown in Fig. 15.

TABLE 19

Buckling Tests of Ordinary Flat Plates

With 1 1/4 Inch Supported Edges

Plate No.	Buckling Load lbs.
F,40,1.5,30A	715
31A	660
32A	760
33A	815

Average value = 738 lbs.

TABLE 20

Theoretically Calculated Loads Carried by Supported Widths

Width of supported strip	Load carried by strip
1/2 inch	63 lbs.
3/4 inch	95 lbs.
1 inch	126 lbs.
1 1/4 inch	158 lbs.

TABLE 21

Buckling Tests of Non-prestressed Flat Plates, .032 inch Thickness With 1 Inch Supported Edges

Plate No.	Buckling Load (Yoshiki's Method)
F,32,1.5,1	320
2	300
3	400
4	365
5	350
6	255
7	270
8	245

Average buckling load 313 lbs.

TABLE 22

Buckling Tests of Non-Prestressed Flat Plates, .051 Inch Thickness With 1 Inch Supported Edges

Plate No.	Buckling Load (Yoshiki's Method)
F,51,1.5,1	980
2	1490
3	1150
4	1100
5	1200

Average buckling load 1175

TABLE 23

Buckling of .040 Prestressed Plates

Plate No.	Initial Radius Inch	Buckling Load Top of knee	Buckling Load Yoshiki's Method	Buckling Behavior Type
C,40,1.5,27	5	800	?	Mode jump
28			?	" "
29		900	810	Normal
30		700	740	"
31		700	740	Mode jump
32		Approx. 700	?	" "
33		Approx. 1900	680	
34		900	980	Normal
35		Approx. 1200	?	Mode jump
36	5	900	860	Normal
C,40,1.5,2	6	?	1480	"
3		1800	1530	"
4		900	1070	"
13		900	770	Mode jump
24		500	?	Normal
25		750	790	"
37		650	580 or 2180	Double Parabola
38		800	710 or 1460	" "
39		650	810 or 920	" "
40		700	640 or 1840	" "
41		550	?	Normal
42	6	700	650 or 1580	
C,40,1.5,5	7	850	?	Normal
6		1150	?	Mode jump
7		900	880	Normal
8		850	850	"
9		700	760	"
10		600	620	"
11	7	650	620	"
12	7	650	620	"

TABLE 23 (continued)

Plate No.	Initial Radius Inch	Buckling Load Top of knee	Buckling Load Yoshiki's Method	Buckling Behavior Type
C,40,1.5,16	8	900	890	Normal
17		700	820	"
18		1100	910	"
19		750	710	"
20		1100	?	Mode jump
21		1050	980	Normal
22		800	820	"
23	8	600	610	"
C,40,1.5,43	10	800	480	"
44		800	540 and 1900	Double Parabola
45		800	580	Normal
46		800	640	"
47		800	?	"
48		950	700	"
49		800	450	"
50	10	1000	680	"

TABLE 24

Buckling of .032 Inch Prestressed Plates

Plate No.	Initial Radius of Curvature	Buckling Load		Buckling Behavior Type
		Top of knee	Yoshiki's Method	
C,32,1.5,1	5	500	510	Normal
2	5	450	430 or 640	Double Parabola
3	5	1700	1650	Normal
4	5	300	300 or 870	Double Parabola
5	5	550	400	Mode jump
6	5	200	215	Normal
7	5	-	250	"
8	5	-	220 or 710	Double Parabola
9	5	250	225 or 610	" "
C,32,1.5,10	6	450	440	Normal
11	6	250	230	"
12	6	(400+)*	340	Mode jump
13	6	400	430 or 1060	Double Parabola
14	6	400	380 or 1190	Normal
15	6	250	-	"
32	6	350	170	Mode jump
33	6	200	220	Normal
34	6	200	200	"
35	6	400	320	"
36	6	375	270	Mode jump
37	6	-	-	" "
C,32,1.5,16	7	375	-	Normal
17	7	400	350	"
18	7	400	460	"
C,32,1.5,19	7	-	400	"
20	7	400	-	Mode jump
21	7	400	390 or 760	Double Parabola
22	7	500	330	Normal
23	7	200	250	Normal (3 half wave

* Not used in finding averages.

TABLE 24 (Continued)

Plate No.	Initial Radius of Curvature	Buckling Load Top of knee	Buckling Load Yoshiki's Method	Buckling Behavior Type
C,32,1.5,24	∞	350	300	Normal
25	∞	375	320 or 490	Double Parabola
26	∞	550	385	Normal
27	∞	-	300	Mode jump
28	∞	525	465	Normal *
29	∞	400	360 or 530	Double Parabola
30	∞	-	330	Mode jump
31	∞	350	290	Normal

* Not used in finding averages.

TABLE 25

Buckling of .051 Inch Prestressed Plates

Plate No.	Initial Radius of Curvature	Buckling Load Top of knee	Buckling Load Yoshiki's Method	Buckling Behavior Type
C,51,1.5,1	6	2200	?	Mode jump
2	6	2000	?	" "
3	6	1400	?	" "
4	6	2000	?	" "
5	6	2800	?	" "
6	6	1400	1200	Normal
7	6	1900	1200 and 2000	Double Parabola
8	6	1900	1500	Normal
C,51,1.5,9	7	1400	1420	"
10	7	1700	1400 and 2700	Double Parabola
11	7	1400	1220	Normal
12	7	1600	1400	"
13	7	1400	1280	"
14	7	2000	?	Mode jump
15	7	1400	1790	Normal
16	7	1400	1200 and 2800	Double Parabola
C,51,1.5,17	7 3/4	1200	900	Normal
18	7 3/4	1800	?	Mode jump
19	7 3/4	1500	1000	Normal
20	7 3/4	1500	1080	"
21	7 3/4	1400	1250	"
22	7 3/4	1600	1200	"
23	7 3/4	1600	?	"
24	7 3/4	1800	?	"
C,51,1.5,25	9	1300	1150	"
26	9	1500	1180	"
27	9	1400	1210	"
28	9	1450	1160	"
29	9	1600	?	"
30	9	1500	1220	"
31	9	1500	1220	"
32	9	1200	1060	"

TABLE 26

Average Buckling Load of .040 Inch Prestressed Plates

Initial	Top of knee Method		Yoshiki's Method	
Radius, in.	Average Load	No. of tests averaged	Average Load	No. of tests av.
5	967	9	802	6
6	809	11	903 or 1362	10
7	813	8	745	6
8	875	8	820	7
10	844	8	581 or 776	7

TABLE 27

Average Buckling Load of .040 Inch Prestressed Plates

Initial	Top of knee Method		Yoshiki's Method	
Radius, in.	Average Load	No. of tests averaged	Average Load	No. of tests av.
5	967	9	802	6
6	809	11	903 or 1362	10
7	813	8	745	6
8	875	8	820	7

TABLE 28

Average Buckling Loads of .051 Inch Prestressed Plates

Initial	Top of Knee Method			
Radius, In.	Average Load	No. of Tests Averaged	Average Load	No. of Tests Av.
6	1950	8	1300 or 1567	3
7	1538	8	1387 or 1801	7
7 3/4	1550	8	1086	5
9	1469	8	1163	6

TABLE 29

Percent Increase of Buckling Load

Initial Radius of Curvature	Thickness	Net Buckling Load	% Increase of Prestressed Over Ordinary Plate(Net Buckling Loads)
5	.032	499 (405 or 589)	101% (63% or 137%)
6	.032	263 (235 or 379)	67% (-5% or 53%)
7	.032	317 (298 or 360)	28% (20% or 45%)
8	.032	360 (279 or 321)	45% (12% or 29%)
	.032	(248)*	-
5	.040	841 (676)	40% (13%)
6	.040	683 (777 or 1236)	47% (29% or 106%)
7	.040	687 (619)	15% (3%)
8	.040	749 (694)	25% (16%)
	.040	(600)	25% (16%)
10	.040	718 (455 or 652)	19.66% (-24% or 8.66%)
	.040	(600)*	-
6	.051	1426 (1038 or 1305)	56.2% (13.7% or 42.9%)
7	.051	1205 (1125 or 1539)	39.64% (23.22% or 68.56%)
7 3/4	.051	1288 (824)	41% (-9.74%)
9	.051	1207 (901)	32.2% (-1.3%)
	.051	(913)*	-

* Used for purposes of comparison

TABLE 30

Coefficients

$$b_{0,2} = \frac{E}{28.44}\left(2w_{1,1}^2+18w_{3,1}^2+50w_{5,1}^2-4w_{1,1}w_{1,5}-36w_{3,1}w_{3,3}\right.$$

$$-4w_{1,5}w_{1,7}-4w_{1,7}w_{1,9}-4w_{1,9}w_{1,11}w_{1,13}-36w_{3,3}w_{3,5}$$

$$\left.+98w_{7,1}^2+162w_{9,1}^2+242w_{11,1}^2+338w_{13,1}^2-36w_{3,5}w_{3,7}\right)$$

$$b_{0,4} = \frac{E}{455.1}\left(16w_{1,1}w_{1,3}-16w_{1,1}w_{1,5}-16w_{1,3}w_{1,7}-16w_{1,5}w_{1,9}-16w_{1,7}w_{1,11}\right.$$

$$-16w_{1,9}w_{1,13}-16w_{1,11}w_{1,15}+144w_{3,1}w_{3,3}-144w_{3,1}w_{3,5}$$

$$\left.-144w_{3,3}w_{3,7}\cdots\right)$$

$$b_{0,6} = \frac{E}{2304}\left(36w_{1,1}w_{1,5}-36w_{1,1}w_{1,7}+18w_{1,3}^2-36w_{1,3}w_{1,9}\right.$$

$$-36w_{1,5}w_{1,11}-36w_{1,7}w_{1,13}-36w_{1,9}w_{1,15}+324w_{3,1}w_{3,5}$$

$$\left.-324w_{3,1}w_{3,7}+162w_{3,3}^2-324w_{3,3}w_{3,9}\cdots\right)$$

$$b_{0,8} = \frac{E}{7282}\left(64w_{1,1}w_{1,7}-64w_{1,1}w_{1,9}+64w_{1,3}w_{1,5}-64w_{1,3}w_{1,11}\right.$$

$$\left.-64w_{1,5}w_{1,13}-64w_{1,7}w_{1,15}+576w_{3,1}w_{3,7}-576w_{3,1}w_{3,9}\cdots\right)$$

$$b_{0,10} = \frac{E}{17778}\,(100w_{1,1}w_{1,9} - 100w_{1,1}w_{1,11} + 100w_{1,3}w_{1,7} - 100w_{1,3}w_{1,13}$$

$$+ 50w_{1,5}^{2} - 100w_{1,5}w_{1,15} + 900w_{3,1}w_{3,9} - 900w_{3,1}w_{3,11}$$

$$+ 900w_{3,3}w_{3,7} \cdots)$$

$$b_{0,12} = \frac{E}{36864}\,(144w_{1,1}w_{1,11} - 144w_{1,1}w_{1,13} + 144w_{1,3}w_{1,9} - 144w_{1,3}w_{1,15}$$

$$+ 144w_{1,5}w_{1,7} + 1296w_{3,1}w_{3,11} - 1296w_{3,1}w_{3,13} + 1296w_{3,3}w_{3,9}$$

$$+ 1296w_{3,5}w_{3,7} \cdots)$$

$$b_{2,0} = \frac{E}{144.0}\,(2w_{1,1}^{2} - 4w_{1,1}w_{3,1} + 18w_{1,3}^{2} - 36w_{1,3}w_{3,3}$$

$$+ 50w_{1,5}^{2} - 100w_{1,5}w_{3,5} + 98w_{1,7}^{2} - 196w_{1,7}w_{3,7}$$

$$+ 162w_{1,9}^{2} + 242w_{1,11}^{2} + 338w_{1,13}^{2} - 4w_{3,1}w_{5,1} \cdots)$$

$$b_{2,2} = \frac{E}{300.4}\,(16w_{1,1}w_{1,3} + 16w_{1,1}w_{3,1} + 64w_{1,3}w_{1,5} - 64w_{1,3}w_{3,1}$$

$$- 16w_{1,3}w_{3,5} + 144w_{1,5}w_{1,7} - 144w_{1,5}w_{3,3} - 64w_{1,5}w_{3,7}$$

$$- 576w_{1,9}w_{3,3} - 784w_{1,11}w_{3,5} \cdots)$$

TABLE 30 (Continued)

$$b_{2,4} = \frac{E}{1111}\,(-4w_{1,1}w_{1,3}+36w_{1,1}w_{1,5}+36w_{1,1}w_{3,3}-4w_{1,1}w_{3,5}$$

$$+100w_{1,3}w_{1,7}+100w_{1,3}w_{3,1}-4w_{1,3}w_{3,7}+196w_{1,5}w_{1,9}$$

$$-196w_{1,5}w_{3,1}-36w_{1,5}w_{3,9}+324w_{1,7}w_{1,11}-324w_{1,7}w_{3,3}$$

$$+484w_{1,9}w_{1,13}-484w_{1,9}w_{3,5}+676w_{1,11}w_{1,15}+196w_{3,1}w_{5,3}\cdots)$$

$$b_{2,6} = \frac{E}{3600}\,(-16w_{1,1}w_{1,5}+64w_{1,1}w_{1,7}+64w_{1,1}w_{3,5}-16w_{1,1}w_{3,7}$$

$$+144w_{1,3}w_{1,9}+144w_{1,3}w_{3,3}+256w_{1,5}w_{1,11}+256w_{1,5}w_{3,1}$$

$$-16w_{1,5}w_{3,11}+400w_{1,7}w_{1,13}-400w_{1,7}w_{3,1}+576w_{1,9}w_{1,15}$$

$$-576w_{1,9}w_{3,3}-784w_{1,11}w_{3,5}\cdots)$$

TABLE 30 (Continued)

$$b_{2,8} = \frac{E}{9474}\,(-36w_{1,1}w_{1,7}+100w_{1,1}w_{1,9}+100w_{1,1}w_{3,7}-36w_{1,1}w_{3,9}$$

$$-4w_{1,3}w_{1,5}+196w_{1,3}w_{1,11}+196w_{1,3}w_{3,5}-4w_{1,3}w_{3,11}$$

$$+324w_{1,5}w_{1,13}+324w_{1,5}w_{3,3}-4w_{1,5}w_{3,13}+484w_{1,7}w_{3,1}$$

$$+484w_{1,7}w_{1,15}-676w_{1,9}w_{3,1}-900w_{1,11}w_{3,3}\cdots)$$

$$b_{2,10} = \frac{E}{21120}\,(-64w_{1,1}w_{1,9}+144w_{1,1}w_{1,11}+144w_{1,1}w_{3,9}-64w_{1,1}w_{3,11}$$

$$-16w_{1,3}w_{1,7}+256w_{1,3}w_{1,13}+256w_{1,3}w_{3,7}-16w_{1,3}w_{3,13}$$

$$+400w_{1,5}w_{1,15}+400w_{1,5}w_{3,5}+576w_{1,7}w_{3,3}+784w_{1,9}w_{3,1}$$

$$-1024w_{1,11}w_{3,1}-1296w_{1,13}w_{3,3}-1600w_{1,15}w_{3,5}\cdots)$$

$$b_{2,12} = \frac{E}{41616}\,(-100w_{1,1}w_{1,11}+196w_{1,1}w_{1,13}+196w_{1,1}w_{3,11}-100w_{1,1}w_{3,13}$$

$$-36w_{1,3}w_{1,9}+324w_{1,3}w_{1,15}+324w_{1,3}w_{3,9}-4w_{1,5}w_{1,7}$$

$$+484w_{1,5}w_{3,7}+676w_{1,7}w_{3,5}+900w_{1,9}w_{3,3}+1156w_{1,11}w_{3,1}$$

$$-144w_{1,13}w_{3,1}-176w_{1,15}w_{3,3}\cdots)$$

TABLE 30 (Continued)

$$b_{4,0} = \frac{E}{2304} \left(16w_{1,1}w_{3,1} - 16w_{1,1}w_{5,1} + 144w_{1,3}w_{3,3} - 144w_{1,3}w_{5,3}\right.$$

$$\left. + 400w_{1,5}w_{3,5} + 784w_{1,7}w_{3,7} \cdots\right)$$

$$b_{4,2} = \frac{E}{2844} \left(-4w_{1,1}w_{3,,} + 36w_{1,1}w_{3,3} + 36w_{1,1}w_{5,1} - 4w_{1,1}w_{5,3}\right.$$

$$+ 100w_{1,3}w_{3,1} + 196w_{1,3}w_{3,5} - 196w_{1,3}w_{5,1} + 324w_{1,5}w_{3,3}$$

$$+ 484w_{1,5}w_{3,7} - 484w_{1,5}w_{5,3} + 676w_{1,7}w_{3,5}$$

$$\left. + 1156w_{1,9}w_{3,7} \cdots\right)$$

$$b_{4,4} = \frac{E}{4807} \left(64w_{1,1}w_{3,5} + 64w_{1,1}w_{5,3} - 64w_{1,3}w_{3,1} + 256w_{1,3}w_{3,7}\right.$$

$$+ 256w_{1,3}w_{5,1} + 256w_{1,5}w_{3,1} + 576w_{1,5}w_{3,9}$$

$$\left. - 576w_{1,5}w_{5,1} + 576w_{1,7}w_{3,3} + 1024w_{1,9}w_{3,5} \cdots\right)$$

$$b_{4,6} = \frac{E}{9216} \left(-4w_{1,1}w_{3,5} + 100w_{1,1}w_{3,7} + 100w_{1,1}w_{5,5} - 36w_{1,3}w_{3,3}\right.$$

TABLE 30 (Continued)

$$+324w_{1,3}w_{3,9}+324w_{1,3}w_{5,3}-196w_{1,5}w_{3,1}+676w_{1,5}w_{3,11}$$

$$+676w_{1,5}w_{5,1}+484w_{1,7}w_{3,1}+900w_{1,9}w_{3,3}+144w_{1,11}w_{3,5}\cdots)$$

$$b_{4,8}=\frac{E}{17778}\ (-16w_{1,1}w_{3,7}+144w_{1,1}w_{3,9}-16w_{1,3}w_{3,5}+400w_{1,3}w_{3,11}$$

$$-144w_{1,5}w_{3,3}+784w_{1,5}w_{3,13}+784w_{1,5}w_{5,3}-400w_{1,7}w_{3,1}$$

$$+784w_{1,9}w_{3,1}+1296w_{1,11}w_{3,3}\cdots)$$

$$b_{6,0}=\frac{E}{11664}\ (36w_{1,1}w_{5,1}+324w_{1,3}w_{5,3}+18w_{3,1}^{2}+162w_{3,3}^{2}\cdots)$$

$$b_{6,2}=\frac{E}{12844}\ (-16w_{1,1}w_{5,1}+64w_{1,1}w_{5,3}+256w_{1,3}w_{5,1}+784w_{1,5}w_{5,3}$$

$$+144w_{3,1}w_{3,3}+576w_{3,3}w_{3,5}\cdots)$$

$$b_{6,4}=\frac{E}{16727}\ (-4w_{1,1}w_{5,3}+100w_{1,1}w_{5,5}-196w_{1,3}w_{5,1}+676w_{1,5}w_{5,1}$$

$$-36w_{3,1}w_{3,3}+324w_{3,1}w_{3,5}+900w_{3,3}w_{3,7}\cdots)$$

TABLE 30 (Continued)

$$b_{6,6} = \frac{E}{24354} \left(-144w_{1,3}w_{5,3} - 576w_{1,5}w_{5,1} - 144w_{3,1}w_{3,5} + 576w_{3,1}w_{3,7} + 1296w_{3,3}w_{3,9} \cdots\right)$$

$$b_{8,0} = \frac{E}{36864} \left(64w_{3,1}w_{5,1} \cdots\right)$$

$$b_{8,2} = \frac{E}{38940} \left(-4w_{3,1}w_{5,1} + 196w_{3,1}w_{5,3} + 324w_{3,3}w_{5,1} \cdots\right)$$

$$b_{8,4} = \frac{E}{45511} \left(-16w_{3,1}w_{5,3} - 144w_{3,3}w_{5,1} \cdots\right)$$

$$b_{10,0} = \frac{E}{90000} \left(50w_{5,1}^{2} \cdots\right)$$

TABLE 31

Coefficients

	D_1	D_2	D_3	D_4	D_5	D_6
$w_{1,1}^3$	1.451	-.02705	-.001497	0	0	0
$w_{1,1}^2 w_{1,3}$	-.972	.448	.01149	-.00805	-.01488	0
$w_{1,1}^2 w_{3,1}$	-.1920	.0410	.264	-.0364	0	-.000711
$w_{1,1}^2 w_{3,3}$	0	-.0542	-.0689	.1298	.00957	.000843
$w_{1,1}^2 w_{1,5}$	0	-.0875	0	.00832	.1492	0
$w_{1,1}^2 w_{5,1}$	0	0	-.00517	.00325	0	.0945
$w_{1,1} w_{1,3}^2$	5.38	0	-.0642	0	.0417	0
$w_{1,1} w_{3,1}^2$	11.30	-.414	0	0	0	.00695
$w_{1,1} w_{3,3}^2$	10.50	0	0	0	.0751	.0213
$w_{1,1} w_{1,5}^2$	10.50	0	-.1382	0	0	0
$w_{1,1} w_{5,1}^2$	29.35	-.811	0	0	0	0
$w_{1,1} w_{1,3} w_{3,1}$	.983	-.459	-.232	.205	.0604	.00918
$w_{1,1} w_{1,3} w_{3,3}$	-1.301	0	.387	0	-.0681	-.0247
$w_{1,1} w_{1,3} w_{1,5}$	-2.095	.490	.0992	-.0593	0	0

TABLE 31 (Continued)

	D_1	D_2	D_3	D_4	D_5	D_6
$w_{1,1}w_{1,3}w_{5,1}$	0	0	.0667	-.0948	0	-.0626
$w_{1,1}w_{3,1}w_{3,3}$	-5.89	1.382	0	0	-.2015	-.01457
$w_{1,1}w_{3,1}w_{1,5}$	0	.354	0	-.1753	-.1680	0
$w_{1,1}w_{3,1}w_{5,1}$	-.443	.238	.1009	-.0559	0	0
$w_{1,1}w_{3,3}w_{1,5}$	1.342	-.400	-.332	.1307	0	.0271
$w_{1,1}w_{3,3}w_{5,1}$	.525	-.642	-.1058	.1637	.1200	0
$w_{1,1}w_{1,5}w_{5,1}$	0	0	0	.1041	0	0
$w_{1,3}^3$	0	1.632	0	-.0640	0	0
$w_{1,3}^2w_{3,1}$	-2.755	0	.740	0	-.1118	-.0209
$w_{1,3}^2w_{3,3}$	0	-1.297	0	.668	0	0
$w_{1,3}^2w_{1,5}$	2.935	0	-.1837	0	.848	0
$w_{1,3}^2w_{5,1}$	0	0	-.1520	0	0	.1998
$w_{1,3}w_{3,1}^2$	-4.96	2.64	0	0	-.2141	-.0253
$w_{1,3}w_{3,3}^2$	0	4.52	0	0	0	0

TABLE 31 (Continued)

	D_1	D_2	D_3	D_4	D_5	D_6
$w_{1,3}w_{1,5}^2$	0	4.99	0	-.397	0	0
$w_{1,3}w_{5,1}^2$	-9.72	5.17	0	0	-.431	0
$w_{1,3}w_{3,1}w_{3,3}$	16.59	0	0	0	.517	.1209
$w_{1,3}w_{3,1}w_{1,5}$	4.25	-1.310	-.704	.450	0	.0647
$w_{1,3}w_{3,1}w_{5,1}$	2.855	-1.087	-.367	.465	.286	0
$w_{1,3}w_{3,3}w_{1,5}$	-4.78	0	.850	0	-.915	-.1031
$w_{1,3}w_{3,3}w_{5,1}$	-7.68	0	.878	0	-.456	0
$w_{1,3}w_{1,5}w_{5,1}$	0	0	.469	-.396	0	-.1952
$w_{3,1}^3$	0	0	2.02	-.324	0	0
$w_{3,1}^2w_{3,3}$	0	0	-1.839	2.165	0	0
$w_{3,1}^2w_{1,5}$	0	-1.257	0	0	1.047	0
$w_{3,1}^2w_{5,1}$	2.155	-.655	0	0	0	.793
$w_{3,1}w_{3,3}^2$	0	0	4.09	0	0	0
$w_{3,1}w_{1,5}^2$	-5.92	0	1.719	0	0	-.0886
$w_{3,1}w_{5,1}^2$	0	0	5.76	-1.120	0	0

TABLE 31 (Continued)

	D_1	D_2	D_3	D_4	D_5	D_6
$w_{3,1}w_{3,3}w_{1,5}$	-14.18	3.040	0	0	0	-.1660
$w_{3,1}w_{3,3}w_{5,1}$	-4.53	3.135	0	0	-.733	-.585
$w_{3,1}w_{1,5}w_{5,1}$	0	1.679	0	-.637	-.782	0
$w_{3,3}^3$	0	0	0	1.451	0	0
$w_{3,3}^2w_{1,5}$	5.27	0	0	0	1.850	.1281
$w_{3,3}^2w_{5,1}$	6.63	0	0	0	.566	.910
$w_{3,3}w_{1,5}^2$	0	-2.685	0	1.608	0	0
$w_{3,3}w_{5,1}^2$	0	0	-2.12	3.50	0	0
$w_{3,3}w_{1,5}w_{5,1}$	8.44	-2.68	-1.205	.984	0	0
$w_{1,5}^3$	0	0	0	0	1.920	0
$w_{1,5}^2w_{5,1}$	0	0	-.642	0	0	.586
$w_{1,5}w_{5,1}^2$	0	-2.53	0	0	2.51	0
$w_{5,1}^3$	0	0	0	0	0	2.12

TABLE 31 (continued)

$(D_7 - D_{12})$

	D_7	D_8	D_9	D_{10}	D_{11}	D_{12}
$w_{1,1}^3$	0	0	0	0	0	0
$w_{1,1}^2 w_{1,3}$	0	0	0	0	0	0
$w_{1,1}^2 w_{3,1}$	0	0	0	0	0	.00000802
$w_{1,1}^2 w_{3,3}$	0	0	0	0	0	-.001499
$w_{1,1}^2 w_{1,5}$	0	0	0	0	0	0
$w_{1,1}^2 w_{5,1}$	-.000203	0	0	0	0	-.02025
$w_{1,1} w_{1,3}^2$	0	0	0	0	0	0
$w_{1,1} w_{3,1}^2$	-.000233	0	0	0	0	-.001217
$w_{1,1} w_{3,3}^2$	-.00250	0	0	0	0	0
$w_{1,1} w_{1,5}^2$	0	0	0	0	0	0
$w_{1,1} w_{5,1}^2$	0	.000509	-.0000531	0	0	0
$w_{1,1} w_{1,3} w_{3,1}$	0	0	0	0	0	-.00650
$w_{1,1} w_{1,3} w_{3,3}$	0	0	0	0	0	0
$w_{1,1} w_{1,3} w_{1,5}$	0	0	0	0	0	0

TABLE 31 (Continued)

	D_7	D_8	D_9	D_{10}	D_{11}	D_{12}
$w_{1,1}w_{1,3}w_{5,1}$	.00462	0	0	0	0	.0931
$w_{1,1}w_{3,1}w_{3,3}$	.001197	0	0	0	0	.01295
$w_{1,1}w_{3,1}w_{1,5}$	0	0	0	0	0	.01490
$w_{1,1}w_{3,1}w_{5,1}$	.00471	-.0002050	0	0	0	0
$w_{1,1}w_{3,3}w_{1,5}$	0	0	0	0	0	-.01303
$w_{3,3}w_{5,1}$	-.00216	.000730	0	0	0	0
$w_{1,1}w_{1,5}w_{5,1}$	0	0	0	0	0	-.0616
$w_{1,3}^3$	0	0	0	0	0	0
$w_{1,3}^2w_{3,1}$	0	0	0	0	0	0
$w_{1,3}^2w_{3,3}$	0	0	0	0	0	-.0404
$w_{1,3}^2w_{1,5}$	0	0	0	0	0	0
$w_{1,3}^2w_{5,1}$	-.00718	0	0	0	0	0
$w_{1,3}w_{3,1}^2$	-.001727	0	0	0	0	.0315
$w_{1,3}w_{3,3}^2$	0	0	0	0	0	.0714
$w_{1,3}w_{1,5}^2$	0	0	0	0	0	0

TABLE 31 (Continued)

	D_7	D_8	D_9	D_{10}	D_{11}	D_{12}
$w_{1,3}w_{5,1}^2$	0	-.002445	.000416	0	0	0
$w_{1,3}w_{3,1}w_{3,3}$	-.01307	0	0	0	0	0
$w_{1,3}w_{3,1}w_{1,5}$	0	0	0	0	0	-.0391
$w_{1,3}w_{3,1}w_{5,1}$	-.01845	.001781	0	0	0	0
$w_{1,3}w_{3,3}w_{1,5}$	0	0	0	0	0	0
$w_{1,3}w_{3,3}w_{5,1}$	.0296	-.00582	0	0	0	0
$w_{1,3}w_{1,5}w_{5,1}$	.0313	0	0	0	0	.1491
$w_{3,1}^3$	0	-.0000201	0	0	0	0
$w_{3,1}^2w_{3,3}$	0	.000292	0	0	0	0
$w_{3,1}^2w_{1,5}$	0	0	0	0	0	-.0493
$w_{3,1}^2w_{5,1}$	0	0	-.0000288	0	0	-.1859
$w_{3,1}w_{3,3}^2$	0	-.001701	0	0	0	0
$w_{3,1}w_{1,5}^2$	0	0	0	0	0	0
$w_{3,1}w_{5,1}^2$	.01522	0	0	-.00001529	0	0
$w_{3,1}w_{3,3}w_{1,5}$	.02185	0	0	0	0	.0822

TABLE 31 (Continued)

	D_7	D_8	D_9	D_{10}	D_{11}	D_{12}
$w_{3,1}w_{3,3}w_{5,1}$	0	0	.000374	0	0	.823
$w_{3,1}w_{1,5}w_{5,1}$	0	0	0	0	0	0
$w_{3,3}^3$	0	0	0	0	0	0
$w_{3,3}^2w_{1,5}$	-.01810	0	0	0	0	0
$w_{3,3}^2w_{5,1}$	0	0	-.001024	0	0	0
$w_{3,3}w_{1,5}^2$	0	0	0	0	0	-.1239
$w_{3,3}w_{5,1}^2$	-.0339	0	0	.0001128	0	0
$w_{3,3}w_{1,5}w_{5,1}$	-.0697	.01172	0	0	0	0
$w_{1,5}^3$	0	0	0	0	0	0
$w_{1,5}^2w_{5,1}$	-.0393	0	0	0	0	0
$w_{1,5}w_{5,1}^2$	0	0	0	0	0	0
$w_{5,1}^3$	0	0	0	0	-.00000263	-.502

TABLE 31 (continued)

$(D_{13} - D_{18})$

	D_{13}	D_{14}	D_{15}	D_{16}	D_{17}	D_{18}
$w_{1,1}^3$	0	0	0	0	0	0
$w_{1,1}^2 w_{1,3}$	0	0	0	0	.0000427	0
$w_{1,1}^2 w_{3,1}$	0	0	0	0	0	0
$w_{1,1}^2 w_{3,3}$	0	0	0	0	-.01541	0
$w_{1,1}^2 w_{1,5}$	0	0	0	0	-.00948	0
$w_{1,1}^2 w_{5,1}$	.00000851	0	0	0	0	0
$w_{1,1} w_{1,3}^2$	0	0	0	0	-.00253	0
$w_{1,1} w_{3,1}^2$	.00000241	0	0	0	0	0
$w_{1,1} w_{3,3}^2$	0	0	0	0	0	0
$w_{1,1} w_{1,5}^2$	0	0	0	0	0	0
$w_{1,1} w_{5,1}^2$	0	-.0000757	.000001522	0	0	0
$w_{1,1} w_{1,3} w_{3,1}$	0	0	0	0	-.0371	.000461
$w_{1,1} w_{1,3} w_{3,3}$	0	0	0	0	.0451	-.001522
$w_{1,1} w_{1,3} w_{1,5}$	0	0	0	0	0	0

TABLE 31 (Continued)

	D_{13}	D_{14}	D_{15}	D_{16}	D_{17}	D_{18}
$w_{1,1}w_{1,3}w_{5,1}$	-.00368	0	0	0	.0227	.000510
$w_{1,1}w_{3,1}w_{3,3}$	-.001042	0	0	0	0	-.00318
$w_{1,1}w_{3,1}w_{1,5}$	0	0	0	0	.1190	0
$w_{1,1}w_{3,1}w_{5,1}$	-.001486	.00000902	0	0	0	0
$w_{1,1}w_{3,3}w_{1,5}$	0	0	0	0	0	0
$w_{1,1}w_{3,3}w_{5,1}$	.00793	-.000534	0	0	-.0522	0
$w_{1,1}w_{1,5}w_{5,1}$	.00897	0	0	0	-.0972	.0725
$w_{1,3}^{3}$	0	0	0	0	0	0
$w_{1,3}^{2}w_{3,1}$	0	0	0	0	.0456	-.00323
$w_{1,3}^{2}w_{3,3}$	0	0	0	0	0	0
$w_{1,3}^{2}w_{1,5}$	0	0	0	0	-.0847	0
$w_{1,3}^{2}w_{5,1}$	0	0	0	0	-.0401	.0266
$w_{1,3}w_{3,1}^{2}$	-.001942	0	0	0	0	-.00828
$w_{1,3}w_{3,3}^{2}$	-.01305	0	0	0	0	0

TABLE 31 (Continued)

	D_{13}	D_{14}	D_{15}	D_{16}	D_{17}	D_{18}
$w_{1,3}w_{1,5}^2$	0	0	0	0	0	0
$w_{1,3}w_{5,1}^2$	0	.00568	-.000708	0	0	0
$w_{1,3}w_{3,1}w_{3,3}$	0	0	0	0	0	.01880
$w_{1,3}w_{3,1}w_{1,5}$	0	0	0	0	0	0
$w_{1,3}w_{3,1}w_{5,1}$	.0312	-.002445	0	0	-.1507	0
$w_{1,3}w_{3,3}w_{1,5}$	0	0	0	0	.467	-.0599
$w_{1,3}w_{3,3}w_{5,1}$	0	0	0	0	.1499	0
$w_{1,3}w_{1,5}w_{5,1}$	-.0203	0	0	0	0	0
$w_{3,1}^3$	0	0	0	0	0	0
$w_{3,1}^2w_{3,3}$	0	-.0002820	0	0	-.408	0
$w_{3,1}^2w_{1,5}$	.00582	0	0	0	0	.0449
$w_{3,1}^2w_{5,1}$	0	0	.0000000316	0	0	0
$w_{3,1}w_{3,3}$	0	0	0	0	.426	0
$w_{3,1}w_{1,5}^2$	0	0	0	0	0	0
$w_{3,1}w_{5,1}^2$	-.00583	0	0	.0000000165	0	0

TABLE 31 (Continued)

	D_{13}	D_{14}	D_{15}	D_{16}	D_{17}	D_{18}
$w_{3,1}w_{3,3}w_{1,5}$	-.01328	0	0	0	0	0
$w_{3,1}w_{3,3}w_{5,1}$	0	0	-.000378	0	0	-.2605
$w_{3,1}w_{1,5}w_{5,1}$	-.0496	.00730	0	0	.485	0
$w_{3,3}^{3}$	0	-.001499	0	0	0	0
$w_{3,3}^{2}w_{1,5}$	0	0	0	0	0	.1514
$w_{3,3}^{2}w_{5,1}$	0	0	0	0	0	.1233
$w_{3,3}w_{1,5}^{2}$	0	0	0	0	0	0
$w_{3,3}w_{5,1}^{2}$	.0738	0	0	-.0001408	-.803	0
$w_{3,3}w_{1,5}w_{5,1}$	.0465	-.00822	0	0	0	0
$w_{1,5}^{3}$	0	0	0	0	-.2065	0
$w_{1,5}^{2}w_{5,1}$	0	0	0	0	0	0
$w_{1,5}w_{5,1}^{2}$	0	-.01147	.00209	0	0	0
$w_{5,1}^{3}$	0	0	0	0	0	0

TABLE 31

$(D_{19} - D_{24})$

	D_{19}	D_{20}	D_{21}	D_{22}	D_{23}	D_{24}
$w_{1,1}^3$	0	0	0	0	0	0
$w_{1,1}^2 w_{1,3}$	0	0	0	0	0	0
$w_{1,1}^2 w_{3,1}$	0	0	0	0	0	0
$w_{1,1}^2 w_{3,3}$	0	0	0	0	0	0
$w_{1,1}^2 w_{1,5}$	0	0	0	0	-.00456	.0000900
$w_{1,1}^2 w_{5,1}$	0	0	0	0	0	0
$w_{1,1} w_{1,3}^2$	0	0	0	0	-.00474	.00001822
$w_{1,1} w_{3,1}^2$	0	0	0	0	0	0
$w_{1,1} w_{3,3}^2$	-.0001518	0	0	0	-.0360	0
$w_{1,1} w_{1,5}^2$	0	0	0	0	0	0
$w_{1,1} w_{5,1}^2$	0	0	0	0	0	0
$w_{1,1} w_{1,3} w_{3,1}$	0	0	0	0	0	0
$w_{1,1} w_{1,3} w_{3,3}$	0	0	0	0	.01611	-.01428
$w_{1,1} w_{1,3} w_{1,5}$	0	0	0	0	.0332	-.00454

TABLE 31 (Continued)

	D_{19}	D_{20}	D_{21}	D_{22}	D_{23}	D_{24}
$w_{1,1}w_{1,3}w_{5,1}$	.000510	0	0	0	0	0
$w_{1,1}w_{3,1}w_{3,3}$	.00001970	0	0	0	0	0
$w_{1,1}w_{3,1}w_{1,5}$	0	0	0	0	.03245	-.02215
$w_{1,1}w_{3,1}w_{5,1}$	0	0	0	0	0	0
$w_{1,1}w_{3,3}w_{1,5}$	0	0	0	0	-.0272	.0251
$w_{1,1}w_{3,3}w_{5,1}$	-.00379	.0000325	0	0	0	0
$w_{1,1}w_{1,5}w_{5,1}$	-.00804	0	0	0	0	.0228
$w_{1,3}^3$	0	0	0	0	0	0
$w_{1,3}^2w_{3,1}$	0	0	0	0	.0208	-.01120
$w_{1,3}^2w_{3,3}$	0	0	0	0	0	0
$w_{1,3}^2w_{1,5}$	0	0	0	0	0	0
$w_{1,3}^2w_{5,1}$	-.001700	0	0	0	0	.01730
$w_{1,3}w_{3,1}^2$	.000284	0	0	0	0	0
$w_{1,3}w_{3,3}^2$	0	0	0	0	0	0
$w_{1,3}w_{1,5}^2$	0	0	0	0	.0750	-.01729

TABLE 31 (Continued)

	D_{19}	D_{20}	D_{21}	D_{22}	D_{23}	D_{24}
$w_{1,3}w_{5,1}^2$	0	-.001925	.0001578	0	0	0
$w_{1,3}w_{3,1}w_{3,3}$	-.002005	0	0	0	-.1502	0
$w_{1,3}w_{3,1}w_{1,5}$	0	0	0	0	-.1124	.0698
$w_{1,3}w_{3,1}w_{5,1}$	-.01086	.000548	0	0	0	0
$w_{1,3}w_{3,3}w_{1,5}$	0	0	0	0	0	0
$w_{1,3}w_{3,3}w_{5,1}$	.01628	-.001613	0	0	.1490	-.0667
$w_{1,3}w_{1,5}w_{5,1}$	0	0	0	0	0	-.0819
$w_{3,1}^3$	0	0	0	0	0	0
$w_{3,1}^2w_{3,3}$	0	.00001907	0	0	0	0
$w_{3,1}^2w_{1,5}$	-.00548	0	0	0	-.1013	0
$w_{3,1}^2w_{5,1}$	0	0	0	0	0	0
$w_{3,1}w_{3,3}^2$	0	-.0002285	0	0	0	-.1757
$w_{3,1}w_{1,5}^2$	0	0	0	0	0	0
$w_{3,1}w_{5,1}^2$	0	0	0	0	0	0

TABLE 31 (Continued)

	D_{19}	D_{20}	D_{21}	D_{22}	D_{23}	D_{24}
$w_{3,1}w_{3,3}w_{1,5}$	0	0	0	0	.273	0
$w_{3,1}w_{3,3}w_{5,1}$	0	0	.0000348	0	0	0
$w_{3,1}w_{1,5}w_{5,1}$	.0594	-.00831	0	0	.2105	-.1268
$w_{3,3}^{3}$	0	0	0	0	0	0
$w_{3,3}^{2}w_{1,5}$	-.01320	0	0	0	0	0
$w_{3,3}^{2}w_{5,1}$	0	0	-.0001857	0	-.219	0
$w_{3,3}w_{1,5}^{2}$	0	0	0	0	-.1600	.1152
$w_{3,3}w_{5,1}^{2}$	-.0314	0	0	.00001683	0	0
$w_{3,3}w_{1,5}w_{5,1}$	0	0	0	0	-.344	.1475
$w_{1,5}^{3}$	0	0	0	0	0	0
$w_{1,5}^{2}w_{5,1}$	0	0	0	0	0	0
$w_{1,5}w_{5,1}^{2}$	0	.01672	-.00285	0	-.2995	0
$w_{5,1}^{2}$	0	0	0	0	0	0

TABLE 31

$(D_{25} - D_{30})$

	D_{25}	D_{26}	D_{27}	D_{28}	D_{29}	D_{30}
$w_{1,1}^3$	0	0	0	0	0	0
$w_{1,1}^2 w_{1,3}$	0	0	0	0	0	0
$w_{1,1}^2 w_{3,1}$	0	0	0	0	0	0
$w_{1,1}^2 w_{3,3}$	0	0	0	0	0	0
$w_{1,1}^2 w_{1,3}$	0	0	0	0	0	0
$w_{1,1}^2 w_{5,1}$	0	0	0	0	0	0
$w_{1,1} w_{1,3}^2$	0	0	0	0	0	0
$w_{1,1} w_{3,1}^2$	0	0	0	0	0	0
$w_{1,1} w_{3,3}^2$	-.000641	0	0	0	0	0
$w_{1,1} w_{1,5}^2$	0	0	0	0	.00706	-.000692
$w_{1,1} w_{5,1}^2$	0	0	0	0	0	0
$w_{1,1} w_{1,3} w_{3,1}$	0	0	0	0	0	0
$w_{1,1} w_{1,3} w_{3,3}$	.0000797	0	0	0	0	0
$w_{1,1} w_{1,3} w_{1,5}$	0	0	0	0	-.00418	.0000860

TABLE 31 (Continued)

	D_{25}	D_{26}	D_{27}	D_{28}	D_{29}	D_{30}
$w_{1,1}w_{1,3}w_{5,1}$	0	0	0	0	0	0
$w_{1,1}w_{3,1}w_{3,3}$	0	0	0	0	0	0
$w_{1,1}w_{3,1}w_{1,5}$	.000920	0	0	0	0	0
$w_{1,1}w_{3,1}w_{5,1}$	0	0	0	0	0	0
$w_{1,1}w_{3,3}w_{1,5}$	-.00352	0	0	0	.01081	-.00813
$w_{1,1}w_{3,3}w_{5,1}$	0	0	0	0	0	0
$w_{1,1}w_{1,5}w_{5,1}$	-.0204	.001021	0	0	0	0
$w_{1,3}^{3}$	0	0	0	0	-.000494	0
$w_{1,3}^{2}w_{3,1}$	.000468	0	0	0	0	0
$w_{1,3}^{2}w_{3,3}$	0	0	0	0	.00505	-.00376
$w_{1,3}^{2}w_{1,5}$	0	0	0	0	0	0
$w_{1,3}^{2}w_{5,1}$	-.01268	.000548	0	0	0	0

TABLE 31 (Continued)

	D_{25}	D_{26}	D_{27}	D_{28}	D_{29}	D_{30}
$w_{1,3}w_{3,1}w_{3,3}$	-.00796	.000274	0	0	0	0
$w_{1,3}w_{3,1}w_{1,5}$	-.00827	0	0	0	.0247	-.01657
$w_{1,3}w_{3,1}w_{5,1}$	0	0	0	0	0	0
$w_{1,3}w_{3,3}w_{1,5}$	0	0	0	0	0	0
$w_{1,3}w_{3,3}w_{5,1}$	0	-.00808	-.000491	0	0	0
$w_{1,3}w_{1,5}w_{5,1}$	.0538	-.00580	0	0	0	.0328
$w_{3,1}^{3}$	0	0	0	0	0	0
$w_{3,1}^{2}w_{3,3}$	0	0	0	0	0	0
$w_{3,1}^{2}w_{1,5}$	-.00999	.000997	0	0	0	0
$w_{3,1}^{2}w_{5,1}$	0	0	0	0	0	0
$w_{3,1}w_{3,3}^{2}$	0	0	.00000880	0	0	0
$w_{3,1}w_{1,5}^{2}$	0	0	0	0	-.0303	.0250
$w_{3,1}w_{5,1}^{2}$	0	0	0	0	0	0

TABLE 31 (Continued)

	D_{25}	D_{26}	D_{27}	D_{28}	D_{29}	D_{30}
$w_{3,1}w_{3,3}w_{1,5}$	.0224	-.00362	0	0	-.0875	0
$w_{3,1}w_{3,1}w_{5,1}$	0	0	0	0	0	0
$w_{3,1}w_{1,5}w_{5,1}$	0	-.01682	.00204	0	0	0
$w_{3,3}^{3}$	0	0	0	0	0	-.0270
$w_{3,3}^{2}w_{1,5}$	0	0	0	0	0	0
$w_{3,3}^{2}w_{5,1}$	-.0774	0	0	.0000268	0	0
$w_{3,3}w_{1,5}^{2}$	-.02025	0	0	0	0	0
$w_{3,3}w_{5,1}^{2}$	0	0	0	0	0	0
$w_{3,3}w_{1,5}w_{5,1}$	0	.01793	-.00331	0	.1218	-.0603
$w_{1,5}^{3}$	0	0	0	0	0	0
$w_{1,5}^{2}w_{5,1}$	0	0	0	0	0	-.0409
$w_{1,5}w_{5,1}^{2}$	0	0	-.00563	.000862	0	0
$w_{5,1}^{3}$	0	0	0	0	0	0

TABLE 32

P, Q, R, and S

P

.028440	0	0	0	0	0	0
0	.0062884	0	0	0	0	0
0	0	.0025823	0	0	0	0
0	0	0	.0013295	0	0	0
0	0	0	0	.00065734	0	0
0	0	0	0	0	.00037190	0
0	0	0	0	0	0	.00022270

Q

.078726	.019711	.0055992	.0022161	.0010798	.00060216	.00036862
.0055245	.0087474	.0060917	.0036414	.0021901	.0013754	.00090551
.0012685	.0029296	.0031490	.0026273	.0019864	.0014557	.0010653
.00047031	.0012280	.0015910	.0016067	.0014323	.0011973	.00097037
.00022287	.00061385	.00087119	.0009796	.00097192	.0008952	.00078857
.00012250	.00034691	.00051761	.00062043	.00065972	.00065063	.00061073
.000074372	.00021404	.00032912	.00041068	.00045729	.00047327	.00046584

TABLE 32 (Continued)

R

.011057	.00077588	.00017816	.000066052	.0000313	.000017204	.000010445
.0027683	.0012285	.00041145	.00017240	.000086209	.000048721	.00003006
.00078637	.00085555	.00044227	.00022345	.00012235	.000072695	.000046223
.00031124	.00051142	.00036899	.00022565	.00013758	.000087134	.000057678
.00015166	.00030758	.00027898	.00020116	.00013650	.000092653	.000064224
.000084569	.00019316	.00020444	.00016815	.00012573	.000091377	.000066469
.00005177	.00012717	.00014961	.00013628	.00011075	.000085773	.000065425

S

.086409	0	0	0	0	0	0
0	.027107	0	0	0	0	0
0	0	.013714	0	0	0	0
0	0	0	.0083576	0	0	0
0	0	0	0	.0053863	0	0
0	0	0	0	0	.0037958	0
0	0	0	0	0	0	.0026981

TABLE 33

Coefficients

$(C_1 - C_7)$

	C_1	C_2	C_3	C_4	C_5	C_6	C_7
$w_{1,1}{}^3$	1.370	-.001497	0	0	0	0	0
$w_{1,1}{}^2 w_{1,3}$	.298	-.01245	0	0	0	0	0
$w_{1,1}{}^2 w_{3,1}$	-.0690	.155	-.000687	0	0	0	0
$w_{1,1}{}^2 w_{3,3}$	-.1148	.2434	-.00365	0	0	0	0
$w_{1,1}{}^2 w_{1,5}$	.452	-.02181	0	0	0	0	0
$w_{1,1}{}^2 w_{5,1}$	0	.00458	.0338	-.000177	0	0	0
$w_{1,1} w_{1,3}{}^2$	5.55	-.0767	0	0	0	0	0
$w_{1,1} w_{3,1}{}^2$	10.06	0	.00330	-.000226	0	0	0
$w_{1,1} w_{3,3}{}^2$	10.59	0	.01681	-.00296	0	0	0
$w_{1,1} w_{1,5}{}^2$	10.55	-.1442	0	0	0	0	0
$w_{1,1} w_{5,1}{}^2$	26.92	0	0	0	.000282	-.0000485	0
$w_{1,1} w_{1,3} w_{3,1}$	-.092	.1975	-.00802	0	0	0	0
$w_{1,1} w_{1,3} w_{3,3}$	-1.528	.512	-.0318	0	0	0	0
$w_{1,1} w_{1,3} w_{1,5}$	-.430	-.1096	0	0	0	0	0
$w_{1,1} w_{1,3} w_{5,1}$	0	-.1042	.0742	-.00387	0	0	0

TABLE 33 (Continued)

	C_1	C_2	C_3	C_4	C_5	C_6	C_7
$w_{1,1}w_{3,1}w_{3,3}$	-2.75	0	.00838	-.001830	0	0	0
$w_{1,1}w_{3,1}w_{1,5}$	.449	-.0860	-.00736	0	0	0	0
$w_{1,1}w_{3,1}w_{5,1}$	.271	-.0668	0	.000252	-.0001779	0	0
$w_{1,1}w_{3,1}w_{1,5}$	.049	.163	-.0344	0	0	0	0
$w_{1,1}w_{3,3}w_{5,1}$	-.801	.1243	0	.00268	-.000710	0	0
$w_{1,1}w_{1,5}w_{5,1}$	0	-.0141	.0349	-.00614	0	0	0
$w_{1,3}^3$	4.89	-.192	0	0	0	0	0
$w_{1,3}^2w_{3,1}$	-3.168	.890	-.0338	0	0	0	0
$w_{1,3}^2w_{3,3}$	-3.85	1.970	-.1208	0	0	0	0
$w_{1,3}^2w_{1,5}$	7.167	-.6072	0	0	0	0	0
$w_{1,3}^2w_{5,1}$	0	-.2314	.2440	-.01184	0	0	0
$w_{1,3}w_{3,1}^2$	1.89	0	.0278	-.00268	0	0	0
$w_{1,3}w_{3,3}^2$	13.31	0	.1975	-.03894	0	0	0
$w_{1,3}w_{1,5}^2$	15.49	-1.312	0	0	0	0	0
$w_{1,3}w_{5,1}^2$	3.64	0	0	0	.00497	-.000919	0
$w_{1,3}w_{3,1}w_{3,3}$	18.12	0	.1592	-.02118	0	0	0

TABLE 33 (Continued)

	C_1	C_2	C_3	C_4	C_5	C_6	C_7
$w_{1,3}w_{3,1}w_{1,5}$	-.24	.985	-.0978	0	0	0	0
$w_{1,3}w_{3,1}w_{5,1}$	1.02	.274	0	.0208	-.002814	0	0
$w_{1,3}w_{3,3}w_{1,5}$	-9.28	3.129	-.400	0	0	0	0
$w_{1,3}w_{3,3}w_{5,1}$	-8.92	1.161	0	.0544	-.01045	0	0
$w_{1,3}w_{1,5}w_{5,1}$	0	-.997	.4212	-.05233	0	0	0
$w_{3,1}^3$	0	1.048	0	0	-.0000201	0	0
$w_{3,1}^2w_{3,3}$	0	2.616	0	0	-.000499	0	0
$w_{3,1}^2w_{1,5}$	.75	0	.0060	-.00296	0	0	0
$w_{3,1}^2w_{5,1}$	.190	0	.235	0	0	-.0000287	0
$w_{3,1}w_{3,3}^2$	0	4.99	0	0	-.002782	0	0
$w_{3,1}w_{1,5}^2$	-6.11	1.875	-.1193	0	0	0	0
$w_{3,1}w_{5,1}^2$	0	2.40	0	-.00227	0	0	-.0000015
$w_{3,1}w_{3,3}w_{1,5}$	-3.95	0	.1526	-.0352	0	0	0
$w_{3,1}w_{3,3}w_{5,1}$	1.21	0	.582	0	0	-.000586	0
$w_{3,1}w_{1,5}w_{5,1}$	2.600	-.374	0	.03046	-.00537	0	0

TABLE 33 (Continued)

	C_1	C_2	C_3	C_4	C_5	C_6	C_7
$w_{3,3}^3$	0	4.11	0	0	-.00450	0	0
$w_{3,3}^2 w_{1,5}$	14.32	0	.361	-.0826	0	0	0
$w_{3,3}^2 w_{5,1}$	7.93	0	.985	0	0	-.001765	0
$w_{3,3} w_{1,5}^2$	-9.14	5.60	-.5116	0	0	0	0
$w_{3,3} w_{5,1}^2$	0	4.37	0	.0305	0	0	-.000225
$w_{3,3} w_{1,5} w_{5,1}$	-.91	2.237	0	.1084	-.02459	0	0
$w_{1,5}^3$	9.60	-1.03	0	0	0	0	0
$w_{1,5}^2 w_{5,1}$	0	-.844	.708	-.0631	0	0	0
$w_{1,5} w_{5,1}^2$	2.86	0	0	0	.00978	-.00426	0
$w_{5,1}^3$	0	0	.614	0	0	0	0

TABLE 33 (Continued)

	C_8	C_9	C_{10}	C_{11}	C_{12}	C_{13}	C_{14}
$w_{1,1}^3$	1.446	-.02705	0	0	0	0	0
$w_{1,1}^2 w_{1,3}$	-.938	.424	-.01475	0	0	0	0
$w_{1,1}^2 w_{3,1}$	.596	-.0682	0	0	0	0	0
$w_{1,1}^2 w_{3,3}$	-.2025	.328	-.0367	0	0	0	0
$w_{1,1}^2 w_{1,5}$	0	-.0625	.1208	-.00429	0	0	0
$w_{1,1}^2 w_{5,1}$	.456	-.0914	0	0	0	0	0
$w_{1,1} w_{1,3}^2$	5.19	0	.0341	-.00469	0	0	0
$w_{1,1} w_{3,1}^2$	11.33	-.420	0	0	0	0	0
$w_{1,1} w_{3,3}^2$	10.59	0	.0740	-.0392	0	0	0
$w_{1,1} w_{1,5}^2$	10.08	0	0	0	.00498	-.001064	0
$w_{1,1} w_{5,1}^2$	29.35	-.812	0	0	0	0	0
$w_{1,1} w_{1,3} w_{3,1}$	.33	.1235	-.0486	0	0	0	0
$w_{1,1} w_{1,3} w_{3,3}$	-.264	0	.0596	-.02633	0	0	0
$w_{1,1} w_{1,3} w_{1,5}$	-1.797	.3121	0	.0196	-.00392	0	0
$w_{1,1} w_{1,3} w_{5,1}$	-.0806	.1553	-.0710	0	0	0	0

TABLE 33 (Continued)

	C_8	C_9	C_{10}	C_{11}	C_{12}	C_{13}	C_{14}
$w_{1,1}w_{3,1}w_{3,3}$	-5.95	1.440	-.2173	0	0	0	0
$w_{1,1}w_{3,1}w_{1,5}$	0	-.0974	.1305	-.0294	0	0	0
$w_{1,1}w_{3,1}w_{5,1}$	-.109	.0600	0	0	0	0	0
$w_{1,1}w_{3,3}w_{1,5}$	.482	-.073	0	.0305	-.01234	0	0
$w_{1,1}w_{3,3}w_{5,1}$	.199	-.100	-.0628	0	0	0	0
$w_{1,1}w_{1,5}w_{5,1}$	0	.0671	.0146	-.0264	0	0	0
$w_{1,3}^3$	0	1.440	0	0	-.000494	0	0
$w_{1,3}^2w_{3,1}$	-.640	0	.00885	-.0105	0	0	0
$w_{1,3}^2w_{3,3}$	0	.510	0	0	-.00600	0	0
$w_{1,3}^2w_{1,5}$	2.384	0	.594	0	0	-.000705	0
$w_{1,3}^2w_{5,1}$	.493	0	.0008	-.0077	0	0	0
$w_{1,3}w_{3,1}^2$	-5.07	2.78	-.2535	0	0	0	0
$w_{1,3}w_{3,3}^2$	0	4.79	0	0	-.0368	0	0
$w_{1,3}w_{1,5}^2$	0	3.79	0	.0231	0	0	-.000376
$w_{1,3}w_{5,1}^2$	-9.74	5.21	-.447	0	0	0	0

TABLE 33 (Continued)

	C_8	C_9	C_{10}	C_{11}	C_{12}	C_{13}	C_{14}
$w_{1,3}w_{3,1}w_{3,3}$	17.10	0	.600	-.1880	0	0	0
$w_{1,3}w_{3,1}w_{1,5}$	2.46	-.156	0	.0556	-.0180	0	0
$w_{1,3}w_{3,1}w_{5,1}$	1.641	.504	-.2372	0	0	0	0
$w_{1,3}w_{3,3}w_{1,5}$	-2.75	0	.1865	0	0	-.00744	0
$w_{1,3}w_{3,3}w_{5,1}$	-4.89	0	.0931	-.104	0	0	0
$w_{1,3}w_{1,5}w_{5,1}$	.650	-.585	0	-.018	-.0029	0	0
$w_{3,1}^3$	6.06	-.972	0	0	0	0	0
$w_{3,1}^2w_{3,3}$	-5.51	6.49	-1.223	0	0	0	0
$w_{3,1}^2w_{1,5}$	0	-1.463	1.233	-.1442	0	0	0
$w_{3,1}^2w_{5,1}$	6.12	-1.584	0	0	0	0	0
$w_{3,1}w_{3,3}^2$	12.25	0	1.276	-.527	0	0	0
$w_{3,1}w_{1,5}^2$	-1.206	0	0	0	.0227	-.00750	0
$w_{3,1}w_{5,1}^2$	17.39	-3.401	0	0	0	0	0
$w_{3,1}w_{3,3}w_{1,5}$	-14.86	3.36	0	.360	-.1282	0	0
$w_{3,1}w_{3,3}w_{5,1}$	-7.45	7.25	-2.035	0	0	0	0

TABLE 33 (Continued)

	C_8	C_9	C_{10}	C_{11}	C_{12}	C_{13}	C_{14}
$w_{3,1}w_{1,5}w_{5,1}$	0	-.514	1.014	-.270	0	0	0
$w_{3,3}^3$	0	4.34	0	0	-.0810	0	0
$w_{3,3}^2w_{1,5}$	5.78	0	2.015	0	0	-.02834	0
$w_{3,3}^2w_{5,1}$	11.17	0	1.180	-.606	0	0	0
$w_{3,3}w_{1,5}^2$	0	1.52	0	.0844	0	0	-.002889
$w_{3,3}w_{5,1}^2$	-6.59	11.01	-2.629	0	0	0	0
$w_{3,3}w_{1,5}w_{5,1}$	4.44	.52	0	.195	-.1153	0	0
$w_{1,5}^3$	0	0	1.300	0	0	0	0
$w_{1,5}^2w_{5,1}$	.639	0	0	0	-.0070	-.00089	0
$w_{1,5}w_{5,1}^2$	0	-2.61	2.63	-.3294	0	0	0
$w_{5,1}^3$	10.60	-2.51	0	0	0	0	0

TABLE 34

P

- 611.61171	- 1739.6884	- 2867.0318	- 3745.0598	- 5135.8373	- 6271.5607	- 7407.9913
- 1739.7368	- 4399.0754	- 7482.6101	- 9762.9057	-13382.199	-16337.694	-19295.619
- 2867.0985	- 7482.5759	-11876.652	-15989.836	-21909.541	-26742.741	-31580.445
- 3745.2551	- 9763.1498	-15990.312	-20087.965	-28548.952	-34841.893	-41140.932
- 5135.9384	-13382.090	-21909.465	-28548.000	-37581.136	-47717.261	-56340.597
- 6271.7552	-16337.746	-26742.950	-34841.124	-47717.798	-55538.337	-68747.095
- 7408.1093	-19295.390	-31580.198	-41139.416	-56340.399	-68746.080	-76673.759

Q

759.4424	1740.7063	2856.0230	3972.9682	5206.9748	6218.0834	7345.9977
2103.5703	4600.0935	7444.9519	10336.612	13547.013	16181.365	19120.476
3473.5510	7595.1523	12235.519	16933.003	22159.176	26453.076	31252.328
4538.9638	9929.3806	15983.990	22089.756	28871.039	34425.131	40660.232
6224.9423	13620.755	21924.432	30283.785	39551.092	47137.821	55623.040
7601.8564	16635.534	26777.873	36980.372	48276.864	57505.755	67816.920
8979.3460	19651.263	31633.497	43682.428	57012.544	67885.252	80018.209

TABLE 34 (Continued)

R

106.66289	295.43607	487.84526	637.45940	874.26953	.067.6398	1261.1198
244.46671	646.02442	1066.6472	1394.4222	1912.8776	2336.2419	2759.8033
401.12485	1045.6048	1718.4228	2244.8117	3079.1982	3760.8014	4442.8137
557.99657	1451.7190	2378.1562	3102.3040	4253.2224	5193.6700	6135 .0251
731.30996	1902.6004	3112.1434	4054.6691	5554.7699	6780.1879	8007.1805
873.31538	2272.5724	3715.1874	4836.0781	6620.2611	8076.3001	9534.1737
1031.7199	2685.3301	4389.1798	5710.2860	7811.9100	9524.3567	11238.100

S

- 119.97987	- 297.91923	- 486.85234	- 676.61114	- 886.51929	- 1058.5626	- 1250.5296
- 297.90260	- 622.80264	- 1069.3927	- 1482.9307	- 1941.4648	- 2317.4507	- 2737.2519
- 486.85180	- 1069.4500	- 1654.4926	- 2392.1002	- 3129.6617	- 3734.3712	- 4409.8588
- 676.60727	- 1483.0055	- 2392.0935	- 3190.3614	- 4328.5695	- 5163.3736	- 6096.1051
- 886.51418	- 1941.5610	- 3129.6497	- 4328.5668	- 5473.0406	- 6748.4553	- 7966.1794
- 1058.5530	- 2317.5475	- 3734.3439	- 5163.3512	- 6748.4317	- 7783.1788	- 9497.3183
- 1250.5079	- 2737.3556	- 4409.7905	- 6096.0289	- 7966.0868	- 9497.2411	- 10837.624

TABLE 35

	H_1 =	H_2 =	H_3 =	H_4 =	H_5 =	H_6 =
$\frac{w_{1,1}^2}{h^3}$	-.620	.09894	.032192	-.011851	.0273624	.00704138
$\frac{w_{1,1}^2 w_{1,3}}{h^3}$	.708	-.308	-.04684	.04367	.02588	-.00761590
$\frac{w_{1,1}^2 w_{3,1}}{h^3}$	.3602	-.0860	-.237	.0402	.00881520	.005427
$\frac{w_{1,1}^2 w_{3,3}}{h^3}$	-.152895	.1052	.073	-.0838	-.02150	-.001807
$\frac{w_{1,1}^2 w_{1,5}}{h^3}$	.13881	.1162	-.00704569	-.02217	-.1244	-.00151685
$\frac{w_{1,1}^2 w_{5,1}}{h^3}$	.14997	-.0340709	.02047	-.01082	-.00391952	-.0906
$\frac{w_{1,1} w_{1,3}^2}{h^3}$	-2.24	.338491	.1619	-.043514	.0784	.0231184
$\frac{w_{1,1} w_{3,1}^2}{h^3}$	-4.95	.875	.249522	-.10613	.196889	.05005
$\frac{w_{1,1} w_{3,3}^2}{h^3}$	-4.34	.619752	.212407	-.0732423	.1467	.0278
$\frac{w_{1,1} w_{1,5}^2}{h^3}$	-4.45	.633899	.3341	-.080868	.219829	.0462826
$\frac{w_{1,1} w_{5,1}^2}{h^3}$	-12.70	2.139	.634673	-.25620	.532422	.145081
$\frac{w_{1,2} w_{1,3} w_{3,1}}{h^3}$	-.933	.457	.252	-.180	-.0744	-.00633
$\frac{w_{1,1} w_{1,3} w_{3,3}}{h^3}$	.770	-.149123	-.357	.040213	.0242	.0266
$\frac{w_{1,1} w_{1,3} w_{1,5}}{h^3}$	1.387	-.406	-.1576	.0829	.00165457	-.0121891
$\frac{w_{1,1} w_{1,3} w_{5,1}}{h^3}$	-.045274	.0339956	-.0727	.1054	-.00780271	.0634
$\frac{w_{1,1} w_{3,1} w_{3,3}}{h^3}$	3.08	-1.156	-.162592	.15480	.1385	-.02126
$\frac{w_{1,1} w_{3,1} w_{1,5}}{h^3}$	.142167	-.330	-.0095535	.1551	.1947	-.00161405
$\frac{w_{1,1} w_{3,1} w_{5,1}}{h^3}$	.479	-.196	-.1106	.0554	.00916206	-.00157925
$\frac{w_{1,1} w_{3,3} w_{1,5}}{h^3}$	-1.169	.369	.354	-.1287	-.00345243	-.0241

$\frac{W_{1,1}W_{1,3}W_{3,1}}{h^3}$	-.683	.539	.1273	-.1575	-.1513	.00377846
$\frac{W_{1,1}W_{1,5}W_{5,1}}{h^3}$	-.108925	.0115347	-.00022887	-.0981	-.000627717	.000716704
$\frac{W_{1,3}^2}{h^3}$	1.14854	-.[illegible]	-.0698371	.1478	.128820	-.0130195
$\frac{W_{1,3}^2W_{3,1}}{h^3}$	1.640	-.300069	-.687	.075359	.0136	.0248
$\frac{W_{1,3}W_{3,3}}{h^3}$	-1.25044	.979	.121571	-.478	-.142396	.00910762
$\frac{W_{1,3}W_{1,5}}{h^3}$	-.161	.591095	.1460	-.105462	-.599	-.00348992
$\frac{W_{1,3}W_{3,3}}{h^3}$	.150982	-.017527	.1602	-.0115270	-.00731889	-.1921
$\frac{W_{1,3}^2W_{3,1}}{h^3}$	3.54	-1.76	-.190364	.244441	.2587	-.0154
$\frac{W_{1,3}^2W_{3,3}}{h^3}$	3.03659	-2.39	-.168085	.340502	.327329	-.0310944
$\frac{W_{1,3}^2W_{3,5}}{h^3}$	3.88759	-2.80	-.243326	.550	.425603	-.0408237
$\frac{W_{1,3}W_{3,1}^2}{h^3}$	7.03	-3.51	-.365587	.456459	.523	-.0789996
$\frac{W_{1,3}W_{3,1}W_{3,3}}{h^3}$	-6.31	1.07862	.334663	-.134903	-.094	-.0414
$\frac{W_{1,3}W_{3,1}W_{1,5}}{h^3}$	-3.58	1.142	.828	-.405	-.0388697	-.0466
$\frac{W_{1,3}W_{3,3}W_{3,1}}{h^3}$	-2.177	1.217	.418	-.402	-.301	.00983973
$\frac{W_{1,3}^2W_{3,3}}{h^3}$	1.[illegible]	-.85955	-.703	.243178	.650	.1029
$\frac{W_{1,3}W_{1,5}W_{5,1}}{h^3}$	2.59	-.69448	-.886	.132948	.229	-.0119026
$\frac{W_{1,3}W_{1,5}W_{5,1}}{h^3}$	.337530	-.11663	-.481	.287	.00393589	.2071
$\frac{W_{3,1}^3}{h^3}$	1.05163	-.42616	-1.78	.301	-.0578184	.0453470
$\frac{W_{1,3}^2W_{3,3}}{h^3}$	-2.77541	1.[illegible]727	1.760	-1.385	-.171502	-.0348002

(Continued)

$\frac{w_{3,1}w_{1,5}}{h^3}$	.420135	1.031	-.0152429	-.171243	-.902	-.00487436
$\frac{w_{3,1}^2w_{5,1}}{h^3}$	-.021	.157	.200557	-.140641	-.0365176	-.745
$\frac{w_{3,1}w_{3,2}^2}{h^3}$	3.50986	-.60812	-3.50	.281172	-.0780122	.0931361
$\frac{w_{3,1}w_{1,5}^2}{h^3}$	3.77	-.58180	-1.610	.153433	-.190819	.0952
$\frac{w_{3,1}w_{5,1}^2}{h^3}$	5.71135	-1.31781	-5.09	.961	-.149982	.129547
$\frac{w_{3,1}w_{3,2}w_{1,5}}{h^3}$	8.09	-2.270	-.441453	.319783	-.0225971	.0696
$\frac{w_{3,1}w_{3,2}w_{5,1}}{h^3}$	1.45	-1.382	-.257200	.713569	.557	.542
$\frac{w_{3,1}w_{1,5}w_{5,1}}{h^3}$	.788188	-1.539	-.0526277	.528	.954	-.00893141
$\frac{w_{3,2}^2}{h^3}$	-.759293	.67890	.159131	-.810	-.112196	.00452134
$\frac{w_{3,2}^2w_{1,5}}{h^3}$	.59	1.07538	.00777411	-.161238	-1.316	-.1215
$\frac{w_{3,2}^2w_{5,1}}{h^3}$	-1.10	.29799	.266925	-.0591174	-.367	-.832
$\frac{w_{3,2}(w_{1,5})^2}{h^3}$	-2.97576	1.958	.329107	-1.079	-.349274	.0193732
$\frac{w_{3,2}(w_{5,1})^2}{h^3}$	-3.82418	2.19899	2.08	-2.16	0.365473	-.0366604
$\frac{w_{3,2}w_{1,5}w_{5,1}}{h^3}$	-7.53	2.47	1.447	-.797	-.105474	.0364934
$\frac{(w_{1,5})^3}{h^3}$	2.77469	.89836	-.165216	-.171174	-1.511	-.0293032
$\frac{(w_{1,5})^2w_{5,1}}{h^3}$	.227024	-.019795	.635	-.0448441	-.0117136	-.551
$\frac{w_{1,5}(w_{5,1})^2}{h^3}$	1.03648	2.28	-.0637866	-.327900	-2.16	-.0173393
$\frac{w_{3,2}^3}{h^3}$	3.56381	-.856[illegible]	.352362	-.218371	-.0811875	-2.03

TABLE 36

Results of Rayleigh-Ritz analysis for buckling parameter, K, using selected terms of series (97)

$$K = \frac{N_y a^2}{\pi^2 D}$$

Coefficients Retained	K (Non-Prestressed Plate)	K (Pre-Stressed Plate)	Percent increase of pre-stressed plate over non-prestressed plate
$w_{1,3}$	9.91	10.59	6.9%
$w_{1,2}$	8.72	10.02	14.9%
$w_{1,2}$ and $w_{1,4}$	8.68	9.97	14.9%
$w_{1,2}$ and $w_{3,2}$	8.38	9.61	14.7%
Accepted value of Ref. 22	8.33	-	-

TABLE 37

Ratio of deflection coefficients used in Rayleigh-Ritz analysis

Coefficients	Ratio for Non-Prestressed Plate	Ratio for Pre-Stressed Plate
$w_{1,2}/w_{1,4}$	-19.1	37.7
$w_{1,2}/w_{3,2}$	12.3	29.2

SECTION XV

Summary and Conclusions

The proposed method of prestressing has been investigated and shown to be capable of raising the buckling load. It has been shown that the buckling load is quite sensitive to changes in the magnitude and distribution of the stresses produced by the prestressing process.

The experimental program was divided into two parts. In the first the deflections and stresses induced in the prestressing process were determined, and the effect these stresses would have upon the buckling load was calculated. The calculations were performed by the Finite Difference Method and by the Rayleigh-Ritz Method. For one plate, which was the only plate for which the Finite Difference Method was used, this method predicted that for the stresses found the Buckling Load would be raised over 100% while the Rayleigh-Ritz method predicted a raise of approximately 130%. Because it was felt that the Finite Difference Method was unreliable for the small number of net points used and also because of the lengthy computations it requires, the Rayleigh-Ritz Method was decided upon for determining the buckling loads of the plates. The Rayleigh-Ritz method showed an increase of about 20% and 13% using the data of two of the other tests. It is interesting to note that for the latter two prestressed plates a symmetric three half-wave buckling mode was predicted and for the non-prestressed plates of this (3:2) aspect ratio an antisymmetric two half-wave buckling mode is predicted.

Thus it was shown that relatively small in-plane stresses (less than 1000 psi) would have a considerable effect on both the buckling mode and load.

The second (and main) phase of the experimental program was that of actually testing prestressed plates to determine their buckling loads. All the plates tested were of the same length and width but were of various thicknesses and had various initial radii of curvature. A number of non-prestressed plates were also tested for purposes of comparison and calibration of the buckling jig.

The average increase of the buckling load by prestressing was 38% measured by the "Top of the Knee" method, although there was considerable scatter. Some plates exhibited raises in their buckling load of over 100% while other plates had their buckling loads slightly lowered.

A need for a more realistic evaluation of the strength of plates has been pointed out since the present concept of the buckling load is based upon the behavior of the ideal plate. In actuality there is no sudden decrease in the strength but only a gradual decrease necessitating some criteria probably based on the magnitude of the deflection as a ratio to the applied load.

The theoretical program also was divided into two parts. The first part consisted of finding the stresses and deflections induced by the prestressing procedure, while the second part consisted of finding their effect upon the Buckling Load by the Rayleigh Ritz Method.

Von Karman's non-linear equations were used in finding the deflections and stresses. These equations normally are used only for deflections of the order of the plate thickness, however, since in this case the major deflection is from one developable (cylindrical) surface to another (flat) developable as to take advantage of this. The method[7] used in solving the non-linear equations is basically one used by Levy in which the terms are expanded in Fourier series which transforms the differential equations into algebraic equations in terms of the trigonometric coefficients. The resulting non-linear algebraic equations are then solved by an iteration method.

The buckling load of one particular is then determined by the Rayleigh Ritz method and it is found that in this case the prestresses found would raise the buckling load approximately 15%. This conclusion, however, can be subjected to questioning, because in the use of Rayleigh-Ritz method some assumptions are made which may not be actually valid.

SECTION XVI

BIBLIOGRAPHY

(1) Teichmann, F.K. and Wang, C.T., "Finite Deflections of Curved Sandwich Cylinders", Sherman M. Fairchild Publication Fund Paper No. FF-4, Institute of the Aeronautical Sciences.

(2) Teichmann, Wang, Gerard, "Buckling of Sandwich Cylinders Under Axial Compression", Journal of the Aeronautical Sciences, Vol. 18, No. 6, p. 398, June 1951.

(3) Welter, C., "The Effect of Radius of Curvature and Preliminary Eccentricities on Buckling Loads of Curved Thin Aluminum Alloy Sheets for Monocoque Construction", Journal of the Aeronautical Sciences, Vol. 13, No. 11, p. 593, November 1946.

(4) Cox, H.L., Letter to the Editor, Journal of the Aeronautical Sciences, Vol. 14, No. 6, p. 333, June 1947.

(5) Cicala, P., "The Effect of Initial Deformations on the Behavior of a Cylindrical Shell under Axial Deformation", Quarterly of Applied Mathematics, Vol. 9, p. 275, October 1951.

(6) Scanlan, R.H. and Rosenbaum, R., "Introduction to the Study of Aircraft Vibration and Flutter", 1st Ed., p. 17, New York, MacMillan Co., 1951

(7) Scarborough, J.B., "Numerical Mathematical Analysis", 1st Edition, pp. 187-195, Baltimore, Md., The John Hopkins Press, 1930.

(8) Southwell, R.V., "An Introduction to the Theory of Elasticity for Engineers and Physicists", 2nd Edition, pp. 424-429, Oxford University Press, 1941.

(9) Donnell, L.H., "Stephen Timoshenko 60th Anniversary Volume, "On the Application of Southwell's Method for the Analysis of Buckling Tests", pp. 27-34, New York, N.Y., The MacMillan Co., December 1948.

(10) Hu, P.C., Lundquist, E.E., and Batdorf, S.B., "Effect of Small Deviations from Flatness or Effective Width and Buckling of Plates in Compression", T.N. 1124, Washington, D.C., N.A.C.A., Sept. 1946.

(11) Yoshiki, M., "A New Method of Determining the Critical Buckling Points of Rectangular Plates in Compression", Journal Society of Applied Mechanics of Japan, Vol. 1, p. 193, 1948. Also presented at the 8th International Congress on Theoretical and Applied Mechanics at Istanbul, 1952.

(12) Levy, S., "Buckling of Rectangular Plates with Built in Edges", Journal of Applied Mechanics, Vol. 64, p. A-171, December 1942.

(13) Love, A.E.H., "A Treatise on the Mathematical Theory of Elasticity", 4th Edition, p. 499, New York, Dover Publications, 1944.

(14) VanDerPol, Balth, and Bremmer, H., "Operational Calculus based on the Two-Sided Laplace Integral", Chap. 5, Cambridge, England, University Press, 1950.

(15) Levy, S., "Square Plate with Clamped Edges under Normal Pressure Producing Large Deflections", N.A.C.A., T.R. No. 740, 1942.

(16) Levy, S., "Large Deflection Theory for Rectangular Plates", Proceeding of Symposis in Applied Mathematics, Vol. 1, pp. 202, 209, New York City, American Mathematical Society, 1949.

(17) Pierce, B.O., "A Short Table of Integrals", 3rd Edition, p. 95, Boston, Mass., Ginn and Co., 1929.

(18) Reiss, E.L., "Pre-stressing Plates and Shells to Increase their Buckling Load", Thesis for M.Ae.E., New York University, May 1952.

(19) Timoshenko, S., "Theory of Plates and Shells", 1st Edition, p. 343, New York, McGraw-Hill Book Co., Inc., 1940.

(20) Levy, S., "Bending of Rectangular Plates with Large Deflections", N.A.C.A. T.R. No. 737, 1942.

(21) Levy, S. and Greenman, S., "Bending with Large Deflection of a Rectangular Plate with Length-Width Ratio of 1.5 Under Normal Pressure", T.N. 853, Washington, D.C., N.A.C.A., July 1952.

SECTION XVII

APPENDIXES

APPENDIX A

VALIDITY OF YOSHIKI'S METHOD FOR DETERMINING THE BUCKLING LOAD OF PLATES

In the section reviewing pertinent literature the method developed by M. Yoshiki (11) was explained with reference to Figs. 1 and 3. The method is based on the parabolic post buckling behavior of plates and which can be proven for clamped plates in the following manner:

The total potential energy in a plate is composed of the strain energy due to bending, membrane stresses and the movement during buckling of the applied load according to

$$W = V_1 + V_2 - T \qquad (A1)$$

For a rectangular plate with clamped edges the strain energy due to bending is

$$V_1 = \frac{D}{2} \iint (\nabla^2 w - \nabla^2 w_0)^2 \, dx \, dy \qquad (A2)$$

while that due to axial compression is

$$V_2 = \frac{h}{2} \int_0^b \int_0^a \sigma_y \, \varepsilon_y \, dx \, dy \qquad (A3)$$

but since $\varepsilon_x = f(x)$ only, and $\sigma_y = E \, \varepsilon_y$

$$V_2 = \frac{Ebh}{2} \int_0^b \varepsilon_y^2 \, dx$$

where w_0 is the initial deflection.

Denoting e as the total strain measured from the unstrained perfect plate, i.e. be is the end shortening of the plate then

$$be = b\varepsilon_y + \frac{1}{2} \int_0^b \left(\frac{\partial w}{\partial y}\right)^2 dy + \frac{1}{2} \int_0^b \left(\frac{\partial w_0}{\partial y}\right)^2 dy$$

or

$$\varepsilon_y = e - \frac{1}{2b}\int_0^b \left[\left(\frac{\partial w}{\partial y}\right)^2 - \left(\frac{\partial w_0}{\partial y}\right)^2\right] dy$$

then eliminating ε_y from the expression for V_2 the following expression is arrived at

$$V_2 = \frac{Ebh}{2}\int_0^a \left\{ e - \frac{1}{2b}\int_0^b \left[\left(\frac{\partial w}{\partial y}\right)^2 - \left(\frac{\partial w_0}{\partial y}\right)^2\right] dy \right\} dx \qquad (A4)$$

and

$$T = \frac{1}{2}\, p\, b\, e \qquad \text{where } p = -a N_y \qquad (A5)$$

Assuming a deflection during buckling of the form

$$w = w_{m,n} \sin\frac{\pi x}{a} \sin\frac{\pi y}{b} \sin\frac{m\pi x}{a} \sin\frac{n\pi y}{b} \qquad (A6)$$

and initial imperfections of the form

$$w_0 = w_{m0',n0} \sin\frac{\pi x}{a} \sin\frac{\pi y}{b} \sin\frac{m_0\pi x}{a} \sin\frac{n_0\pi y}{b} \qquad (A7)$$

which satisfy the boundary conditions $w = 0$ and $\frac{\partial w}{\partial n} = 0$

The energy expressions become

$$\frac{128a^2}{D\pi^4} V_1 = w_{m,n}^2 \left\{ \left(\frac{a}{b}\right)^3 (2+\delta_1^m)\, 2(n^2+1)^2 + 8n^2 + \left(\frac{b}{a}\right)(2+\delta_1^n) 2(m^2+1)^2 \right.$$

$$\left. + 8m^2 + 8\left(\frac{a}{b}\right)(m^2+1)(n^2+1) \right\}$$

$$+ w_{m0,n0}^2 \left\{ \left(\frac{a}{b}\right)^3 (2+\delta_1^{m_0}) 2(n_0^2+1)^2 + 8n_0^2 + \left(\frac{b}{a}\right)(2+\delta_1^{n_0}) 2(m_0^2+1)^2 \right.$$

$$+8m_0^2+8\left(\frac{a}{b}\right)(m_0^2+1)(n_0^2+1)\Big\}$$

$$-2\frac{a}{b}\,w_{m,n}w_{m0,}w_{n0}\Big\{-\Big[(n+1)^2+(n-1)^2\Big]\,\delta^n_{n0}+(n+1)^2\delta^n_{n0-2}$$

$$-(n-1)^2\,\delta^n_{2-n0}+(n-1)^2\delta^n_{2+n0}\Big\}\Big\{-\Big[(m_0+1)^2+(m_0-1)^2\Big]\delta^{n_0}_{m0}$$

$$-(m_0-1)^2\delta^m_{2-m0}+(m_0-1)^2\delta^m_{m0-2}+(m_0+1)^2\delta^m_{2+m0}\Big\}$$

$$-2\frac{b}{a}\,w_{m,n}w_{m0,n0}\Big\{\Big[(m+1)^2(m_0+1)^2+(m-1)^2(m_0-1)^2\Big]\,\delta^m_{m0}$$

$$-(m-1)^2(m_0+1)^2\delta^m_{2+m0}-(m+1)^2(m_0-1)^2\delta^m_{m0-2}+(m-1)^2(m_0-1)^2\delta^m_{2-m0}\Big\}$$

$$\Big\{2\delta^n_{n0}-\delta^n_{2+n0}-\delta^n_{n0-2}+\delta^n_{2-n0}\Big\}$$

$$-2\left(\frac{a}{b}\right)^3 w_{m,n}w_{m0,n0}\Big\{\Big[(n+1)^2(n_0+1)^2+(n-1)^2(n_0-1)^2\Big]\delta^n_{n0}$$

$$-(n-1)^2(n_0+1)^2\delta^n_{2+n0}-(n+1)^2(n_0-1)^2\delta^n_{n0-2}+(n-1)^2(n_0-1)^2\delta^n_{2-n0}$$

$$\Big\{2\delta^m_{m0}-\delta^m_{2+m0}-\delta^m_{m0-2}+\delta^m_{2-m0}\Big\}-2\frac{a}{b}\,w_{m,n}w_{m0,n0}$$

$$\left\{-\left[(m+1)^2+(m-1)^2\right]\delta^{m}_{m0}+(m+1)^2\delta^{m}_{m0-2}-(m-1)^2\delta^{m}_{2-m0}+(m-1)^2\delta^{m0}_{2+m0}\right\}$$

$$\left\{-\left[(n_0+1)^2+(n_0-1)^2\right]\delta^{n}_{n0}-(n_0-1)^2\delta^{n}_{2-n0}+(n_0-1)^2\delta^{n}_{n0-2}\right.$$

$$\left.+(n_0+1)^2\delta^{n}_{2+n_0}\right\} \qquad (A8)$$

which may be written in the form

$$V_1 = a_1 w_{m,n}^2 + a_2 w_{m0,n0} + a_3 w_{m,n} w_{m0,n0} \qquad (A9)$$

where a_1, a_2, and a_3 are constants which are functions of m,n,m0,n0,a, and b only and $a_3 = 0$ if $m = n+1^{+}-p$ or $m0 = n0+1^{+}-p$ where p is any even integer.

For the special case where w and w_0 are of the same form, i.e., $m = m_0 = r$, $n = n_0 = p$ then

$$V_1 = a_4 \left(w_{m,n} - w_{m0,n0}\right)^2 \qquad (A10)$$

where

$$a_4 = \frac{D\pi^4}{64a^2}\left\{\left(\frac{a}{b}\right)^3(2+\delta^{n}_{1})(p^4+6p^2+1)+\left(\frac{b}{a}\right)(2+\delta^{p}_{1})(r^4+6r^2+1)\right.$$

$$\left.+4\left(\frac{a}{b}\right)(r^2+1)(p^2+1)(1+\delta^{r}_{1}\,\delta^{p}_{1})\right\}$$

Also

$$\frac{65536b^3}{Eh\pi^4 a} V_2 = \frac{32768b^4}{\pi^4} e^2 + w_{m,n}^4 \left\{ \left[18+17\delta_1^{(m)} - 4\delta_2^{(m)} \right] \left[4+8n^2 \right.\right.$$

$$\left.\left. +4n^4 - (n-1)^2(3n^2+2n+3)\delta_1^{(n)} \right\} + w_{m0,n0}^4 \left\{ \left[18+17\delta_1^{(m0)} - 4\delta_2^{(m0)} \right.\right.\right.$$

$$\left.\left.\left. 4+8n_0^2+4n_0^4 - (n_0-1)^2(3n_0^2+2n_0+3)\delta_0^{(n)} \right\} - 2w_{m,n}^2 w_{m0,n0}^2 \right.$$

$$\left\{ \left[12+8\delta_1^{(m)} - 2\delta_2^{(m)} + 8\delta_1^{(m0)} - 2\delta_2^{(m0)} + 6\delta_{m0}^{(m)} - 4\delta_{m0+1}^{(m)} - 4\delta_{m0-1}^{(m)} + \delta_{m0+2}^{(m)} \right.\right.$$

$$\left.\left. + \delta_{m0-2}^{(m)} - 4\delta_{1-m0}^{(m)} + \delta_{2-m0}^{(m)} \right] \left[4+4n^2 - 2(n-1)^2\delta_1^{(n)} + 4n_0^2 + 4n^2 n_0^2 \right.\right.$$

$$\left.\left. -2n_0^2(n-1)^2\delta_1^{(n)} + (n_0-1)^4\delta_1^{(n)}\delta_1^{(n0)} - 2(1+n^2)(n_0-1)^2\delta_1^{(n0)} \right] \right.$$

$$\left. - \frac{1024}{\pi^4} e \left\{ w_{m,n}^2 \left[1+\delta_1^{(m)} \right] \left[2+2n^2 - (n-1)^2\delta_1^{(n)} \right] \right.\right.$$

$$\left.\left. - w_{m0,n0}^2 \left[1+\delta_1^{(m0)} \right] \left[2+2n_0^2 - (n_0-1)^2\delta_1^{(n0)} \right] \right\} \right. \qquad \text{(A11)}$$

which may be written in the form

$$V_2 = \beta_1 w_{m,n}^4 + \beta_2 w_{m0,n0}^4 + \beta_3 w_{m,n}^2 w_{m0,n0}^2 + \beta_4 e^2 + \beta_5 e w_{m,n}^2 + \beta_6 e w_{m0,n0}^2 \qquad \text{(A12)}$$

Again for the special case $m = m_0 = r$ and $n = n_0 = p$

$$V_2 = \gamma_1 e^2 + \gamma_2 (w_{m,n}^2 - w_{m0,n0}^2)^2 + \gamma_3 (w_{m,n}^2 - w_{m0,n0}^2) e \tag{A13}$$

where

$$\gamma_1 = \frac{Ehab}{2}$$

$$\gamma_2 = \frac{Eh\pi^4 a}{65536 b^3} \left\{ 18 + 17\delta_1^{(m)} - 4\delta_2^{(m)} \right\} \left\{ 4(p^2+1)^2 (p-1)^2 \left[(p-1)^2 - 4p^2 - 4 \right] \delta_1^{(n)} \right\}$$

$$\gamma_3 = \frac{1024Eah}{65536 b^3} \left\{ (1+\delta_1^{(m)}) \left[2 + 2p^2 - (p-1)^2 \delta_1^{(n)} \right] \right\}$$

The total potential energy defined according to Eq. C1 can be found for the special case where $m = m_0 = r$ and $n = n_0 = p$ to be

$$W = \alpha_4 (w_{m,n} - w_{m0,n0})^2 + \gamma_1 e^2 + \gamma_2 (w_{m,n}^2 - w_{m0,n0}^2)^2 + \gamma_3 (w_{m,n}^2 - w_{m0,n0}^2) e - \frac{1}{2} Pbe \tag{A14}$$

Now minimizing with respect to e and $w_{m,n}$

$$\frac{\partial W}{\partial e} = 2\gamma_1 e + \gamma_3 (w_{m,n}^2 - w_{m0,n0}^2) - \frac{1}{2} p b = 0 \tag{A15}$$

$$\frac{\partial W}{\partial w_{m,n}} = 2\alpha_4 (w_{m,n} - w_{m0,n0}) + 4\gamma_2 w_{m,n} (w_{m,n}^2 - w_{m0,n0}^2) + 2\gamma_3 w_{m,n} e = 0 \tag{A16}$$

Solving Eqs. (C15) and C16) for e there results

$$\epsilon = \bar{\gamma}_1 P + \bar{\gamma}_2 (w_{m,n}^2 - w_{m0,n0}^2) \tag{A17}$$

and

$$\epsilon = \frac{\bar{\alpha}_1 (w_{m,n} - w_{m0,n0})}{w_{m,n}} + \bar{\alpha}_2 (w_{m,n}^2 - w_{m0,n0}^2) \tag{A18}$$

Equating Eqs. (A17) and (A18) there results for P

$$P = \bar{\beta}_1 (w_{m,n}^2 - w_{m0,n0}^2) + \bar{\beta}_2 \frac{w_{m0,n0}}{w_{m,n}} - \bar{\beta}_2 \tag{A19}$$

now setting $w_{m,n} - w_{m0,n0} = \delta$ there results

$$w_{m,n}^2 - w_{m0,n0}^2 = \delta^2 \left(1 + \frac{2 w_{m0,n0}}{\delta}\right) \tag{A20}$$

and

$$P = \bar{\beta}_1 \delta^2 \left(1 + \frac{2 w_{m0,n0}}{\delta}\right) + \bar{\beta}_2 \frac{w_{m0,n0}}{w_{m,n}} - \bar{\beta}_2 \tag{A21}$$

However in the post-buckling region the deflection w becomes large, relative to the initial deflection w_0, that is

$$1 \gg \frac{w_{m0,n0}}{w_{m,n}} > \frac{w_{m0,n0}}{w_{m,n}} \tag{A22}$$

and

$$P = \bar{\beta}_1 \delta^2 - \bar{\beta}_2 \tag{A23}$$

Since the strain gage readings taken during the buckling tests were assumed proportional to the deflection caused by the applied load, Eq. (A23) demonstrates the parabolic post-buckling behavior of clamped plates assuming the plate to buckle in a mode similar to the initial deflections.

For the prestressed plate of aspect ratio 3/2 which is under consideration the deflection forms which will predominate are

$$w = w_{1,2} \sin^2 \frac{\pi x}{a} \sin \frac{\pi y}{b} \sin \frac{2\pi y}{b} \tag{A24}$$

$$w_0 = w_{1_0,1_0} \sin^2 \frac{\pi x}{a} \sin^2 \frac{\pi y}{b} \tag{A25}$$

For these forms of deflections the bending and membrane strain energies can be found to be

$$\frac{128a^2}{D\pi^4} V_1 = w_{1,2}^2 \left\{246\left(\frac{a}{b}\right)^3 + 32\left(\frac{b}{a}\right) + 80\left(\frac{a}{b}\right)\right\}$$

$$+ w_{1_0,1_0}^2 \left\{48\left(\frac{a}{b}\right)^3 + 48\left(\frac{b}{a}\right) + 32\left(\frac{a}{b}\right)\right\}$$

$$-216\, w_{1_0,1_0} w_{1,2} \left(\frac{a}{b}\right)^3 \tag{A26}$$

$$\frac{16384b^3}{Eh\pi^4 a} V_2 = \frac{8192b^4}{\pi^4} e^2 + 875 w_{1,2}^4 + 140 w_{1_0,1_0}^4 - 680 w_{1_0,1_0}^2 w_{1,2}^2$$

$$- \frac{5120}{\pi^4} e w_{1,2}^2 + \frac{2048}{\pi^4} e w_{1_0,1_0}^2 \tag{A27}$$

The conditions that $\frac{\partial w}{\partial e} = 0$ and $\frac{\partial w}{\partial w_{1,2}} = 0$ will yield

$$75w_{1,2}^2 - 20w_{1_0,1_0}^2 - \frac{6912D}{Eh}\frac{w_{1_0,1_0}}{w_{1,2}} - \frac{1280Pb^4}{Eah} + \frac{128}{Eh}\left[123 + 16\frac{b^4}{a^4} + 40\frac{b^2}{a^2}\right] = 0$$

letting $w_{1,2} - w_{1_0,1_0} = \delta$ and using Eq. (A29)

$$75\delta^2\left(1 + \frac{2w_{1_0,1_0}}{\delta}\right) + 55w_{1_0,1_0}^2 - \frac{6912D}{Eh}\frac{w_{1_0,1_0}}{w_{1,2}} - \frac{1280Pb^4}{Eah} + \frac{128}{Eh}$$

$$\left[123 + 16\frac{b^4}{a^4} + 140\frac{b^2}{a^2}\right] = 0 \qquad \text{(A28)}$$

but according to relations (A23) resulting from the fact that $w_{m,n}$, $w_{m0,n0}$ Eq. (A28) may be written as

$$75\delta^2 - \frac{1280Pb^4}{Eah} + \frac{128}{Eh}\left[123 + 16\frac{b^4}{a^4} + 40\frac{b^2}{a^2}\right] = 0 \qquad \text{(A29)}$$

or just as in Eq. (A23)

$$P = \bar{\gamma}_1\delta^2 + \bar{\gamma}_2 \qquad \text{(A30)}$$

Thus it is demonstrated the parabolic nature of the post-buckling behavior of flat plates with initial deflections. Since the above did not depend on the actual values of m, m_0, n_0 the above derivation will apply for assumed deflections of the general forms of Eqs. (A6) and (A7).

APPENDIX B

DERIVATION OF EQUATIONS GOVERNING STRESS FUNCTION COEFFICIENTS

Upon substituting (71) into the expression $\nabla^4 F$

$$\nabla^4 F = \pi^4 \sum_{p=0}^{\infty} \sum_{q=0}^{\infty} b_{p,q} \left(\frac{p^2}{a^2} + \frac{q^2}{b^2} \right)^2 \cos \frac{p\pi x}{a} \cos \frac{q\pi y}{b} \qquad \text{(B1)}$$

also by substitution of (70)

$$\left(\frac{\partial^2 w}{\partial x \partial y} \right)^2 - \frac{\partial^2 w}{\partial x^2} \frac{\partial^2 w}{\partial y^2} = \frac{\pi^4}{4a^2 b^2} \sum_{m=1}^{\infty} \sum_{n=1}^{\infty} \sum_{r=2}^{\infty} \sum_{s=2}^{\infty} m(s-n) \Big[(r-m)n$$

$$-m(s-n) \Big] w_{m,n} w_{r-m,s-n} \cos \frac{r\pi x}{a} \cos \frac{s\pi y}{b} + \frac{\pi^4}{4a^2 b^2} \sum_{m=1}^{\infty} \sum_{n=1}^{\infty} \sum_{r=2}^{\infty} \sum_{u=-\infty}^{\infty}$$

$$m(n-u) \Big[(r-m)n+m(n-u) \Big] w_{m,n} w_{r-m,n-u} \cos \frac{r\pi x}{a} \cos \frac{u\pi y}{b}$$

$$+ \frac{\pi^4}{4a^2 b^2} \sum_{m=1}^{\infty} \sum_{n=1}^{\infty} \sum_{t=-\infty}^{\infty} \sum_{s=2}^{\infty} m(s-n) \Big[(m-t)n+m(s-n) \Big] w_{m,n} w_{m-t,s-n}$$

$$\cos \frac{t\pi x}{a} \cos \frac{s\pi y}{b} + \frac{\pi^4}{4a^2 b^2} \sum_{m=1}^{\infty} \sum_{n=1}^{\infty} \sum_{t=-\infty}^{\infty} \sum_{u=-\infty}^{\infty} m(n-u)$$

$$\Big[(m-t)n-m(n-u) \Big] w_{m,n} w_{m-t,n-u} \cos \frac{t\pi x}{a} \cos \frac{u\pi y}{b} \qquad \text{(B2)}$$

Since (B1) has indices running from zero to ∞ (B2) will be transformed into a similar form making use of the identity $\cos(-\alpha) = \cos(+\alpha)$ and for purposes of simplification the four summations of (B2) will be labelled Σ A, Σ B, Σ C, Σ D, in the same order as they appear above.

$$\Sigma A = \frac{\pi^4}{4a^2b^2} \sum_{m=1}^{\infty} \sum_{n=1}^{\infty} \sum_{r=2}^{\infty} \sum_{s=2}^{\infty} m(s-n) \left[(r-m)n-m(s-n)\right] w_{m,n} w_{r-m,s-n} \cos\frac{r\pi x}{a} \cos\frac{s\pi y}{b}$$

$$\Sigma B = \frac{\pi^4}{4a^2b^2} \sum_{m=1}^{\infty} \sum_{n=1}^{\infty} \sum_{r=2}^{\infty} \sum_{u=1}^{\infty} m(n-u) \left[(r-m)n+m(n-u)\right]$$

$$w_{m,n} w_{r-m,n-u} \cos\frac{r\pi x}{a} \cos\frac{u\pi y}{b} + \frac{\pi^4}{4a^2b^2} \sum_{m=1}^{\infty} \sum_{n=1}^{\infty} \sum_{r=2}^{\infty} \sum_{u=0}^{\infty}$$

$$m(n+u) \left[(r-m)n+m(n+u)\right] w_{m,n} w_{r-m,n+u} \cos\frac{r\pi x}{a} \cos\frac{u\pi y}{b}$$

$$\Sigma C = \frac{\pi^4}{4a^2b^2} \sum_{m=1}^{\infty} \sum_{n=1}^{\infty} \sum_{t=1}^{\infty} \sum_{s=2}^{\infty} m(s-n) \left[(m-t)n+m(s-n)\right] w_{m,n} w_{m-t,s-n} \cos\frac{t\pi x}{a} \cos\frac{s\pi y}{b}$$

$$+ \frac{\pi^4}{4a^2b^2} \sum_{m=1}^{\infty} \sum_{n=1}^{\infty} \sum_{t=0}^{\infty} \sum_{s=2}^{\infty} m(s-n) \left[(m+t)n+m(s-n)\right] w_{m,n} w_{m+t,s-n} \cos\frac{t\pi x}{a} \cos\frac{s\pi y}{b}$$

(B3)

$$\Sigma D = \frac{\pi^4}{4a^2b^2} \sum_{m=1}^{\infty} \sum_{n=1}^{\infty} \sum_{t=1}^{\infty} \sum_{u=0}^{\infty} m(n-u) \left[(m-t)n-m(n-u)\right]$$

$$w_{m,n} w_{m-t,n-u} \cos\frac{t\pi x}{a} \cos\frac{u\pi y}{b}$$

$$+ \frac{\pi^4}{4a^2b^2} \sum_{m=1}^{\infty} \sum_{n=1}^{\infty} \sum_{t=0}^{\infty} \sum_{u=1}^{\infty} m(n+u) \left[(m+t)n-m(n+u)\right]$$

$$w_{m,n} w_{m+t,n+u} \cos\frac{t\pi x}{a} \cos\frac{u\pi y}{b}$$

$$+\frac{\pi^4}{4a^2b^2}\sum_{m=1}^{\infty}\sum_{n=1}^{\infty}\sum_{t=1}^{\infty}\sum_{u=1}^{\infty} m(n+u)\left[(m-t)n-m(n+u)\right]$$

$$w_{m,n}w_{m-t,n+u}\cos\frac{t\pi x}{a}\cos\frac{u\pi y}{b}$$

$$+\frac{\pi^4}{4a^2b^2}\sum_{m=1}^{\infty}\sum_{n=1}^{\infty}\sum_{t=0}^{\infty}\sum_{u=0}^{\infty} m(n-u)\left[(m+t)n-m(n-u)\right]$$

$$w_{m,n}w_{m+t,n-u}\cos\frac{t\pi x}{a}\cos\frac{u\pi y}{b}$$

therefore

$$\left(\frac{\partial^2 w}{\partial x\partial y}\right)^2-\frac{\partial^2 w}{\partial x^2}\frac{\partial^2 w}{\partial y^2}=\Sigma A+\Sigma B+\Sigma C+\Sigma D \qquad (B4)$$

Equating coefficients of (B1) and (B4) according to eq. (67) the following results:

$$\pi^4 b_{pq}\left[\frac{p^2}{a^2}+\frac{q^2}{b^2}\right]^2=\frac{E\pi^4}{4a^2b^2}\left[\bar{A}_1+\sum_{k=1}^{2}\bar{B}_k+\sum_{k=1}^{2}\bar{C}_k+\sum_{k=1}^{4}\bar{D}_k\right]$$

where $\bar{A}_1=\sum_{m=1}^{p-1}\sum_{n=1}^{q-1} m(q-n)\left[(p-m)n-m(q-n)\right]w_{m,n}w_{p-m,q-n}$

if $p \neq 0, 1$ and $q \neq 0, 1$

$\bar{A}_1 = 0$, if $p = 0$ or 1, or $q = 0$ or 1

$$\bar{B}_1 = \sum_{m=1}^{p-1} \sum_{n=q+1}^{\infty} m(n-q) \left[(p-m)n+m(n-q)\right] w_{m,n} w_{p-m,n-q}$$

if $p \neq 0, 1$ and $q \neq 0$

$\bar{B}_1 = 0$, if $p = 0$ or 1, or $q = 0$

$$\bar{B}_2 = \sum_{m=1}^{p-1} \sum_{n=1}^{\infty} m(n+q) \left[(p-m)n+m(n+q)\right] w_{m,n} w_{p-m,n+q}$$

if $p \neq 0, 1$

$\bar{B}_2 = 0$, if $p = 0$ or 1

$$\bar{C}_1 = \sum_{m=p+1}^{\infty} \sum_{n=1} m(q-n) \left[(m-p)n+m(q-n)\right] w_{m,n} w_{m-p,q-n}$$

if $p \neq 0$ and $q \neq 0, 1$

$\bar{C}_1 = 0$, if $p = 0$, or $q = 0$ or 1

$$\bar{C}_2 = \sum_{m=1}^{\infty} \sum_{n=1}^{q-1} m(q-n) \left[(m+p)n+m(q-n)\right] w_{m,n} w_{m+p,q-n}$$

if $q \neq 0, 1$

$\bar{C}_2 = 0$, if $q = 0$ or 1

$$\bar{D}_1 = \sum_{m=1+p}^{\infty} \sum_{n=1+q}^{\infty} m(n-q) \left[(m-p)n-m(n-q)\right] w_{m,n} w_{m-p,n-q}$$

if $p \neq 0$

$\bar{D}_1 = 0$, if $p = 0$

$$\bar{D}_2 = \sum_{m=1}^{\infty} \sum_{n=1}^{\infty} m(n+q) \left[(m+p)n-m(n+q)\right] w_{m,n} w_{m+p,n+q}$$

if $q \neq 0$

$\bar{D}_2 = 0$, if $q = 0$

$$\bar{D}_3 = \sum_{m=1+p}^{\infty} \sum_{n=1}^{\infty} m(n+q) \left[(m-p)n-m(n+q)\right] w_{m,n} w_{m-p,n+q}$$

if $p \neq 0$ and $q \neq 0$

$\bar{D}_3 = 0$, if $p = 0$ or $q = 0$

$$\bar{D}_4 = \sum_{m=1}^{} \sum_{n=1+q}^{} m(n-q) \left[(m+p)n-m(n-q)\right] w_{m,n} w_{m+p,n-q}$$

if $p \neq 0$ or $q \neq 0$

$\bar{D}_4 = 0$ if $p = 0$ and $q = 0$

Making the indicated transformations (B5) can be put in the required form as shown below:

$$b_{p,q} = \frac{E}{4(p^2 \frac{b}{a} + q^2 \frac{a}{b})^2} \sum_{n=1}^{9} B_n \qquad (B6)$$

letting $m = k$ and $n = t$ in $\bar{A}_1$

$$B_1 = \sum_{k=1}^{p-1} \sum_{t=1}^{q-1} \left[kt(p-k)(q-t) - k^2(q-t)^2\right] w_{k,t} w_{p-k,q-t}$$

if $p \neq 0, 1$ and $q = 0, 1$

$B_1 = 0$, if $p = 0$ or 1, or $q = 0$ or 1

letting $m = k$ and $n = t$ in $\bar{C}_2$

$$B_2 = \sum_{k=1}^{\infty} \sum_{t=1}^{q-1} \left[kt(k+p)(q-t) + k^2(q-t)^2\right] w_{k,t} w_{(k+p),(q-t)}$$

if $q \neq 0, 1$

$B_2 = 0$, if $q = 0$ or 1

letting $m = k+p$ and $n = t$ in $\bar{C}_1$

$$B_3 = \sum_{k=1}^{\infty} \sum_{t=1}^{q-1} \left[(k+p)(t)(k)(q-t) + (k+p)^2(q-t)^2\right] w_{(k+p),t} w_{k,(q-t)}$$

if $q \neq 0, 1$ and $p \neq 0$

$B_3 = 0$, if $q = 0$ or 1, or $p = 0$

letting m = k and n = t in $\bar{B}_2$

$$B_4 = \sum_{k=1}^{p-1} \sum_{t=1}^{\infty} \left[kt(p-k)(t+q)+k^2(t+q)^2 \right] w_{k,t} w_{(p-k),(t+q)}$$

if $p \neq 0, 1$

$B_4 = 0$, if $p = 0$ or 1

letting m = k and n = q+t in $\bar{B}_1$

$$B_5 = \sum_{k=1}^{p-1} \sum_{t=1}^{\infty} \left[k(t+q)(p-k)t+k^2t^2 \right] w_{k,(t+q)} w_{(p-k),t}$$

if $q \neq 0$ and $p \neq 0, 1$

$B_5 = 0$, if $q = 0$, or $p = 0$ or 1

letting m = k and n = t in $\bar{D}_1$

$$B_6 = \sum_{k=1}^{\infty} \sum_{t=1}^{\infty} \left[kt(k+p)(t+q)-k^2(t+q)^2 \right] w_{k,t} w_{(k+p),(t+q)}$$

if $q \neq 0$

$B_6 = 0$, if $q = 0$

letting $m = k$ and $n = t+q$ in $\bar{D}_2$

$$B_7 = \sum_{k=1}^{\infty} \sum_{t=1}^{\infty} \left[k(t+q)(k+p)t - k^2t^2\right] w_{k,(t+q)} w_{(k+p),t}$$

if $q \neq 0$ or $p \neq 0$

$B_7 = 0$, if $p = q = 0$

letting $m = k+p$ and $n = t$ in $\bar{D}_3$

$$B_8 = \sum_{k=1}^{\infty} \sum_{t=1}^{\infty} \left[(k+p)tk(t+q) - (k+p)^2(t+q)^2\right] w_{(k+p),t} w_{k,(t+q)}$$

if $q \neq 0$ and $p \neq 0$

$B_8 = 0$, if $q = 0$ or $p = 0$

letting $m = k+p$ and $n = t+q$ in $\bar{D}_4$

$$B_9 = \sum_{k=1}^{\infty} \sum_{t=1}^{\infty} \left[(k+p)(t+q)kt - (k+p)^2t^2\right] w_{(k+p),(t+q)} w_{k,t}$$

if $p \neq 0$

$B_9 = 0$, if $p = 0$

APPENDIX C

DERIVATION OF EQUATIONS GOVERNING RELATION OF PRESSURE AND DEFLECTION COEFFICIENTS

Upon substituting (70) into the expression $\nabla^4 w$

$$\nabla^4 w = \pi^4 \sum_{m=1}^{\infty} \sum_{n=1}^{\infty} w_{m,n} \left(\frac{m^2}{a^2} + \frac{n^2}{b^2}\right)^2 \sin \frac{m\pi x}{a} \sin \frac{n\pi y}{b} \qquad (C1)$$

also by substitution of (70) and (71)

$$\frac{\partial^2 F}{\partial y^2} \frac{\partial^2 w}{\partial x^2} + \frac{\partial^2 F}{\partial x^2} \frac{\partial^2 w}{\partial y^2} - 2 \frac{\partial^2 F}{\partial x \partial y} \frac{\partial^2 w}{\partial x \partial y} =$$

$$\frac{\pi^4}{4a^2b^2} \sum_{m=1}^{\infty} \sum_{n=1}^{\infty} \sum_{p=0}^{\infty} \sum_{q=0}^{\infty} \left\{ (mq-np)^2 b_{p,q} w_{m,n} \sin \frac{(p+m)\pi x}{a} \sin \frac{(n+q)\pi y}{b} \right.$$

$$+ (mq+np)^2 b_{p,q} w_{m,n} \sin \frac{(p+m)\pi x}{a} \sin \frac{(n-q)\pi y}{b}$$

$$+ (mq+np)^2 b_{p,q} w_{m,n} \sin \frac{(m-p)\pi x}{a} \sin \frac{(n+q)\pi y}{b}$$

$$\left. + (mq-np)^2 b_{p,q} w_{m,n} \sin \frac{(m-p)\pi x}{a} \sin \frac{(n-q)\pi y}{b} \right\} \qquad (C2)$$

To change (C2) into a form similar to (C1) the following transformations will be made

$$p+m = r$$

$$q+n = s$$

$$m-p = t$$

$$n-q = u$$

Substituting the above transformations and making use of the identity $\sum_{-\infty}^{-1} f(u) = \sum_{1}^{\infty} f(-u)$ in (C2) the following equation results:

$$\frac{\partial^2 F}{\partial y^2}\frac{\partial^2 w}{\partial x^2} + \frac{\partial^2 F}{\partial x^2}\frac{\partial^2 w}{\partial y^2} - 2\frac{\partial^2 F}{\partial x \partial y}\frac{\partial^2 F}{\partial x \partial y} =$$

$$\frac{\pi^4}{4a^2b^2}\sum_{m=1}^{\infty}\sum_{n=1}^{\infty}\sum_{r=1}^{\infty}\sum_{s=1}^{\infty}\left[(s-n)m-(r-m)n\right]^2 b_{r-m,s-n} w_{m,n} \sin\frac{r\pi x}{a}\sin\frac{s\pi y}{b}$$

$$+\sum_{m=1}^{\infty}\sum_{n=1}^{\infty}\sum_{r=1}^{\infty}\sum_{u=1}^{\infty}\left[(n-u)m+(r-m)n\right]^2 b_{r-m,n-u} w_{m,n} \sin\frac{r\pi x}{a}\sin\frac{u\pi y}{b}$$

$$-\sum_{m=1}^{\infty}\sum_{n=1}^{\infty}\sum_{r=1}^{\infty}\sum_{u=1}^{\infty}\left[(n+u)m+(r-m)n\right]^2 b_{r-m,n+u} w_{m,n} \sin\frac{r\pi x}{a}\sin\frac{u\pi y}{b}$$

$$+\sum_{m=1}^{\infty}\sum_{n=1}^{\infty}\sum_{t=1}^{\infty}\sum_{s=1}^{\infty}\left[(s-n)m+(m-t)n\right]^2 b_{m-t,s-n} w_{m,n} \sin\frac{t\pi x}{a}\sin\frac{s\pi y}{b}$$

$$-\sum_{m=1}^{\infty}\sum_{n=1}^{\infty}\sum_{t=1}^{\infty}\sum_{s=1}^{\infty}\left[(s-n)m+(m+t)n\right]^2 b_{m+t,s-n} w_{m,n} \sin\frac{t\pi x}{a}\sin\frac{s\pi y}{b}$$

$$+\sum_{m=1}^{\infty}\sum_{n=1}^{\infty}\sum_{t=1}^{\infty}\sum_{u=1}^{\infty}\left[(n-u)m-(m-t)n\right]^2 b_{m-t,n-u} w_{m,n} \sin\frac{t\pi x}{a}\sin\frac{u\pi y}{b}$$

$$+\sum_{m=1}^{\infty}\sum_{n=1}^{\infty}\sum_{t=1}^{\infty}\sum_{u=1}^{\infty}\left[(n+u)m-(m+t)n\right]^2 b_{m+t,n-u} w_{m,n} \sin\frac{t\pi x}{a}\sin\frac{u\pi y}{b}$$

$$- \sum_{m=1}^{\infty} \sum_{n=1}^{\infty} \sum_{t=1}^{\infty} \sum_{u=1}^{\infty} \left[(n-u)m-(m+t)n\right]^2 b_{m+t,n-u} w_{m,n} \sin \frac{t\pi x}{a} \sin \frac{u\pi y}{b}$$

$$- \sum_{m=1}^{\infty} \sum_{n=1}^{\infty} \sum_{t=1}^{\infty} \sum_{u=1}^{\infty} \left[(n+u)m-(m-t)n\right]^2 b_{m-t,n+u} w_{m,n} \sin \frac{t\pi x}{a} \sin \frac{u\pi y}{b}$$

$$= \frac{\pi^4}{4a^2b^2} \sum_{n=1}^{9} A_n \qquad (C3)$$

Equating coefficients of (C1) and (C3) according to equation (66) and noting that

$$p_T = \sum_{r=1}^{\infty} \sum_{s=1}^{\infty} p_{r,s} \sin \frac{r\pi x}{a} \sin \frac{s\pi y}{b}$$

odd integers only

$$p_{r,s} = D\pi^4 w_{r,s} \left(\frac{r^2}{a^2} + \frac{s^2}{b^2}\right)^2 - \frac{h\pi^4}{4a^2b^2} \sum_{n=1} \bar{A}_n$$

$$\bar{A}_1 = \sum_{m=1}^{r} \sum_{n=1}^{s} \left[(s-n)m-(r-m)n\right]^2 b_{r-m,s-n} w_{m,n}$$

$$\bar{A}_2 = \sum_{m=1}^{r} \sum_{n=s}^{\infty} \left[(n-s)m+(r-m)n\right]^2 b_{r-m,n-s} w_{m,n}$$

$$\bar{A}_3 = -\sum_{m=1}^{r} \sum_{n=-s}^{\infty} \left[(n+s)m+(r-m)n\right]^2 b_{r-m,n+s} w_{m,n}$$

$$\bar{A}_4 = \sum_{m=r}^{\infty} \sum_{n=1}^{s} \left[(s-n)m+(m-r)n\right]^2 b_{m-r,s-n} W_{m,n}$$

$$\bar{A}_5 = \sum_{m=-r}^{\infty} \sum_{n=1}^{s} \left[(s-n)m+(m+r)n\right]^2 b_{m+r,s-n} W_{m,n}$$

$$\bar{A}_6 = \sum_{m=r}^{\infty} \sum_{n=s}^{\infty} \left[(n-s)m-(m-r)n\right]^2 b_{m-r,n-s} W_{m,n}$$

$$\bar{A}_7 = \sum_{m=-r}^{\infty} \sum_{n=-s}^{\infty} \left[(n+s)m-(m+r)n\right]^2 b_{m+r,n+s} W_{m,n}$$

$$\bar{A}_8 = \sum_{m=-r}^{\infty} \sum_{n=s}^{\infty} \left[(n-s)m-(m+r)n\right]^2 b_{m+r,n-s} W_{m,n}$$

$$\bar{A}_9 = \sum_{m=r}^{\infty} \sum_{n=-s}^{\infty} \left[(n+s)m-(m-r)n\right]^2 b_{m-r,n+s} W_{m,n} \qquad \text{(C4)}$$

Equation (C4) is put into the required form by making the indicated transformations

$$p_{r,s} = D\pi^4 W_{r,s} \left(\frac{r^2}{a^2} + \frac{s^2}{b^2}\right)^2 + \frac{h\pi^4}{4a^2b^2} \sum_{n=1}^{9} \bar{A}_n \qquad \text{(C5)}$$

letting $m = k$ and $n = t$ in $\bar{A}_1$

$$\bar{A}_1 = \sum_{k=1}^{r} \sum_{t=1}^{s} \left[(s-t)k-(r-k)t\right]^2 b_{r-k,s-t} W_{k,t}$$

letting $m = k+r$ and $n = t+s$ in $\bar{A}_4$

$$A_2 = \sum_{k=0}^{\infty} \sum_{t=0}^{\infty} \left[t(k+r)-k(t+s)\right]^2 b_{k,t} w_{k+r,t+s}$$

letting $m = k+r$ and $n = t$ in $\bar{A}_9$

$$A_3 = \sum_{k=0}^{\infty} \sum_{t=1}^{\infty} \left[(t+s)(k+r)-kt\right]^2 b_{k,t+s} w_{k+r,t}$$

letting $m = k$ and $n = t+s$ in $\bar{A}_8$

$$A_4 = \sum_{k=1}^{\infty} \sum_{t=0}^{\infty} \left[tk-(k+r)(t+s)\right]^2 b_{k+r,t} w_{k,t+s}$$

letting $m = k$ and $n = t$ in $\bar{A}_7$

$$A_5 = \sum_{k=1}^{\infty} \sum_{t=1}^{\infty} \left[(t+s)k-(k+r)t\right]^2 b_{k+r,t+s} w_{k,t}$$

letting $m = k$ and $n = t+s$ in $\bar{A}_2$

$$A_6 = \sum_{k=1}^{r} \sum_{t=0}^{\infty} \left[tk+(r-k)(t+s)\right]^2 b_{r-k,t} w_{k,t+s}$$

letting $m = k$ and $n = t$ in $\bar{A}_3$

$$A_7 = \sum_{k=1}^{r} \sum_{t=1}^{\infty} \left[(t+s)k+(r-k)t\right]^2 b_{r-k,t+s} w_{k,t}$$

letting $m = k+r$ and $n = t$ in $\bar{A}_4$

$$A_8 = \sum_{k=0}^{\infty} \sum_{t=1}^{s} \left[(s-t)(k+r)+kt\right]^2 b_{k,s-t} w_{k+r,t}$$

letting $m = k$ and $n = t$ in $\bar{A}_5$

$$A_9 = \sum_{k=1}^{\infty} \sum_{t=1}^{s} \left[(s-t)k+(k+r)t\right]^2 b_{k+r,s-t} w_{k,t}$$

APPENDIX D

SATISFACTION OF STRAIGHT EDGE BOUNDARY CONDITION

It can be shown that the assumed form of the stress function, F, and the deflection form w, will automatically satisfy the boundary condition that the edges of the plate must remain straight. This is done by showing that the end shortening of the plate is independent of x and y and must therefore be constant along each edge.

Substituting (70) and (71) into (83) and then into (81) the following relationship is arrived at

$$\delta_x = \int_0^a \left\{ \frac{\pi^2}{E} \sum_{p=0}^{\infty} \sum_{q=0}^{\infty} b_{p,q} \left(\nu \frac{p^2}{a^2} - \frac{q^2}{b^2} \right) \cos \frac{p\pi x}{a} \cos \frac{q\pi y}{b} \right.$$

$$- \frac{\pi^2}{2a^2} \sum_{m=1}^{\infty} \sum_{n=1}^{\infty} \sum_{m'=1}^{\infty} \sum_{n'=1}^{\infty} m\, m'\, w_{m,n} w_{m',n'} \cos \frac{m\pi x}{a}$$

$$\left. \cos \frac{m'\pi x}{a} \sin \frac{n\pi y}{b} \sin \frac{n'\pi y}{b} \right\} dx \qquad \text{(D1)}$$

It can be seen from Eq. (B6) that $b_{00} = 0$ and also that

$$b_{0,q} = \frac{E}{4q^4} \frac{b^2}{a^2} \left\{ \sum_{k=1}^{\infty} \sum_{t=1}^{q-1} k^2 (q-t) q\, w_{k,t} w_{k,q-t} - \sum_{k=1}^{\infty} \sum_{t=1}^{\infty} k^2 q^2 w_{k,t} w_{k,q+t} \right\} \qquad \text{(D2)}$$

Integrating (81) and setting $b_{0,0} = 0$

$$\delta_x = - \frac{\pi^2}{E} \frac{a^2}{b^2} \sum_{q=1}^{\infty} b_{0,q} q^2 \cos \frac{q\pi y}{b} - \frac{\pi^2}{4a} \sum_{m=1}^{\infty} \sum_{n=1}^{\infty} \sum_{n'=1}^{\infty} m^2 w_{m,n} w_{m,n'} \sin \frac{n\pi y}{b} \sin \frac{n'\pi y}{b}$$

or

$$\sigma_x = -\frac{\pi^2}{E}\frac{a}{b^2}\sum_{q=0}^{\infty} b_{0,q}\, q^2 \cos\frac{q\pi y}{b} - \frac{\pi^2}{8a}\sum_{m=1}\sum_{n=1}\sum_{n'=1} m^2 w_{m,n} w_{m,n'}$$

$$\left[\cos(n-n')\frac{\pi y}{b} - \cos(n+n')\frac{\pi y}{b}\right] \qquad \text{(D3)}$$

The first summation of (D3) will be examined separately. Using (D2) it may be written

$$-\frac{\pi^2}{E}\frac{a}{b^2}\sum_{q=1}^{\infty} b_{0,q} q^2 \cos\frac{q\pi y}{b} = -\frac{\pi^2}{4a}\sum_{k=1}^{\infty}\sum_{t=1}^{q-1}\sum_{q=2}^{\infty}\frac{k^2(q-t)}{q} w_{k,t}$$

$$w_{k,q-t}\cos\frac{q\pi y}{b} + \frac{\pi^2}{4a}\sum_{k=1}^{\infty}\sum_{t=1}^{\infty}\sum_{q=1}^{\infty} k^2 w_{k,t} w_{k,q+t}\cos\frac{q\pi y}{b}$$

or

$$-\frac{\pi^2}{E}\frac{a}{b^2}\sum_{q=1}^{\infty} b_{0,q} q^2 \cos\frac{q\pi y}{b} = -\frac{\pi^2}{4a}\sum_{k=1}^{\infty}\sum_{t=1}^{q-1}\sum_{q=2}^{\infty} k^2 w_{k,t} w_{k,q-t}\cos\frac{q\pi y}{b}$$

$$+\frac{\pi^2}{4a}\sum_{k=1}^{\infty}\sum_{t=1}^{q-1}\sum_{q=2}^{\infty} k^2\frac{t}{q} w_{k,t} w_{k,q-t}\cos\frac{q\pi y}{b}$$

$$+\frac{\pi^2}{4a}\sum_{k=1}^{\infty}\sum_{t=1}^{\infty}\sum_{q=1}^{\infty} k^2 w_{k,t} w_{k,q+t}\cos\frac{q\pi y}{b}$$

which may be written

$$-\frac{\pi^2}{E}\frac{a}{b^2}\sum_{q=1}^{\infty} b_{0,q}q^2\cos\frac{q\pi y}{b} = -\frac{\pi^2}{4a}\sum_{k=1}^{\infty}\sum_{t=1}^{q-1}\sum_{q=2}^{\infty} k^2 w_{k,t}w_{k,q-t}\cos\frac{q\pi y}{b}$$

$$+\frac{\pi^2}{4a}\sum_{k=1}^{\infty}\sum_{t=1}^{q-1}\sum_{q=2}^{\infty} k^2\frac{t}{q}w_{k,t}w_{k,q-t}\cos\frac{q\pi y}{b}$$

where $t \quad q-t$

$$+\frac{\pi^2}{4a}\sum_{k=1}^{\infty}\sum_{t=1}^{q-1}\sum_{q=2}^{\infty} k^2\frac{t}{q}w_{k,t}w_{k,q-t}\cos\frac{q\pi y}{b}$$

where $q-t \quad t$

$$+\frac{\pi^2}{4a}\sum_{k=1}^{\infty}\sum_{t=1}^{\infty}\frac{k^2}{2}w_{k,t}^2\cos\frac{2t\pi y}{b}$$

where $q-t = t$, i.e., $q = 2t$

$$+\frac{\pi^2}{4a}\sum_{k=1}^{\infty}\sum_{t=1}^{\infty}\sum_{q=1}^{\infty} k^2 w_{k,t}w_{k,q+t}\cos\frac{q\pi y}{b}$$

Here note that if we restrict the first summation of the above equations to t $q-t$ then

$$-\frac{\pi^2}{4a}\sum_{k=1}^{\infty}\sum_{t=1}^{q-1}\sum_{q=2}^{\infty} k^2 w_{k,t}w_{k,q-t}\cos\frac{q\pi y}{b} = -\frac{\pi^2}{2a}\sum_{k=1}^{\infty}\sum_{t=1}^{q-1}\sum_{q=2}^{\infty} k^2 w_{k,t}w_{k,q-t}\cos\frac{q\pi y}{b}$$

where $t > q-t$

$$-\frac{\pi^2}{4a}\sum_{k=1}^{\infty} k^2 w_{k,t}^2 \cos\frac{2t\pi y}{b}$$

where $t = q-t$

then changing subscripts by the noted transformations in order to clarify the combining of terms the following results:

$$-\frac{\pi^2}{E}\frac{a}{b^2}\sum_{q=1}^{\infty} b_{0,q} q^2 \cos\frac{q\pi y}{b} = -\frac{\pi^2}{2a}\sum_{k=1}^{\infty}\sum_{t=1}^{q-1}\sum_{q=2}^{\infty} k^2 w_{k,t} w_{k,q-t} \cos\frac{q\pi y}{b}$$

where $t > q-t$

$$-\frac{\pi^2}{4a}\sum_{k=1}^{\infty} k^2 w_{k,t}^2 \cos\frac{2t\pi y}{b} + \frac{\pi^2}{4a}\sum_{k=1}^{\infty}\sum_{s=1}^{q-1}\sum_{q=2}^{\infty} k^2 \frac{a}{q} w_{k,s} w_{k,q-s} \cos\frac{q\pi y}{b}$$

where $s > q-s$ let $t = s$

$$+\frac{\pi^2}{4a}\sum_{k=1}^{\infty}\sum_{s=1}^{q-1}\sum_{q=2}^{\infty} k^2 \frac{q-s}{q} w_{k,q-s} w_{k,s} \cos\frac{q\pi y}{b}$$

where $s > q-s$ let $q-t = s$

$$+\frac{\pi^2}{4a}\sum_{k=1}^{\infty}\sum_{t=1}^{\infty}\sum_{q=1}^{\infty} k^2 w_{k,t} w_{k,q+t} \cos\frac{q\pi y}{b}$$

$$+\frac{\pi^2}{8a}\sum_{k=1}^{\infty}\sum_{t=1}^{\infty} k^2 w_{k,t}^2 \cos\frac{2t\pi y}{b}$$

After noting that the third and fourth summations of this equation may be combined as follows:

$$\sum_{k=1}^{\infty}\sum_{s=1}^{q-1}\sum_{q=2}^{\infty}\left(k^2\frac{s}{q}w_{k,s}w_{k,q-s}+k^2\frac{q-s}{q}w_{k,q-s}w_{k,s}\right)\cos\frac{q\pi y}{b}$$

where $s>q-s$

$$=\sum_{k=1}^{\infty}\sum_{t=1}^{q-1}\sum_{q=2}^{\infty}k^2w_{k,t}w_{k,q-t}\cos\frac{q\pi y}{b}$$

where $t>q-t$

the equation may be written

$$-\frac{\pi^2}{E}\frac{\varepsilon}{b^2}\sum_{q=1}^{\infty}b_{0,q}q^2\cos\frac{q\pi y}{b}=-\frac{\pi^2}{4a}\sum_{k=1}^{\infty}\sum_{t=1}^{q-1}\sum_{q=2}^{\infty}k^2w_{k,t}w_{k,q-t}\cos\frac{q\pi y}{b}$$

where $t>q-t$

$$+\frac{\pi^2}{4a}\sum_{k=1}^{\infty}\sum_{t=1}^{\infty}\sum_{q=1}^{\infty}k^2w_{k,t}w_{k,q+t}\cos\frac{q\pi y}{b}$$

$$-\frac{\pi^2}{8a}\sum_{k=1}^{\infty}\sum_{t=1}^{\infty}k^2w_{k,t}^2\cos\frac{2t\pi y}{b} \qquad (D4)$$

Upon examination of the second term of eq. (D3) and noting the two cases which may occur, i.e., $n = n'$ and $n \neq n'$ the following results:

$$-\frac{\pi^2}{8a}\sum_{m=1}^{\infty}\sum_{n=1}^{\infty}\sum_{n'=1}^{\infty}m^2w_{m,n}w_{m,n'}\left[\cos(n-n')\frac{\pi y}{b}-\cos(n+n')\frac{\pi y}{b}\right]$$

$$= -\frac{\pi^2}{8a}\sum_{m=1}^{\infty}\sum_{n=1}^{\infty} m^2 w_{m,n}^2 + \frac{\pi^2}{8a}\sum_{m=1}^{\infty}\sum_{n=1}^{\infty} m^2 w_{m,n}^2 \cos\frac{2n\pi y}{b}$$

$$-\frac{\pi^2}{8a}\sum_{m=1}^{\infty}\sum_{n=1}^{\infty}\sum_{n'=1}^{\infty} m^2 w_{m,n} w_{m,n'} \cos(n-n')\frac{\pi y}{b}$$

$$n \neq n'$$

$$+\frac{\pi^2}{8a}\sum_{m=1}^{\infty}\sum_{n=1}^{\infty}\sum_{n'=1}^{\infty} m^2 w_{m,n} w_{m,n} \cos(n+n')\frac{\pi y}{b}$$

$$n \neq n'$$

Noting that

$$\frac{\pi^2}{8a}\sum_{m=1}^{\infty}\sum_{n=1}^{\infty}\sum_{n'=1}^{\infty} m^2 w_{m,n} w_{m,n'} \cos(n+n')\frac{\pi y}{b} = \frac{\pi^2}{4a}\sum_{m=1}^{\infty}\sum_{n=1}^{\infty}\sum_{n'=1}^{\infty}$$

$$m^2 w_{m,n} w_{m,n'} \cos(n+n')\frac{\pi y}{b}$$

$$n' > n$$

and

$$-\frac{\pi^2}{8a}\sum_{m=1}^{\infty}\sum_{n=1}^{\infty}\sum_{n'=1}^{\infty} m^2 w_{m,n} w_{m,n'} \cos(n-n')\frac{\pi y}{b} = -\frac{\pi^2}{b}\sum_{m=1}^{\infty}\sum_{n=1}^{\infty}\sum_{n'=1}^{\infty}$$

$$m^2 w_{m,n} w_{m,n'} \cos(n-n')\frac{\pi y}{b}$$

$$n > n'$$

the above may be written as follows:

$$-\frac{\pi^2}{8a}\sum_{n=1}^{\infty}\sum_{n=1}^{\infty}\sum_{n'=1}^{\infty} m^2 w_{m,n} w_{m,n'}\left[\cos(n-n')\frac{\pi y}{b} - \cos(n+n')\frac{\pi y}{b}\right] =$$

$$-\frac{\pi^2}{8a}\sum_{m=1}^{\infty}\sum_{n=1}^{\infty} m^2 w_{m,n}^2 - \frac{\pi^2}{4a}\sum_{m=1}^{}\sum_{n=1}^{}\sum_{n'=1}^{} m^2 w_{m,n} w_{m,n'} \cos(n-n')\frac{\pi y}{b}$$

$$n > n'$$

$$+\frac{\pi^2}{4a}\sum_{m=1}^{\infty}\sum_{n=1}^{\infty}\sum_{n'=1}^{\infty} m^2 w_{m,n} w_{m,n'} \cos(n+n')\frac{\pi y}{b}$$

$$+\frac{\pi^2}{8a}\sum_{m=1}^{\infty}\sum_{n=1}^{\infty} m^2 w_{m,n}^2 \cos\frac{2n\pi y}{b}$$

Or making the indicated transformations

$$-\frac{\pi^2}{8a}\sum_{m=1}^{\infty}\sum_{n=1}^{\infty}\sum_{n'=1}^{\infty} m^2 w_{m,n} w_{m,n'} \cos(n-n')\frac{\pi y}{b} - \cos(n+n')\frac{\pi y}{b}$$

where $n > n'$ let $n-n' = q$

$$-\frac{\pi^2}{8a}\sum_{m=1}^{\infty}\sum_{n=1}^{\infty} m^2 w_{m,n}^2 - \frac{\pi^2}{4a}\sum_{m=1}^{\infty}\sum_{q=1}^{\infty}\sum_{n'=1}^{\infty} m^2 w_{m,q+n'} w_{m,n'} \cos\frac{q\pi y}{b}$$

where $n' > q-n$ since n' n let $n+n' = q$

$$+\frac{\pi^2}{4a}\sum_{m=1}^{\infty}\sum_{q=1}^{\infty}\sum_{n'=1}^{\infty} m^2 w_{m,q-n'} w_{m,n'} \cos\frac{q\pi y}{b}$$

$$+\frac{\pi^2}{8a}\sum_{m=1}^{\infty}\sum_{n=1}^{\infty} m^2 w_{m,n}^2 \cos\frac{2n\pi y}{b} \qquad \text{(D5)}$$

Substituting (D4) and (D5) in (D3) the following relationship results for the end shortening of the plate in the x-direction.

$$\delta_x = -\frac{\pi^2}{8a}\sum_{m=1}^{\infty}\sum_{n=1}^{\infty} m^2 w_{m,n}^2 \qquad \text{(D6)}$$

similarly

$$\delta_y = -\frac{\pi^2}{8b}\sum_{m=1}^{\infty}\sum_{n=1}^{\infty} n^2 w_{m,n}^2 \qquad \text{(D7)}$$